Nitrous Oxide Dynamics in a Riparian Wetland of an Agricultural Catchment in Southern Ontario

by

Jamee DeSimone

A thesis
presented to the University of Waterloo
in fulfillment of the
thesis requirement for the degree of
Master of Science
in
Geography

Waterloo, Ontario, Canada, 2009

AUTHOR'S DECLARATION

I hereby declare that I am the sole author of this thesis. This is a true copy of the thesis, including any required final revisions, as accepted by my examiners.

I understand that my thesis may be made electronically available to the public.

Abstract

Riparian zones (RZ) are known to act as buffers, reducing the transfer of potentially harmful nutrients from agricultural fields to surface water bodies. However, many of the same processes in the subsurface that help to reduce this nutrient loading, may also be leading to greenhouse gas (GHG) production and emissions from these areas. Agricultural riparian zones in Southern Ontario are often characterized by a sloped topography, with the highest topographic position being closest to the field edge, decreasing towards an adjacent stream or other surface water body. This topographic variability, combined with lateral chemical inputs from both upland areas and the stream, is expected to cause variable hydrochemical environments throughout the RZ, which may therefore lead to variable N_2O dynamics between upland, mid-riparian and lowland areas. The objectives of this study were to examine these spatial trends in N_2O production and resulting emissions, as related to the hydrochemical environment in these three distinct zones. Objectives were achieved by instrumenting 6 sites across two transects running perpendicular from the agricultural field edge, towards the stream edge, analyzing for subsurface N_2O, moisture and temperature, groundwater NO_3, NH_4, dissolved organic carbon (DOC), dissolved oxygen, and surface fluxes of N_2O.

Subsurface N_2O concentrations and ground water nutrient concentrations displayed distinct spatial and temporal/seasonal trends in the three positions across the RZ, however N_2O fluxes across the soil-atmosphere interface did not display strong or consistent spatial trends. There was a disconnect between the subsurface variables and the fluxes at the surface, in that N_2O emissions did not reflect the N_2O concentrations produced in the shallow soil profile (150 cm deep), nor were they significantly related to the geochemical environment at each position. The lack of visible spatial trends in N_2O fluxes may have been due to an "oxic blanket" effect which may divide the surface from the subsurface soil profile. As N_2O fluxes in this study (-0.28 to 1.3 nmol m^{-2} s^{-1}) were within the range observed at other, similar study sites, the oxic blanket doesn't appear to impede concentrations of N_2O reaching the soil-atmosphere interface. This may suggest that the N_2O released as a flux was being produced in the very shallow soil profile (0 – 5 cm), above the soil gas profile arrays installed at this site. Subsurface concentrations of N_2O were fairly high at certain depths and times, which was not reflected in the fluxes. This may have resulted from nitrifier denitrification reducing N_2O to N_2 before it reached the surface, in aerobic zones above the water table. Another potential reason for the lack of connection between subsurface processes and surface emissions was the high heterogeneity observed across the RZ, which may have overshadowed potential differences

between positions. Physical soil properties like porosity and bulk density across the RZ also potentially impacted the N_2O movement through the soil profile, resulting in similar fluxes among positions, and over time. The missing connection between subsurface N_2O concentrations, ground water nutrients, and the surface fluxes was not a hypothesized result, and requires further research and analysis for a better understanding of the production and consequent movement of N_2O.

Acknowledgements

I would like to thank my dedicated, patient and always available advisors, Drs. Merrin Macrae and Rick Bourbonniere, for their ever-present support and assistance. Thank you to Merrin who, on more than one occasion, allowed me to take hours out of her day to sit down and stare at my data until our eyes started to water, and then let us play with her kids for a fun brain break! And thank you to Rick, who has generously opened his home to me on countless occasions, and allowed me to bask in the heaven that is his Thai and Chinese cooking!

Thank you to all the wonderful field help (and companionship) at the VaRRG field site, including Emily Cho, Lauren Cymbaly (vegetation description), Bobby Katanchi, Joseph Lance, Meagan Leach, Miranda Lewis, Amy Nicol, Jen Owens, Jenn Parrot, Angie Straathof, and Zheng Zhang, – field days would have felt much longer without sharing smiles, laughter, and Dee's famous buttertarts!

Thanks to the special assistance of my favourite CCIW folk, Frank Dunnett and Karen Edmondson, for their tireless construction and lab help, and constant willingness to lend an ear, share a cup of coffee, and even share some office gossip!

Thank you to the technical assistance from Richard Elgood and Alex Maclean, who were always willing to help me, despite their often busy schedules.

Thank you to my friends here at UW who have always supported me and helped to push me along. And thank you to my family, whom I love dearly, but especially when they stopped asking me "are you done yet?"!

I would like to dedicate this paper to John Mount, who sadly passed away December 26th, 2008. As the "overseer" of the property on which we did our field work, John was always outside to greet us in the mornings, and to say goodbye to us in the evenings. He was known for his kindness and interest in our pursuits, as well as his ability to remember every one of our names, positions, and what kinds of things we liked to do in our personal lives (which he often shared with all)! He will be missed.

Table of Contents

List of Figures

List of Tables

Chapter 1
Introduction and Problem Statement

Climate change has become a significant concern on the minds of politicians, scientists and the general public within the last decade. A major contributor to the publicized "global warming" effect, is the increase in greenhouse gases (GHGs). Although these are produced naturally, anthropogenic activities, especially since the industrial revolution, have caused an increase in the production and emission of these gases. Such activities act directly to increase human-made emissions, or indirectly augment natural GHG production in wetlands and other ecosystems (IPCC, 2001). Changes in the natural concentrations of GHGs in the atmosphere can have significant consequences for the planet's ecosystems by changing the Earth's radiative balance (Conrad, 1996). Three gases attributed to the greenhouse effect are carbon dioxide (CO_2), methane (CH_4), and nitrous oxide (N_2O). Carbon dioxide is present in the atmosphere in higher concentrations than either CH_4 or N_2O, however the latter two gases have the ability to disrupt the radiative balance more powerfully than CO_2 on a per mole basis (Lashof and Ahuja, 1990). Global warming potential (GWP) is a term used to describe the ability of a gas to trap heat as compared to a standard reference gas (CO_2). Despite the larger concentration of CO_2 in the atmosphere, both CH_4 and N_2O are more efficient GHGs as they have a GWP of approximately 23 and 296, respectively (IPCC,2001; Akimoto *et al*., 2005). Many studies have examined the influence of increased CO_2 on the environment, and CH_4 is largely studied as a GHG released in both natural and anthropogenic processes. However N_2O, one of the most potent GHGs, and its production mechanisms, has more recently come into light as an important trace gas in the global warming scientific arena. Due to its powerful GWP, and the relatively smaller amount of research conducted on N_2O, it is important to improve the scientific understanding of N_2O dynamics in various landscapes in order to create more accurate climate change models.

Wetlands have been identified as important landforms regulating GHG dynamics, although processes within them vary with wetland type and location. The physical characteristics of wetlands make them a natural source of GHGs to the global budget, and they are largely studied in this respect. Riparian zone wetlands are often used as "buffers" to mitigate nutrient rich inputs from adjacent agricultural fields to surface water bodies (Burt, 2005; Cey *et al.*, 1999; Willems *et al.*, 1997; Peterjohn and Correll, 1984). These lateral inputs are from both surface runoff and groundwater, and contain nitrogen and phosphorus species, such as nitrate (NO_3) and phosphate, as well as organic carbon (Sutka *et al.*, 2006; Banaszuk *et al.*, 2005; Peterjohn and Correll, 1984). The anoxic, inundated

soils present in riparian wetlands provide a reducing environment conducive to processes such as denitrification, the conversion of NO_3 to dinitrogen (Hill *et al.*, 2004). Although agricultural riparian wetlands provide an important ecological service by their buffering activities, a by-product of these activities is the production and release of GHGs. Of specific interest here is the potential for enhanced production of N_2O as a result of NO_3 and carbon loading to these systems.

1.1 Study Rationale and Objectives

There is a 30% discrepancy in the mass balance calculations between atmospheric N_2O sources and sinks (Bowden *et al.*, 2000). Since GHG measurements from wetlands affected by agriculture, like temperate forested riparian wetlands, are under-represented in the literature, and are zones of production for N_2O, studies in these types of environments might help to close this 30% mass balance gap. An understanding of the production and concentrations of GHGs as a result of surface and subsurface input of nutrients and the hydrochemical environment at depth, would help to improve the scientific understanding of nitrogen dynamics in these landscapes. An understanding of the processes leading to the production of N_2O in response to variable moisture, temperature, nutrient supply and substrate availability is fairly well understood (Hanson *et al.*, 1994a). However, the combination of these process controls and the soil physical properties *in situ*, are difficult to predict and require a better understanding (Ball *et al.*, 1997). Despite the number of N_2O studies performed in various environments around the world, there is still little understanding of how N_2O concentrations in subsoils contribute (or not) to N_2O emissions (Reth *et al.*, 2008). The site chosen to perform this research has two transects that display differing topographic gradients, which would theoretically result in variable hydrology and nutrient transport, both of which are important controllers of N_2O production. Therefore, it was reasoned that spatial trends in N_2O emissions at the soil-atmosphere interface would result from trends in nutrient supply and subsurface gases, especially in light of sites' proximities to an agricultural field.

In order to understand and predict changes in sources and sinks for global change modeling, it is important to understand the processes that are involved in creating the soil-atmosphere flux (Conrad and Smith, 1995). The overlying objective of this study was to examine the dynamics of N_2O across an agriculturally-impacted riparian wetland. Specific research questions are:

1) Is there spatial variability in N_2O fluxes from the field edge to the lowland/stream edge?
2) Are these patterns more strongly driven by:
    a. Nutrient/chemical supply?

i. Nutrient supply in groundwater (nitrate, ammonium, dissolved organic carbon (DOC)),
ii. Nutrient supply in soils (extractable N and soil C:N)
iii. Supply of gaseous N_2O in subsurface soil pores

b. Soil physical and moisture characteristics and topography?

It was hypothesized that spatial differences in N_2O fluxes across the riparian zone would be most strongly related to N supply from different sources (agricultural field and stream), whereas temporal-induced spatial variability at each site would be driven by changes in soil moisture.

The following sections of this introduction will discuss riparian zones and their role in mediating non-point source pollution, with the potential of creating another type of pollution (N_2O), specifically in agricultural landscapes. Nutrient cycling, with specific references to denitrification and nitrification will follow, along with a discussion of controlling factors. Gaps or weaknesses in the literature will also be brought to light.

1.2 Riparian Zone Definition and Function

Riparian Zones (RZ) are commonly defined as the interface between aquatic and terrestrial ecosystems, where structural and process changes occur discontinuously over space (Naiman and Décamps, 1997). They are found adjacent to surface water bodies such as streams, and the general direction of flow (both surface and subsurface) is often towards the channel (Triska *et al.*, 1993), although this is not always the case. There are two main interfaces of concern in riparian zones: that which occurs at the upland-RZ boundary, and one that occurs at the stream-RZ boundary (Triska *et al.*, 1993). The former is controlled by upland hydrodynamics with a dominant groundwater flux direction towards the channel, and the latter is strongly influenced by stream hydrodynamics and experiences bi-directional flow of nutrients and water (Triska *et al.*, 1993). Hydrology is therefore, one of the main factors contributing to the form and function of these ecosystems (Burt *et al.*, 2005; Hill *et al.*, 2000; Naiman and Décamps, 1997).

1.2.1 Role of Riparian Zones in Reducing Effects of Contaminants in Agricultural Runoff

Artificial and natural fertilizers can contain high concentrations of nutrients such as NO_3 and phosphate, which can cause negative effects for aquatic ecosystem health, such as eutrophication (Carpenter *et al.*, 1998). The USEPA (1996) suggests that eutrophication of surface water bodies is a major issue, and that agricultural activity is a major contributor of "causative nutrients" in 50% of

lakes and 60% of rivers whose quality has been compromised. Over the past several decades, agriculture has expanded, increasing the volume of these nutrients into the natural environment (Sutka *et al.*, 2006). Nitrate is now considered one of the most common contaminants found in groundwater (Gierczak *et al.*, 2007; Korom, 1998). Nitrate is not only hazardous to the natural ecosystems, but also to human health, where if found in drinking water at levels greater than 10 mg N L^{-1} (World Health Organization), it can lead to methemoglobinemia (blue baby syndrome) and cancer (Gierczak *et al.*, 2007).

Nitrous oxide, a byproduct of nitrogen transformations in natural and anthropogenically-impacted systems, is one of the major GHGs present in the atmosphere, with a radiative forcing effect 296 times that of CO_2 (IPCC, 2001) and a residence time in the atmosphere of up to 160 years (Zumft, 1997; Lashof and Ahuja, 1990). With increases in N fixation due in large part to agricultural practices, the quantity and availability of both ammonium (NH_4) and NO_3 for biochemical conversion to N_2O has increased (Vitousek *et al.*, 1997). The Intergovernmental Panel on Climate Change (IPCC) has suggested that approximately 30% of applied fertilizer is found in runoff and leachate from agricultural fields. Recent studies emphasize how RZs adjacent to agricultural fields can act as buffers for non-point source pollution from agricultural inputs to the stream, by transforming nitrates through biological pathways (Banaszuk *et al.*, 2005; Hill *et al.*, 2000; Cey *et al.*, 1999; Willems *et al.*, 1997; Peterjohn and Correll, 1984). One major byproduct of these pathways is commonly N_2O. So the additions of NO_3 from fertilizers in runoff and leachate, could account for up to 75% of indirect N_2O emissions (Groffman *et al.*, 2000).

1.2.2 Nitrogen Cycling in Riparian Wetlands

The nitrogen cycle is one of the most complex of the elemental cycles; N has seven oxidation states, several different mechanisms for species conversion, and experiences many transport and storage processes (Galloway *et al.*, 2004) (Figure 1). This makes examination of the cycle difficult, especially when considering the human impact. Over the past several decades, anthropogenic impacts upon the environment have lead to shifts in the N cycle (Sutka *et al.*, 2006; Vitousek *et al.*, 1997). Major activities causing these changes include fossil fuel combustion, industrial N fixation and increased fertilization, and cultivation of N-fixing crops (Vitousek *et al.*, 1997). Two out of these four are directly related to agricultural practices, suggesting that agricultural activities contribute a great deal to the total anthropogenic impact on the N cycle. The part of the N cycle experiencing the most change is N fixation (Vitousek *et al.*, 1997) (Figure 1, pathway number 1). Approximately 78% of the

Earth's atmosphere is made up of nitrogen gas (N_2), which is biologically inert (den Elzen *et al.*, 1997). Nitrogen fixation is the process by which N_2 is removed from the atmosphere and converted into ammonia (see Eq. 1, Figure 1).The reaction requires a supply of electrons and protons as well as nitrogenase enzyme complex. The enzyme is extremely sensitive to oxygen, and when exposed, becomes inactivated (Deacon, 2007).

Once nitrogen is fixed or introduced via anthropogenic pathways (like fertilizer additions), and in a viable form for bacterial consumption and conversion, it can return to its inert form via two pathways: nitrification and denitrification (Conrad, 2002) (Figure 1, pathways 4 and 5, respectively). A seminal study by Peterjohn and Correll (1984) illustrated the importance of RZs as important buffers of biologically available nutrients from agriculture. They studied nutrient inputs and transformations in an agricultural watershed over a one year period and determined that a seasonal cycle existed in which certain nutrients were released to the RZ during specific periods of time, and that many of these nutrients were stored and transformed within the RZ. The end products of both nitrification and denitrification can be N_2O or N_2 (and to a lesser extent, nitric oxide (NO)). However, geochemical conditions in the soil environment determine the end product ratio of N_2 to N_2O (Clough *et al.*, 2005; Cannavo *et al.*, 2004; Simek *et al.*, 2002). Conrad (2002) points out in his review of the experimental methods available to study these nitrogen transformations that it is experimentally difficult to separate the processes from each other because: 1) many studies are performed in nitrate-rich environments with little ammonium, 2) ammonium can be oxidized to nitrate, which can then be reduced to N_2O, and 3) heterogeneities and "hot spots" in the riparian zone soils may bias the study and lead to false results. Despite these difficulties, many researchers refer to denitrification as the main process of NO_3 removal from RZ systems, and the primary source of N_2O in terrestrial ecosystems (Hefting *et al.*, 2006; Cannavo *et al.*, 2004; Vidon and Hill, 2004; Hill *et al.*, 2000; Peterjohn and Correll, 1984). Other studies have suggested that the relative contribution of denitrification and nitrification processes to N_2O production is based upon water-filled pore space, and at certain WFPS values, nitrification dominates (ex. Bateman and Baggs, 2005).

1 Nitrogen Fixation
($N_2 + 8H^+ + 16$ ATP $\rightarrow 2NH_3 + H_2 + 16ADP + 16Pi$) (1)
(ATP and ADP are energy molecules, Pi is phosphate)

2 Ammonification/Mineralization
(organic N + microorganisms $\rightarrow NH_3/NH_4^+$) (2)

3 Immobilization

4 Nitrification
($NH_4^+ + 2O_2 + \rightarrow 2H^+ + H_2O + NO_2^- \rightarrow NO_3^-$) (3)

5 Denitrification
($NO_3^- \rightarrow NO_2^- \rightarrow NO \rightarrow N_2O \rightarrow N_2$) (4)

Figure 1. A simplified version of the nitrogen cycle (adapted from Deacon, 2007).

In the past, most of the denitrification was shown to occur in the upper, organic-rich portion of the soil column, with little activity in subsurface layers. However, recent studies have determined that denitrification is in fact occurring in the deeper layers due to groundwater movement through the RZ. Through *in situ* measurements using isotopic signatures of N and O, Cey *et al.* (1999) found that much of their site's denitrification occurred 7 m below the surface, in certain regions of their transect. Willems *et al.* (1997), in laboratory experiments, also established a high, and partially unused denitrification potential in their subsurface soils. So it remains unclear where denitrification most often takes place, and/or whether the entire soil column should be considered, or merely the top several centimeters.

1.2.2.1 Geochemical Factors Affecting Denitrification *in situ*

There are many geochemical factors affecting the denitrification process; N_2O has been found to be the dominant end product in many environments, and therefore factors affecting denitrification are those that affect the production of N_2O in the subsurface (Table 1). Antecedent weather conditions, which can control the amount of reductase enzymes required for denitrification (Dendooven *et al.*,

1996), soil redox conditions, NO_3 concentrations, temperature, and C supply (Clough *et al.*, 2005; Dhont *et al.*, 2004) have all been shown to affect the end products of this process.

Table 1. Geochemical factors affecting denitrification and N_2O production

Geochemical Factor	Relationship	Reference
NO_3-N	• $R^2 = 0.409$ ($P<0.01$) • No significant relationship	Hill *et al.*, 2000 Willems *et al.*, 1997; Walker *et al.*, 1992
NH_4-N	• Positive ($P<0.0001$)	Ashby *et al.*, 1998
pH	• Positive ($P<0.0001$) • No relationship	Ashby *et al.*, 1998 Walker *et al.*, 1992
Eh	• Positive weak correlation	Cey *et al.*, 1999
DOC	• $R^2 = 0.84$ ($P<0.001$) • Positive strong correlation • Positive relationship	Dhont *et al.*, 2004 Hill *et al.*, 2000 Willems *et al.*, 1997
WFPS	• Positive correlation	Clough *et al.*, 2005; Machefert and Dise, 2004; Ashby *et al.*, 1998
DO	• Negative weak • Negative strong ($r = 0.73$, $P<0.05$)	Cey *et al.*, 1999 Willems *et al.*, 1997

The soil system is a complex environment and it is therefore difficult to determine the most important influence on denitrification *in situ*, especially due to the interactions between variables. However, Clough *et al.* (2005), in a review article, found that in sandy soils, water-filled pore space (WFPS) was one of the most important controls on N_2O production and concentration, even more so than available carbon or nitrogen substrate. Anaerobic conditions can be reached at a WFPS of 75-85% (Cannavo, *et al.*, 2005; Machefert *et al.*, 2002), and reducing environments develop in anaerobic conditions. Cey *et al.* (1999) determined that the optimum redox potential for denitrification occurred at an Eh of approximately 200 mV. Clays and small particle-sized soils were found to accommodate N_2O production at rates three times greater than those of sandy soils (Chantigny *et al.*, 2002). Anaerobic conditions are more easily attained in clay soils, because they hold onto soil moisture, a controlling factor in gas and solute transport (Cannavo *et al.*, 2004). Oxygen content must be low for the soil atmosphere to reach a state of anaerobiosis. Chantigny *et al.* (2002) found that when O_2 content in the soil dropped below 6%, N_2O accumulation reached a maximum, suggesting denitrification activity had peaked. Hill *et al.* (2000) found a strong linear correlation between dissolved oxygen (DO) content and NO_3-N concentration, which corresponds to the relationship

found by Cey *et al.* (1999). As oxygen in the soil pores and soil water is used up by respiring bacteria, denitrifiers switch to NO_3 as a terminal electron acceptor in the denitrification process (Gierczak *et al.*, 2007).

Hotspots are defined as "patches" that exhibit significantly higher reaction rates than areas surrounding it, and hot moments as periods of time in which reaction rates are significantly higher than in intervening time (McClain *et al.*, 2003). Hot spots and moments can occur when hydrologic flow paths carrying complementary nutrients converge, when a flow path carrying nutrients interacts with zones of high organic matter and other conditions suitable for biological cycling (McClain *et al.*, 2003; Hill *et al.*, 2000; Hedin *et al.*, 1996) (Figure 2), and/or at the interface between ecosystem "compartments" (McClain *et al.*, 2003). Hot moments can occur as a result of disturbance, natural or anthropogenic (McClain *et al.*, 2003). These can occur for denitrification activity in the subsurface where some areas the main environmental factors that encourage N_2O production.

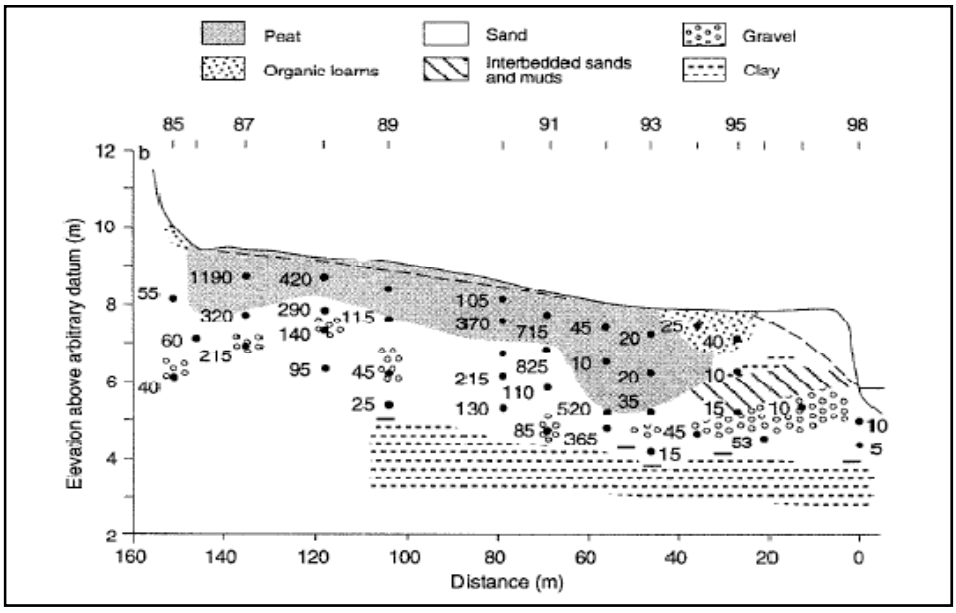

Figure 2. N_2O-N concentrations (μg L^{-1}) across a soil profile transect. High N_2O concentrations are indicative of denitrification activity, which can occur several metres below the surface.

1.3 Nitrous Oxide Emissions from Riparian Zones

Nitrous oxide is the byproduct of denitrification and nitrification, and is more readily produced under certain conditions (see above). Agricultural and forest soils were studied largely in attempts to model GHGs and global budgets (ex. Butterbach-Bahl *et al.*, 2004; Hosen *et al.*, 2000; Mosier *et al.*, 1996). Adjacent riparian zones received less attention in the literature, despite maintaining conditions

conducive for enhanced N_2O production and emissions (Groffman *et al.*, 2000). Of greatest importance to the GHG community, are accurate predictions and a good understanding of N_2O production in various landscapes for use in models. The IPCC developed protocols for estimating N_2O release from industrial, agricultural and natural systems, but did not specifically account for riparian areas in their estimates (IPCC, 2001; Groffman *et al.*, 2000). To fill this knowledge gap, studies are required to increase our understanding of N_2O dynamics in these specific landscapes.

Table 2 is a collection of some of the research that has been completed in riparian zones and forested wetlands, as well as in non-agriculturally impacted forests for comparison. Typical fluxes from riparian areas ranged from < 0.1 – 4 nmol m^{-2} s^{-1}, with fluxes from temperate forests generally smaller in magnitude than agriculturally-impacted ecosystems, as expected (Skiba *et al.*, 1999).

Table 2. Typical fluxes from riparian zones and forested wetlands, and natural forests.

Location	Ecosystem	N_2O Flux (nmol m^{-2} s^{-1})	Source
Netherlands	Forested Riparian Zone	0.5 – 4.0	Hefting *et al.*, 2003
Europe (n = 3)	Riparian Zones and Forested Wetlands	0.05 – 2.76	Machefert *et al.*, 2002
Louisiana, USA	Coastal Riparian Zone	0.05 (mean)	Yu *et al.*, 2008
Brittany, France	Forested Riparian Zone	3.73 (mean)	Clement *et al.*, 2002
Saxony, Germany	Forest	0.01 – 0.71	Butterbach-Bahl *et al.*, 2000

1.3.1 Heterogeneity and the Occurrence of Hot Spots in Riparian Zones

Greenhouse gas fluxes to the atmosphere are a result of processes occurring in the subsurface. In order for these gases to reach the surface, they must be transported vertically. The flux of a gas towards the surface (at the surface-atmosphere interface) is the sum of advective and diffusive fluxes (Clough *et al.*, 2005; Livingston and Hutchinson, 1995). Fick's Law describes the diffusion of solutes in water through porous media, across a concentration gradient (Fetter, 1999; Livingston and Hutchinson, 1995). It is generally used for dissolved solutes, however can be adapted to express the diffusion of soil gases through the unsaturated zone (Fetter, 1999). The basic equation is as follows:

$$J = -D_s^* \partial C/\partial z \quad (5)$$

where J ($M\ L^{-2}\ T^{-1}$) is the mass flux of the solute, D_s^* ($L^2\ T^{-1}$) is the soil gas diffusion coefficient (a function of the tortuosity and water-filled pore space of the soil in question) and $\partial C/\partial z$ ($M\ L^{-2}$) is the concentration gradient of the solute in question. According to Graham's law, the effusion rate of a gas is inversely proportional to the square root of its molecular mass (Clough *et al.*, 2005). Advective transport is based on the difference of pressure between soil air and the overlying atmosphere, which is impacted by moisture, temperature and wind at the surface (Livingston and Hutchinson, 1995). When permeability is low, in soils such as silts and clays, molecular diffusion is the dominant gas transfer process (Livingston and Hutchinson, 1995). As permeability and tortuosity are so important to gas transport in the subsurface, changing moisture conditions, which can have significant impacts on these variables, would also affect gas transfer from zones of production towards the surface-atmosphere interface. This will also impact the development of microsites, contributing to heterogeneity.

Heterogeneity is often observed in natural systems, especially those maintaining variable moisture conditions and seasonally changing hydrology. It can be caused by many factors, often compounding, and therefore difficult to sift out. In a heterogeneous natural system, with multiple inputs of nutrients and hydrologic flow paths, "hot spots" and "hot moments" can be observed in anoxic microsites of the soil column (Hill *et al.*, 2000; Peterjohn and Correll, 1984), at the interfaces between the field and the riparian zone (Lowrance, 1992), and/or the riparian zone and the SE (Hedin *et al.*, 1996). Hot moments can arise with the input of nutrients after spring melt, as a result of flooding, or during the wetting up period after a drought. Riparian zones themselves have also been thought of as "hot spots" in the larger watershed ecosystem (Groffman *et al.*, 2000). The microbiological and hydrological heterogeneity, often caused by hotspot developments in these natural systems, make it difficult to predict the fate of non-point source pollution (Balestrini *et al*., 2007), therefore leading to difficulties in predicting the general dynamics of N_2O in these systems. Hotspots result, in part, from heterogeneity of physical soil characteristics and moisture variability, and according to most climate change predictions, moisture and temperature conditions will change. This will lead to changes in soil moisture dynamics, and therefore production and movement of subsurface gases like N_2O are likely to be altered. There is a need to understand *in situ* transformations of nitrogen in the soil profile, and resulting chemistry thereof. More research studies in riparian environments can only help to enhance our understanding of nitrogen dynamics and the consequential release of N_2O.

1.3.2 The Influence of Topography on Nitrous Oxide in Riparian Zones

Riparian zones are often characterized by a sloped topography, with the highest elevation closest to the field edge, decreasing towards the stream, especially in Southern Ontario. Several researchers have examined the effects of topography upon N_2O emissions due to the influence of topographic sequence on controlling variables such as moisture and nutrient supply. Highest emissions and denitrification rates have been found at the lower landforms (footslopes) and poorly drained soils (Ashby *et al.*, 1998; van Kessel *et al.*, 1993) as N_2O emissions are affected by the pooling of organic matter and soil moisture resulting from of slope geometry (Florinsky *et al.*, 2004). So sites lying in concave portions of a slope, or in depressions, might maintain conditions more suitable for N_2O production and emission. Clement *et al.* (2002) also emphasized the importance of topography as a controlling variable for denitrification activity (and therefore N_2O production), and concluded that at the upland-wetland border specifically (i.e. where the water table is deeper below the surface), denitrification in the entire soil profile should be considered as opposed to just the upper horizon, which has normally been the case.

1.3.3 Nitrous Oxide Studies

Greenhouse gas experiments, and especially those based upon N_2O, have most commonly featured three main datasets, including fluxes (static chamber method), nutrient concentrations (namely NO_3/NH_4, DOC) and cycling, and hydrophysicochemical parameters (such as soil moisture and temperature) (Whalen, 2000; Ashby *et al.*, 1998; Lemke *et al.*, 1998). In addition to these measurements, denitrification, mineralization and nitrification rates are also often examined, especially in order to determine the dominant production mechanism of the N_2O produced (ex. Cannavo *et al.*, 2004; van Kessel *et al.*, 1993; Robertson and Tiedje, 1987); denitrification is often the main variable of interest (ex. Hanson *et al.*, 1994a; Groffman and Tiedje, 1988). Many studies have suggested a rapid reduction (or reduction potential) of NO_3 to N_2O in the shallow groundwater, but an understanding of the movement of this N_2O to surface emissions is still lacking in the literature (Well *et al.*, 2001). Also, many of these studies employ laboratory techniques, but stress the importance of understanding processes and interactions *in situ*.

Muller *et al.* (2004) performed a study on N_2O production in a temperate grassland, examining gas emissions, NO_3 concentrations, and a somewhat novel dataset of soil profile N_2O concentrations, in order to identify production processes that were dominant (i.e. denitrification, nitrification, nitrifier denitrification, etc); this was a fairly complete set of data. However, most studies on N_2O emissions

include hydrophysicochemical parameters plus *either* surface fluxes and nutrients, or surface fluxes and subsurface gas concentrations (ex. Yu *et al.*, 2006); the latter are found in much smaller numbers. Few studies contain a dataset of surface emissions, groundwater nutrients *and* subsurface gas concentrations. This research project is one of the first studies to incorporate all three datasets (nutrients, subsurface gases and surface emissions), in addition to hydrogeochemical variables, in order to examine the effects of nutrient supply and the physical environment on surface fluxes.

Chapter 2

Study Site and Methods

2.1 Experimental Design and Methods

In order to explore differences in N_2O production spatially across the riparian zone, a detailed study was carried out during the 2007 growing season, exploring both subsurface concentrations and surface-atmosphere fluxes of N_2O, and the hydrochemical environment at each of four topographic positions on two separate portions of the riparian zone. Two intensive transects were selected for study, one ending at the Spencer Creek, and the other into the Beverly Swamp (T4), where the stream disappears beneath the peat (T5) (Warren *et al.*, 2001). Four distinct positions along the riparian zone's topographic gradient were delineated and used for sampling: Field Edge (FE), Riparian Level (RL), Riparian Slope (RS), and Stream Edge (SE). Transect 5 has a gradient of approximately 7%, significantly greater than T4 (0.5%), which is largely flat and poorly drained (Figure 3). The upland zones of both transects border the agricultural FE. The mid-riparian zones (namely the RS and RL

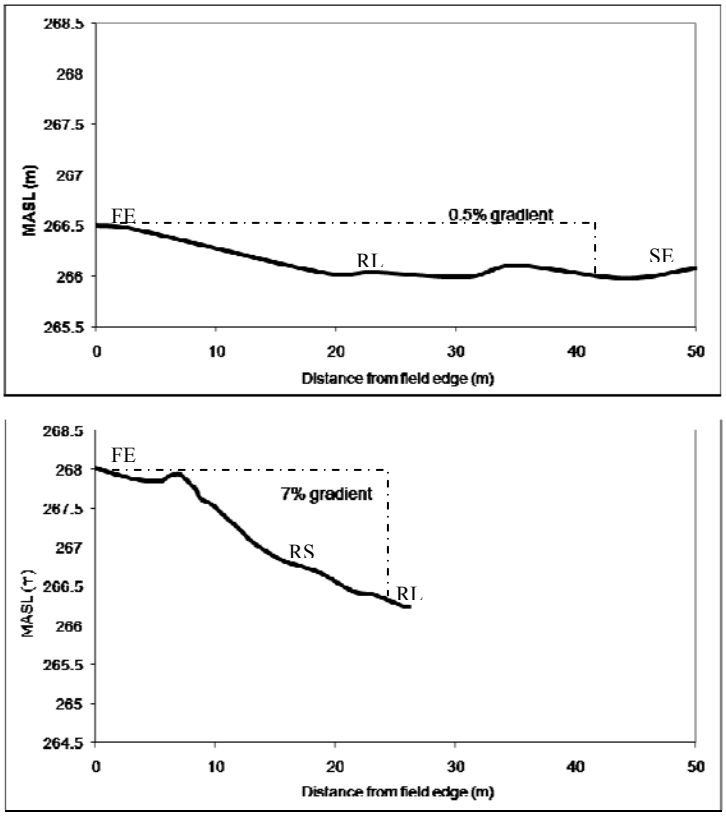

Figure 3. Ground level surface along T4 and T5. Study sites (positions) are marked along each transect.

positions) are different between transects. Affected by stream mediation and artificial flooding, the RL of T4 is in a zone of high surface moisture and groundwater flux as well as in a slight depression in the transect topography. The mid riparian zone on T5 (RS) is on the concave portion of the downward slope.

Along each transect, three sites have been established, each of which contain: one greenhouse gas depth profiler, one thermocouple temperature profiler, three greenhouse gas flux collars, six piezometers, one well, and TDR probes. Both gas and temperature profilers and the six piezometers were installed to depths of 15, 30, 50, 75, 100 and 150cm below the surface (Figure 4).

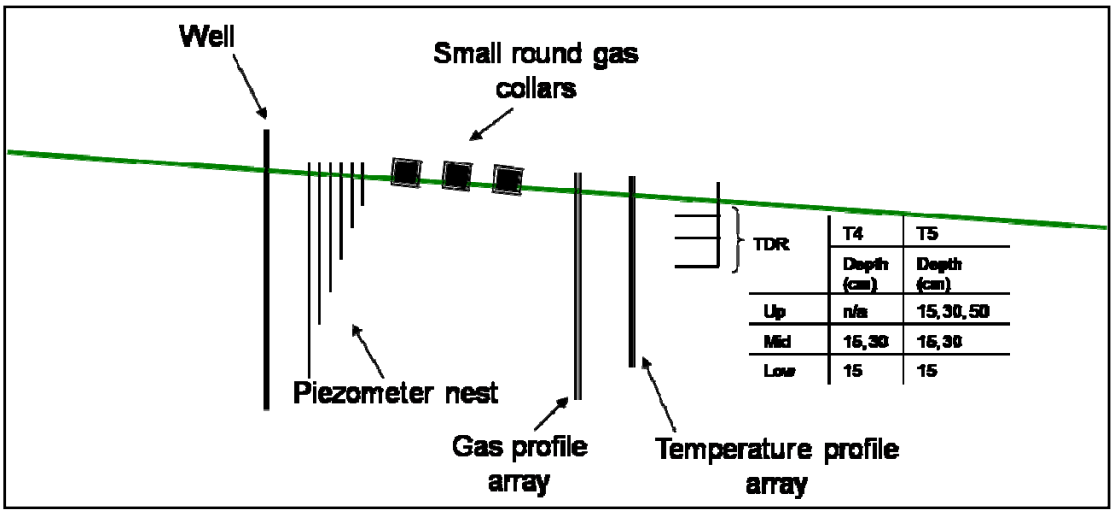

Figure 4. Experimental setup. Each site along transects 4 and 5 were instrumented with a well, piezometer nest, gas and temperature profilers, gas collars and TDR probes.

Sampling was carried out over 12 dates during the growing season of 2007, between June and November. The objective was to sample during periods of baseflow as well as during changing hydrologic conditions – namely before and after rain events. As weather conditions are difficult to predict, before and after rainfall event sampling was carried out on only two occasions. The rest of the sampling events occurred after precipitation events or during baseflow and one sampling event during the annual flood caused by releasing water from the reservoir upstream in preparation for winter.

During each event, a suite of samples and measurements were always taken: soil gas samples, GHG fluxes, water table depth, hydraulic head, DO, nitrogen chemistry, temperature profiles, and TDR probes. The entire sampling event took approximately 8 hours to complete, and was done in the same sequence on each occasion.

2.2 Study Site

The Beverly Swamp is located in Southern Ontario, approximately 40 km northwest of Hamilton, Ontario (43° 22'N, 80° 07'W), and is approximately 2324 ha in size (Heagy, 1993). The swamp is located in the Flamborough Plain physiographic region (Heagy, 1993), in two dolomitic depressions (Young, 2001). Bedrock is thought to be shallow, consisting of approximately 40 m of Guelph formation dolostone under the majority of the swamp's area (Heagy, 1995). Bedrock is overlain with glacial till (1-6 m) and then 0.5 to 1 m of marl, over which up to 1.5 m of peat has developed (Young, 2001; Heagy, 1995). The average pH of the swamp's soil and surface water falls between 7.5 and 8.5 due to the carbonate bedrock (Galloway and Branfireun, 2004). The larger extent of the swamp maintains an elevation above sea level between 265 and 270 m (Woo, 1979).

The Valens Riparian Research Group (VaRRG) study site is located in the north western corner of the Beverly Swamp (Figure 5). The site sits on the outskirts of the swamp, bordering the John Mount farm, in a forested riparian wetland. The stream adjacent to this riparian zone, Spencer Creek, is a second order stream, and runs through the Beverly Swamp. It is controlled by the Valens dam and reservoir 1 km north of the VaRRG site. The area is within the Spencer Creek watershed, which primarily drains agricultural land. The Beverly Swamp area has been used by various research teams since the 1970s, however much of that research has taken place within the swamp proper (ex. Galloway and Branfireun, 2005; Kaufman *et al.*, 2005; Warren *et al.*, 2001; Woo and Valverde, 1981).

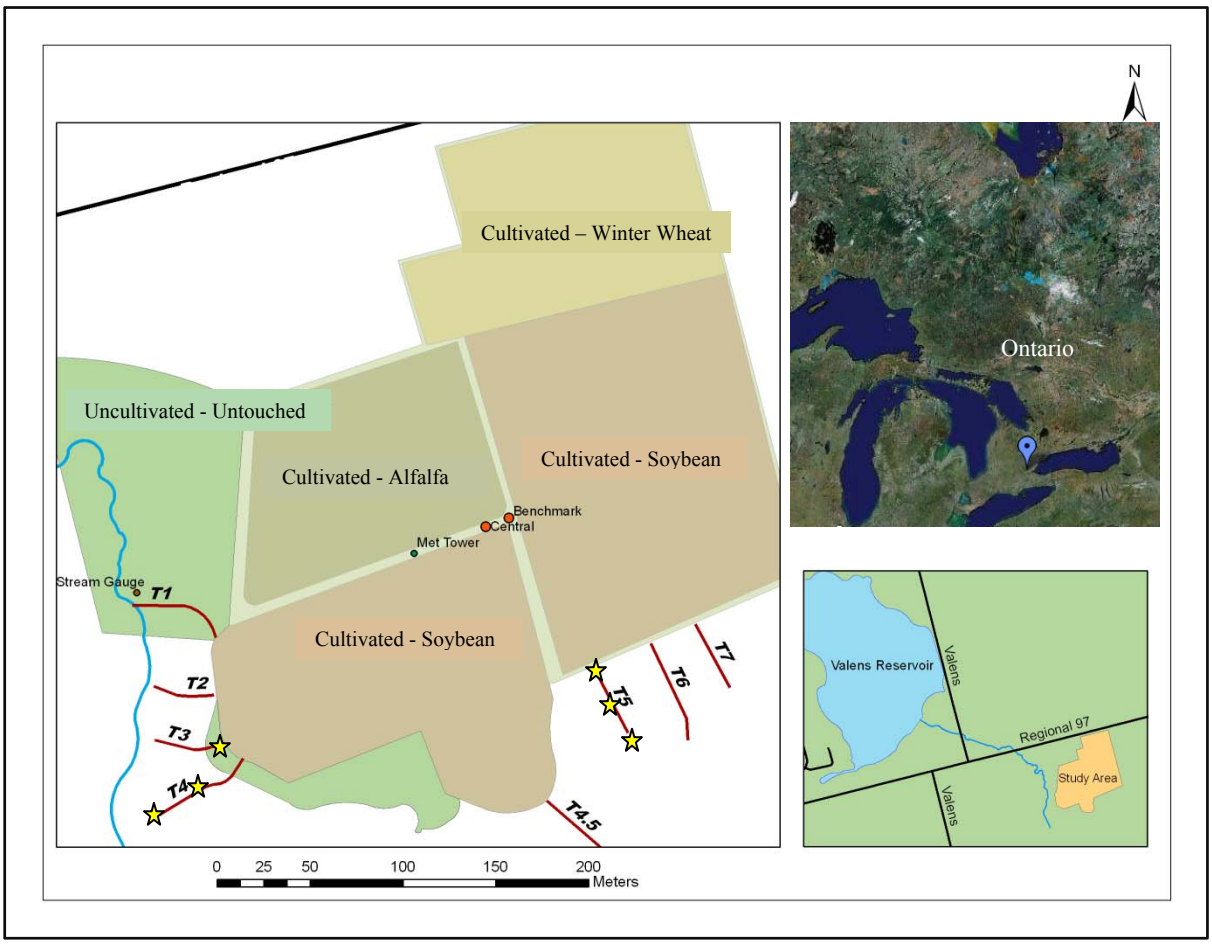

Figure 5. Valens Riparian Research Site (VaRRG). Two transects were used for this study's data collection sites, each with three sets of instrumentation: T4 running perpendicular to the south-west field, and T5, running perpendicular to the south-east field. The met tower was used for site meteorological data, and the "central" and "benchmark" points were used for site surveys.

2.2.1 Vegetation Survey

A recently conducted vegetation survey revealed a dominance of broadleaf deciduous trees with a mean canopy basal area of 17 m^2 ha^{-1}. It is primarily composed of large Silver Maple (*Acer saccharinum L.*), with a relative dominance of 96%, Black Ash (*Fraxinus nigra* Marsh.), White Elm (*Ulmus americana* L.), Eastern White Cedar (*Thuja occidentalis* L.), and Speckled Alder (*Alnus incana*). The area is also sporadically scattered with Red Ash (*Fraxinus pennsylvanica* Marsh.), Trembling Aspen (*Populus tremuloides* Michx.), and Ironwood (*Ostrya virginiana*). The patchy subcanopy includes small trees and shrubs including Choke Cherry (*Prunus virginiana* L.), Elderberry (*Sambucus canadensis* L.), Sweet Viburnum (*Viburnum lentago* L.), and Common Buckthorn (*Rhamnus cathartica* L.). The understory vegetation is diverse whereby the field edge is dominated by grasses and herbaceous flora such as Goldenrod (*Solidago* spp.) and Aster (*Aster* spp.),

and in places, there is dense covered by Ostrich Fern (*Matteuccia struthiopteris*). The understory in riparian wetland consists primarily of Jewelweed (*Impatiens capensis*), Tall Meadow Rue (*halictrum polygamum*), Virginia Creeper (*Parthenocissus quinquefolia*), Marsh Merigold (*Caltha palustris*), Dewberry (*Rubus flagellaris*), nettles (e.g. *Laportea Canadensis* and various *Urtica* spp.), violets (*viola* spp.), ferns (predominantly *Onoclea sensibilis*, and *Dryopteris* spp.), sedges (*Carex* spp., especially *Carex comosa*) and some Reedcanary Grass (*Phalaris arundinacea*). An array of aquatic grasses (e.g. *Scirpus* spp.), Smartweeds (*Polygonum* spp.), and native loosestrifes (e.g. *Lysimachia ciliate* and *Lysimachia thyrsiflora*) are also found thriving within 1 m from the stream edge.

2.2.2 Climate and Hydrology

Climate in the Beverly Swamp area is classified as humid continental (Warren *et al.*, 2001). Historic annual rainfall is approximately 787 mm; annual snowfall is 127cm. Average annual temperature is 7˚C. During the study period, from May to November of 2007, total rainfall reached 263 mm and the average temperature was 14.8 ºC (Table 3). The 2007 field season was abnormally dry. An examination of climate normals for the area reveals a discrepancy in monthly precipitation between the field season and the 30-year averages, as well as with monthly temperatures (Table 3). The average temperature, from May to November was one degree warmer in 2007 than for climate normals, and total precipitation for that same period yielded less than half of what is expected. Runoff and precipitation are the main sources of water to the swamp, with a minimal amount of lateral groundwater movement (Heagy, 1993).

Hydrologic data collected during the 2006 field season by Zhang (2007) at this site suggested a slow moving system with low hydraulic conductivities. The dominant direction of groundwater flow was laterally through the riparian zone, from T1 to T4 (Figure 6). Although water flowed from the FE to the SE (or lowland), in the south-east direction, flow was oblique throughout the riparian zone. This pattern was shown to be reversed on some occasions during the 2007 field season, with groundwater traveling from the lowland areas towards the upland, specifically during DOYs 220, 238 and 255 of this study. These dates correspond to the driest part of the summer. Hydrological study of this riparian zone was not within the scope of this project, however some data were collected during each sampling event, specifically hydraulic heads.

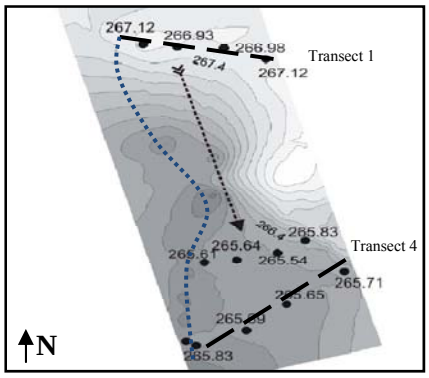

Figure 6. Plan view of shallow groundwater flow direction. Dotted line is the stream, dashed lines represent transects. (adapted from Zhang, 2007)

Table 3. Climate normals for the Galt Region, 17 km from the VaRRG field site. Recorded values collected during the 2007 field season.

Climate Normals from Cambridge Galt MOE								(1971 to 2000)
	May	June	July	Aug	Sept	Oct	Nov	Total Precip and Average Temp
Daily Avg T	13.1	17.7	20.5	19.5	14.8	8.3	2.8	13.8
Rainfall (mm)	83.9	74.5	95.2	89.7	87.4	71.8	74.4	576.9
Snowfall (cm)	0	0	0	0	0	0.6	7.7	8.3
Recorded Values for VaRRG SITE *2007*								
	May	June	July	Aug	Sept	Oct	Nov	Total Precip and Average Temp
Daily Avg T	14.3	19.5	19.4	20.1	16.0	12.5	2.1	14.9
Rainfall (mm)	39.4	24	26.6	31.4	22.2	71.4	47.8	262.8

2.2.3 Soil Properties and Characteristics

Soil pits (0.75 x 0.75 m) were dug at the site for this study in order to better characterize the soil structure along each sampling transect. Ten cm long soil cores could be taken for bulk density, porosity, loss on ignition (LOI), and textural analysis measurements. The soil cores were brought back to the lab where they were weighed at "field moist" conditions prior to being saturated from

below for at least 24 hours. Saturation masses (Ms) were recorded and then the cores were dried at 105˚C for 12-24 hours and weighed again (Md). A subsample of each core was removed and crushed using a mortar and pestle to allow for disaggregation of particles for textural analysis using the hydrometer method. Another subsample was used for LOI analysis, in which a small mass (Mb) of sample was put into a muffle furnace at 500˚C to burn off organic matter, and weighed (Ma). The following equations were used (except textural):

$$\text{Bulk Density } (g/cm^3) = Md / \text{Core Volume} \quad (6)$$

$$\text{Porosity } (\%) = (Ms-Md) / \text{Core Volume} * 100 \quad (7)$$

$$\text{LOI } (\%) = (Mb-Ma) / Mb * 100 \quad (8)$$

Textural analysis for grain size distribution was carried out via the hydrometer method. A known volume of sample was mixed into a 1 L graduated cylinder of distilled water for 30 seconds to 1 min before it was left to settle. The hydrometer was put into the graduated cylinder and values were read from the meniscus of the water surrounding the head of the hydrometer. Measurements were taken every 30 seconds for the first 3-5 minutes, and then every few minutes (depending on the sample) for 30-45 minutes. Once the hydrometer movement slowed down, measurements were taken once per hour until the value remained the same for 2 measurements. Results were recorded in a spreadsheet – sample calculations can be seen in Appendix 1.

At the VaRRG site, on average, the top 50cm of the soil profile is organic, underlain by marl, sand, clay, silt and gravel (Galloway and Branfireun, 2004). The marl layer beneath the study site is thin (Warren *et al.*, 2001), and may act as a confining layer for groundwater movement, causing a perched water table under normal conditions (Woo, 1979). Along the edge of the swamp, elevation above sea level is approximately 268 m, and changes no more than 2 m from the field edge to the stream. An examination of soil pits dug for this study within 10 m of each sampling site revealed subsurface characteristics unavailable through non-invasive means, and expressed here as an enhancement to the information from previous studies. The site's soil properties are characterized by increasing bulk density and decreasing porosity with depth into the soil profile (Table 4). Porosity increases towards the lowland along both transects, while bulk density decreases at the lowland, suggesting high organic content, and perhaps a layer of low density peat. Transect 4 can be characterized by increasing depth of an A horizon with distance from the FE, underlain by loamy, mineral soils. The A horizon at the FE is approximate 25 cm deep, increasing to 30 cm at the RL, and becoming more peaty (organic layer) and deeper (up to 90 cm) at the lowland SE. Iron oxide and sand lenses were visible 10 – 90 cm deep in the mid riparian zone, indicative of a fluctuating water table with periods of both anoxic and

aerobic conditions (Mitsch and Gosselink, 2007). A similar depth increase in the A horizon with distance from the FE was present along T5, however less organic material was present along this transect than along T4. Underlying the A horizon along T5 was an orange-coloured mineral sand layer. Large macropores were present throughout the FE profile. In the lowland riparian level, a shallow 50 cm layer of peaty, rooted matrix was present above a layer of dense clay, along with a 2-3 cm layer of a marl.

Table 4. Physical soil properties and extractable nutrient supplies.

Position	Depth	Bulk Density (g/cm3)		Porosity (%)		Organic Content (%)		C:N ratios		Extractable NO3-N (ug/g)		Soil Type	
		T4	T5	T4	T5	T4	T5	T4	T5	T4	T5	T4	T5
Upland	15	0.27	0.82	49.67	40.27	42.4	6.9	12.74	9.63	5.03	2.69		
	30	1.20	1.01	31.34	31.78	1.8	6.5	10.53	10.48	6.71	4.89		Silt Loam
	50	1.04	1.04	24.90	32.31	1.4	6.1	9.82		1.91			Loam
	75	1.03	1.39	31.82	25.30	1.2						Loamy sand	
	100	1.32	1.13	35.15	26.65	1.7						Sandy loam	
Mid-RZ	15	0.27	0.49	54.20	38.50	39.4		10.99	8.50	1.27	2.55		
	30	0.95	0.79	40.09	32.93	5.6		8.63	10.56	1.27	1.33		
	50	1.29	1.29	29.83	26.22	2.4		7.01	8.46	0.61	1.53		
	75	no data	1.42	no data	27.26	No data		13.13		0.51			
	100	0.40	1.51	17.88	27.42	8.7		9.23		0.43		Silt loam	
Low-land	15	0.29	0.16	50.91	65.17	33.9	54.6	13.87	13.31	7.41	2.87		
	30	0.32	0.13	61.37	68.54	32.2	86.0	14.57	14.41	3.73	2.95		
	50	0.34	0.42	59.39	55.14	25.7	13.7	15.34	15.19	1.62	0.75	Sandy loam	Loam
	75	0.49	1.36	53.72	26.25	22.2	1.6	16.85	24.41	1.30	0.67		Silt Loam
	100	0.65	No data	44.29	no data	11.0	no data	11.38	23.07	0.73	0.48	Sandy loam	

2.2.4 Gas Flux Collection and Analysis

Nitrous oxide fluxes were collected using the non-steady state, closed vented chamber technique (Hutchinson and Mosier, 1981), with a 5 x 18cm cylindrical chamber (approximately 4L volume), equipped with a sampling tube and a gas vent. Samples were collected at ten minute intervals for at total of thirty minutes, and were preserved in evacuated 12 ml Exetainers® containing desiccant. Chambers were lowered onto pre-installed (permanent) collars. All collars were regularly clipped of vegetation, so that the data collected represented soil and not vegetation processes. At the time of each sampling period, collar volumes were measured so that the total volume of the collar + chamber system was adjusted for present conditions. Samples were collected with a syringe equipped with a 3-way stopcock, and a needle tip. Air was sucked out of the chamber and then stopcock was turned off

towards the chamber and opened towards the syringe needle tip. The tips were purged with sample air until 20 ml remained inside the syringe. The syringe tip was then inserted into the Exetainer® septum. Because the Exetainers® were evacuated, approximately 10 ml of air from the syringe was sucked in. The remaining 10 ml was manually pushed in to over pressurize the container. Once all samples were collected, Exetainers® were brought to the Canada Centre for Inland Waters (CCIW) where they were analyzed with an SRI Model 8610C gas chromatograph (GC) equipped with an electron capture detector. The samples are manually injected and pass through a pre-column, with the primary objective of isolating undesired gases (ex. O_2) from the N_2O. The gas then travels through the 2 m x 3.2 m OD analytical column, packed with Hayesep D. The carrier gas used is Helium at 30 psi. Concentrations for each sample are derived from peak areas as determined using the Peak Simple software package by comparison to average daily response factors obtained by running a calibration standard every 12th injection. The slope of the concentration gradient from beginning of the run (ambient) to the end represented the flux of gas from the soil (see sample calculations in Appendix 1). These flux values were corrected for ambient temperature and barometric pressure. The detection limit for N_2O sample analysis was 0.017 uL L^{-1}.

2.2.5 Gas Profiler Production, Sampling and Analysis

The gas profile arrays were created using 1 inch in diameter silicone tubing, shown to be gas-permeable for methane, carbon dioxide and nitrous oxide gases (Kammann *et al.*, 2001). The tubing was cut into desired lengths so that four 15 cm and two 10 cm lengths were used for each profiler array. Using silicone septa and silicone adhesive, one end of the tubing chamber was completely sealed. The other end was sealed with a septum that had been pierced by a length of stainless steel tubing (1/16”), fixed in Swagelok® fittings on either side of the septum, and also sealed with adhesive silicone. This setup was used to collect the gas sample from the silicone chamber. Once all tubing chambers were completed, they were left for 24 hours to cure the adhesive silicone, and each was tested for air and water leaks by collapsing and over-pressuring the chambers in water. After testing was completed, the silicone chambers with their tubing were inserted into a 1 inch PVC pipe, which had been previously perforated at the desired depths to allow for subsurface air exchange with the silicone chambers. The silicone chambers were inserted to depths of 15, 30, 50, 75, 100 and 150cm below the surface. The steel tubing pieces at the top of the apparatus were outfitted with Swagelok® and syringe fittings to allow for above-surface sample collection. Expandable foam was pumped into the empty spaces between each of the silicone chambers to isolate each one from its nearest neighbour (Figure 7).

Figure 7. Gas Profiler Apparatus. Profilers were made from silicone tubing and PVC pipes, along with stainless steel tubing and swagelock fittings. Six ndividual profilers were made to be installed at each of the six sites used in this study.

A 1 inch auger was used to prepare a hole down to 150 cm so that the gas profile samplers could be installed. Careful attention was paid to the diameter of the hole so that a high degree of contact could be maintained between the surrounding soil and the gas profile apparatus. Once dug, the profilers were inserted (often with difficulty) and left to equilibrate for at least one week in the subsurface before sampling.

Gas profilers were sampled using a syringe with a 3-way stopcock attachment and a syringe tip (see gas flux collection method). Thirty ml of air was pulled out of the 15 cm long chambers (those occupying depths of 50 to 150 cm below the surface) and 25 ml of air was pulled out of the 10 cm long chambers (occupying the 15 and 30 cm depths below the surface). All samples were returned to CCIW and analyzed by GC. The detection limit for N_2O sample GC analysis for the profile samples was 0.034 uL L^{-1}; all samples were at least 4 times the detection limit.

2.2.6 Water and Soil Chemistry Sampling and Analysis

Piezometers were made from 1" PVC pipes that were cut to the proper dimensions and capped on the bottom. The sampling zones were drilled and protected by two layers of polyester window screen secured by electrical tape. Each of the 15 and 30 cm piezometers have sample lengths of 10 cm, while the rest have lengths of 15 cm, and reservoirs of 5 cm. A piezometer's sampling depth was defined

from the ground surface to the midpoint of the screened zone. The piezometers were carefully placed into pre-augered holes in much the same way as the gas profile samplers.

Water samples were collected using a peristaltic pump and silicone tubing. Due to the low hydraulic conductivities of the soils and deep water table at this site, sample was often limited. For this reason, only a small volume was pumped out of the tubing as a rinse before sampling. Following this, HDPE bottles were used to collect as much water as possible from each of the piezometers. On most occasions, only the lowland sites produced water from all piezometer depths. All samples were stored in a cooler with ice packs until returned to the lab, where they were stored in a fridge overnight before processing.

Analysis of water samples was carried out in the laboratory the day after sample collection. Samples were filtered through a 0.45 μm cellulose acetate filter to be analyzed for NO_3 and NH_4. These samples were analyzed with a continuous flow analysis system on a Bran+Luebbe AutoAnalyzer3 (AAIII), with a phototube colorimeter detection system (5 mm flow cell). Samples were pumped at 0.23 ml min^{-1} through the system. Nitrate was reduced to nitrite by hydrazine in an alkaline solution with a copper catalyst, followed by a colour reaction with sulphanimide and NEDD, which was measured at 520 nm. For NH_4 analysis, salicylate chemistry was used to produce a blue coloured solution measured at 660 nm. The detection limit for NO_3 was 0.5 mg-N L^{-1}, and 0.05 mg-N L^{-1} for NH_4. Remaining sample water was filtered through a 0.4 μm glass fiber filter (Macherey-Nagel, GF5) for dissolved organic carbon (DOC) an Apollo 9000 carbon analyzer at 800 ºC.

Soil samples for total C and N analysis were sent to the Earth Sciences Department at the University of Waterloo for analysis. Prior to sample submission, soils were "acid washed" to release inorganic carbon sources (carbonates). Samples were poured into test tubes sitting in a warm water bath. One molar hydrochloric acid (HCl) was poured into each test tube and left over night. Acid was decanted and samples were washed with deionized (DI) water 2-3 times a day until a solution pH of 6 was attained, a level that approximates equilibration with atmospheric CO_2. Samples were run for Nitrogen and Carbon analysis on an Isochrom Continuous Flow Stable Isotope Mass Spectrometer (Micromass) coupled to a Carla Erba Elemental Analyzer (CHNS-O EA1108).

Dissolved oxygen measurements were taken at the same time as hydrology measurements, using a Model 5740 DO probe connected to a YSI Model 57 meter (Yellow Springs Instrument Co., Yellow Springs, OH). To minimize the effects of atmospheric oxygen changing DO levels of water in the piezometers, the probe was always carefully lowered to the bottom of the piezometer and then raised

by 1-2 cm to take the reading (recorded in mg L^{-1}) while slowly moving the probe vertically up and down while taking the reading. However, these measurements must be taken with some caution: due to water limitations, a closed flow-cell was not created. Piezometers were capped, but potentially open to the atmosphere. In addition, because the water table was often deeper than many of the piezometers, and as a result of a large probe, not all piezometers were measured at each sampling event.

2.2.7 Environmental Variables and Hydrology

Soil temperature and moisture were both measured during each sampling event. Temperature profilers were used to measure real-time temperature below the surface at 15, 30, 50, 75 and 100 cm deep. These were made using 1" wooden dowels, with 1/8" holes at each of the required depths. Type T (Copper-Constantan) thermocouple wire was used. Two cm was stripped off the end of each wire length and the copper and constantan wires were twisted tightly together. The twisted ends were then put through the holes in the dowel and 5 min epoxy was used to fill the holes and keep the wires protected from subsurface water. The other ends of the wires were run up the dowel to be exposed at the surface. Surface wires were outfitted with plugs that fit into a hand-held device to measure temperature with an accuracy of 0.01˚C.

Temperature was also measured at a 5 cm depth beside each GHG collar. Moisture measurements were collected at the same locations using a Delta-T theta probe, which integrates over the top 6 cm of soil. Volumetric water content and water-filled pore space (WFPS) were determined from those readings via a calibration study performed in the laboratory at the Canada Centre for Inland Waters (sample calibration values and calculations available in Appendix 1).

A centrally-located Hobo Weather Station (Onset Computer Inc.) at the site has been recording wind speed, wind direction, air temperature, relative humidity, rainfall, total solar radiation, photosynthetically active radiation (PAR) and station pressure logged at 15 minute intervals since 2003. The data collected was used to compare seasonal climate variables, namely precipitation and temperature, to climate normals for the area. Barometric pressure from the weather station was used to calculate water table elevations using Hobo water level recorders at the stream's stilling well (located upstream of T4), two upland wells and two lowland wells, also logged at 15 minute intervals.

Water table elevations and hydraulic head were measured during every sampling event. Electronic water tape (Mr. Beep) was used to measure depth to water level from the top of the piezometer tube. "Stick-up", or depth from ground surface to top of piezometer, was measured on several occasions

throughout the study period in order to calculate the hydraulic head from the ground to the water surface. These measurements were augmented by a survey of the site completed by a Technical Operations crew from Environment Canada (CCIW).

2.2.8 Intra-Site Variability and the Impact of a Rainfall Event on Nitrous Oxide

It has been recorded that intra-site variability in surface-atmosphere GHG fluxes can be very high, and may dwarf extra-site variability (Foloronuso and Rolston, 1984). Such variability was noted in many of the sites studied along T4 and T5 during the 2007 study period. Questions that arose from these data include: 1) how can we minimize detection of spatial heterogeneity within small areas; 2) would a larger chamber, covering a greater surface area, demonstrate significantly different fluxes than an average of the three small chambers; 3) is there one small chamber that might be more representative of a larger surface area (i.e. compare well with the large chamber)? These questions were answered in an experiment that tested the fluxes derived from the three small collars used for this thesis, compared to one large collar equal to 2.4 times the surface area of the combined smaller collars. Five common sampling dates in 2007 and 2008 were utilized for this test, when fluxes were collected at the same time of day (+/- 2hrs) in both the small collars and the large ones. Except for the RL at T4, all collars (large and small) were within 1 m of each other. At the RL of T4, the average flux from two large collars was used, one four and one eight metres away from the group of small collars. Site specific analysis was carried out to determine whether or not one site (ex. FE) behaved differently than the rest of the dataset, as well as whether or not one of the collars within each site behaved more similarly to the large square collar than the others. Along with the closed-chamber method of flux measurement, GHG profilers were also sampled during this experiment, within +/- 1 hour of measuring fluxes from the chambers.

Measurements from a rainfall event were taken to examine the impact of precipitation events on both subsurface and flux values of N_2O. As moisture levels and water table are defining controls on subsurface concentrations of N_2O, and changes therein might occur with precipitation input, this event was used to examine moisture-related subsurface concentration changes and infer production. One main event was captured at the beginning of the season, DOY 170 and 171. Several days before (DOY 165), during the day immediately before and after the rain event, and the following day gases were collected from the GHG profilers. Fluxes were measured on DOY 165, immediately following the event, as well as the day after the event.

2.3 Statistical Analyses

Analysis was carried out in SPSS (versions 15 and 16) to determine whether or not GHG flux values were normally distributed. A one-sample Kolmogorov-Smirnov Test was used for this purpose. N_2O distributions were significantly different from normal ($p<0.05$). Therefore, non-parametric statistics were used when grouping or comparing any of the data sets associated with these fluxes. Gas profiles were analyzed in the same manner as GHG fluxes, and were deemed not to be normally distributed as well ($p<0.05$).

Hotspots and hot moments were determined statistically by looking for significant outliers in the datasets. In order to measure "hot" spots and moments in this study, by this definition, rates of denitrification would need to be determined during each sampling period. As this was not feasible, an indirect measurement of reaction rates was used: measuring GHG fluxes at the surface-atmosphere interface, and using GHG concentrations in the subsurface as a proxy for zones of production. It was assumed that subsurface gas concentrations are a representation of production within that zone of the soil profile due to the slow gas diffusion rates in the soil profile, especially when saturated. Gas fluxes, as measured with the closed chamber method, were assumed to represent the near-surface production (and any gases that may have been produced in the subsurface that have been able to diffuse towards the surface before being chemically altered by microbes) by microbial activity. Hotspots/moments were determined statistically by looking for significant outliers in the datasets. This was not possible with the subsurface GHGs due to their large variability, even within one day's profile, therefore these data were examined visually instead.

Chapter 3

Results

3.1 Introduction

The following results chapter will detail data collected over the 2007 field season. It was postulated that there were three distinct positions along each transect, and therefore six distinct sites in total. These sites were hypothesized to be differentiated on the basis of their physical and hydrological characteristics, in addition to the nutrient supplies at each (biogeochemical). This differentiation was hypothesized to create variability and spatial trends in the release of N_2O at the surface-atmosphere interface. Therefore, the following data are presented in three main sections, with connections between each: physical/hydrological properties of the field site, indicating the differences between each of the six sites; a review of N_2O fluxes, nutrients and subsurface N_2O as a function of distance into the riparian zone (spatial); and N_2O, nutrients and subsurface N_2O through time, based on three seasons, in order to examine spatial trends without the confounding variable of time.

3.2 Spatial Trends in Nitrous Oxide Emissions and Related Chemistry

In this section, general spatial trends of each data set (soil physical/hydrological characteristics, N_2O fluxes, subsurface supply) will be discussed (Figure 8). High spatial variability, both within each site, and between sites, was found for N_2O fluxes, with no visible trends. Trends were visible in all other datasets, however variability was still high.

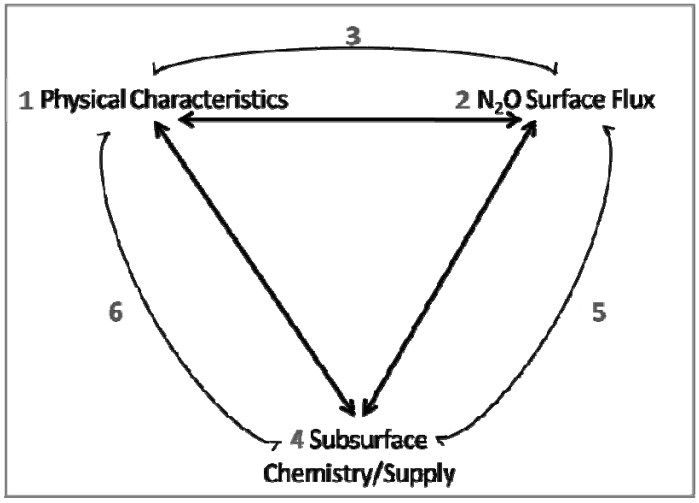

Figure 8. Conceptual diagram of part one of the results section. Numbers indicate the order in which the topics will be covered.

3.2.1 Physical/Hydrological Characteristics

An understanding of processes leading to the release of N_2O at the surface requires an understanding of water table and groundwater movement throughout the riparian zone. From previous work, it is known that groundwater movement is slow through this site, and runs obliquely through the RZ, from T1 to T4 (Zhang, 2007). Hydraulic head values, taken at each well at every site during sampling events, were consistent with those observed by Zhang (2007), indicating that flow was lateral during the 2007 field season, as in his 2006 study. Transect 5 appears to be more closely aligned along a flow path, however this is inconclusive without installing and sampling a network of wells at this site.

Within each of the six zones located along both transects 4 and 5, analysis of hydraulic head from piezometer nests was undertaken during each sampling event, and suggested an upwelling of deeper groundwater towards the surface at one site in particular: the RS of T5. The water table, was generally higher at this mid-riparian site (Figure 9), and therefore experienced flow towards both the FE during dry periods, and always towards the lowland riparian. At all other sites, including those at T4, there was generally minimal head difference with depth and therefore no up or down movement of groundwater.

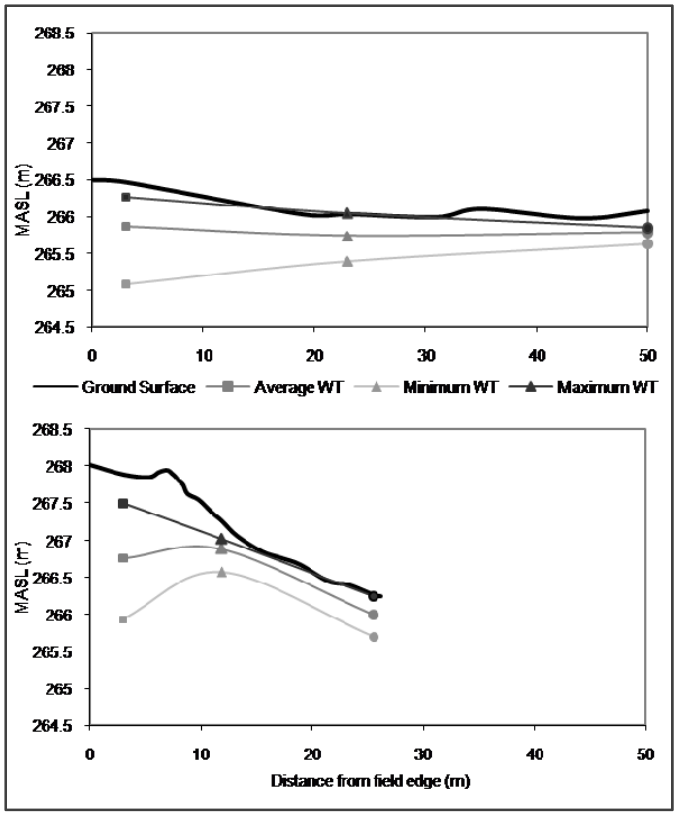

Figure 9. Water table elevations below ground surface. Maximum, average and minimum water table elevations are displayed with respect to ground surface. (■ field edge, △ riparian level and riparian slope (T4 and T5, respectively), ● stream edge and riparian level (T4 and T5, respectively).

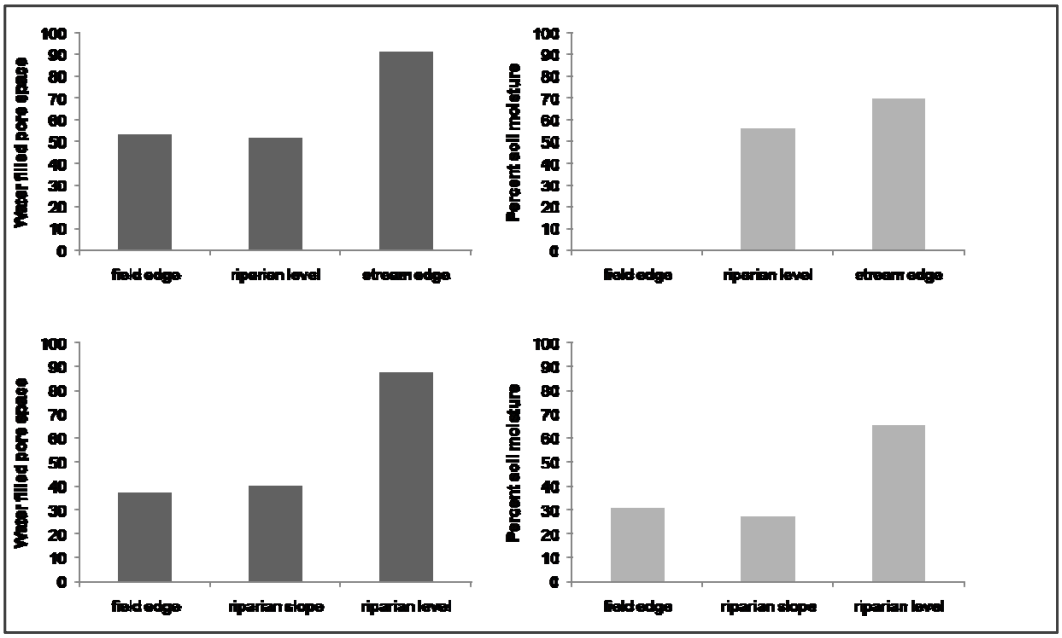

Figure 10. Water filled pore space and soil moisture seasonal medians for each position (T4 (top), T5 (bottom)). WFPS measurements (%) are integrated over the top 6 cm, and soil moisture values are at 15 cm deep.

Water table position was both spatially and temporally variable in the RZ. Fluctuations were greatest at the FE positions of both transects, and on T4, fluctuations decreased with distance into the riparian zone. On T5, however, the mid-riparian zone RS fluctuated the least, likely due to the influence of deeper grounder. Throughout the season, each of the six positions maintained different water table elevations from each other (Figure 9). Both high and low water table elevations were detected at all sites (relatively), with conditions for both denitrification and nitrification. Fluctuations suggest that these processes would occur at varying depths below the surface, potentially changing the volume and flux of N_2O reaching the surface.

Along with water table variations among sites, differences in surface and shallow soil moisture conditions resulted in differences between positions, as expected. Both FEs and mid-riparian zone positions displayed similar moisture conditions, with lowland moisture higher (Figure 10).

3.2.1.1 Soil Physical Characteristics

Soil profiles revealed variability between positions along both transects (Figure 11). Transect 4 was characterized by increasing thickness of the A horizon with distance from the FE, becoming deeper and more peaty (up to 90 cm) at the lowland SE, underlain by loamy, mineral soils. Iron oxide and sand lenses were visible at depths from 10 – 90 cm at the mid riparian zone, indicative of a long-term

fluctuating water table with periods of both anoxic and aerobic conditions (Mitsch and Gosselink, 2007). A similar increase in the A horizon thickness with distance from the FE was present along T5, however less of the visible peaty organic material was present along this transect than along T4. Underlying the A horizon along T5 was an orange-coloured mineral sand layer. In the lowland RL, a shallow 50 cm layer of peaty, rooted matrix, was present above a layer of clay, along with a 2 – 3 cm layer of a marl, which is known to lie at approximately 1m deep below soils of the Beverly Swamp proper (Warren *et al.*, 2001).

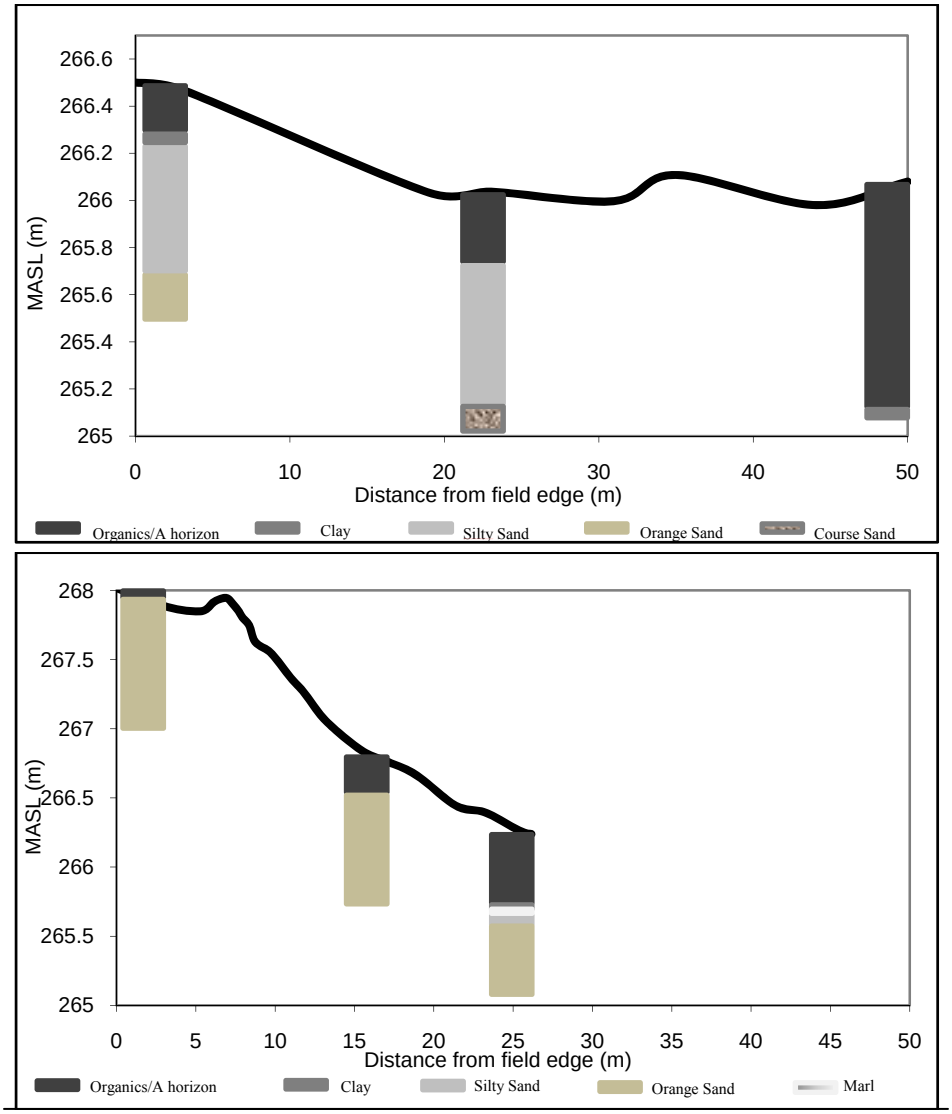

Figure 11. Transect cross-sections with soil physical information. Organics increase with distance into the riparian zone, and mineral layers are more prevalent closer to the FE on both transects.

3.2.2 Nitrous Oxide Surface Fluxes

Highly variable fluxes were observed across the riparian zone, ranging from -0.28 to 1.3 nmol m^{-2} s^{-1}. A frequency distribution of fluxes indicates a skewness to the right (1.6981) and a peaked curve (kurtosis = 4.002), meaning that most of the flux values fell within only a few bins and the majority of that data was below the median, in the lower portion of the range. This distribution was considered non-normal (p=0.054), and therefore non-parametric statistical tests were used throughout to test for statistical relationships.

Contrary to the hypothesis of this thesis, nitrous oxide flux data did not display significant differences between sites along either transect ($p > 0.05$) (Figure 12). High variability was found at all sites when medians were taken from the combined data. Slightly higher fluxes were seen in the RL positions on both transects, with the highest overall variability. Flux data contained several significant outliers in the datasets, which may have been responsible for the large variations visible by error bars. The location of most efflux outliers was in the riparian level position on T5, and on DOY 220, which was dry and warm. Consumption outliers were found predominantly at the FE and RS positions of T5, during the flooding period of DOY 333, which was very wet and cool. This suggests temporal and/or seasonal controls on N_2O flux variability, which will be explored in section 3.3.2.

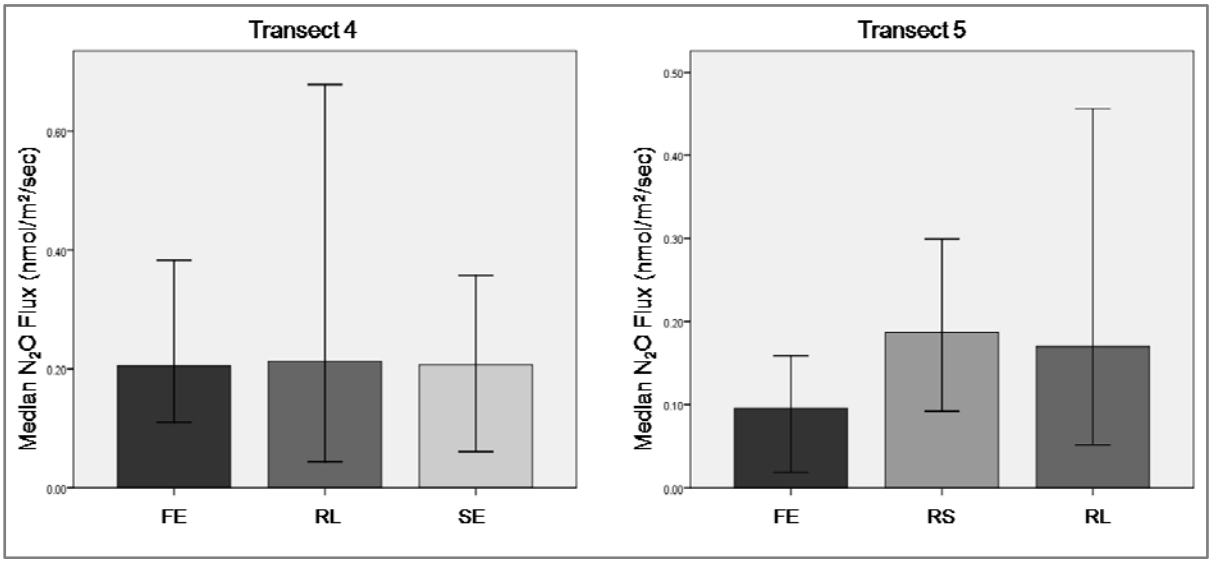

Figure 12. Spatial N_2O flux variability across the riparian zone. Flux medians (derived from the entire season's data) were used to examine the riarian zone's spatial variability, from field edge towards the stream. Error bars represent confidence intervals (95%) and display no significant differences between sites.

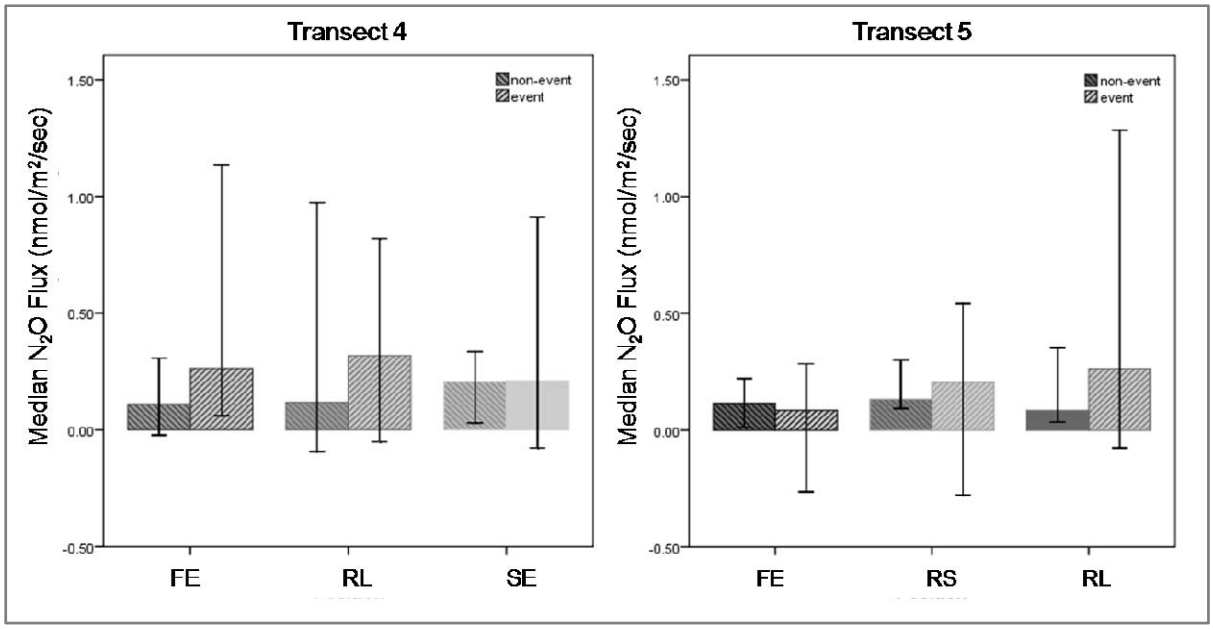

Figure 13. Event vs. non-event N_2O fluxes. Fluxes were were split between sampling events that occurred immediately following precipitation (event), or during baseflow periods (non-event).

To try to reduce the variability in the data, fluxes were "binned" or separated into either event fluxes (n=8) or non-event fluxes (n=5) (event = post precipitation). Binning the flux data by event vs. non-event periods, event fluxes encompassed the total range (above), while the non-event values ranged from -0.09 to 0.97 nmol m^{-2} s^{-1} (Figure 13). There appears to be slightly higher variability under event-related conditions. On T4, there were higher N_2O fluxes found in the SE position during non-event days. On T5, however, the RS position experienced the highest fluxes. Except for the SE, which exhibited no change (event vs. non-event) and the FE of T5, event-based fluxes were higher than non-event fluxes. Spatial variability with position across the riparian zone did not differ significantly from site to site, nor from one transect to another.

3.2.2.1 N_2O Intra-site vs. among-site variability

The sampling technique employed in this study helped to elucidate the heterogeneity of soil microbial processes. Three GHG collars were used at each site to obtain three flux values that were later averaged to obtain one value for each position. However, often these three fluxes produced high standard deviations, demonstrating high spatial heterogeneity within one site. To assist interpretation of the observed fluxes, it is important to compare "intra-site" variability (or heterogeneity) with "among-site" variability. Such comparisons can show whether spatial differences among the three topographic positions along each transect was hidden by intra-site heterogeneity.

Variability was highest at the FE positions on both transects and for each matched set of collars (*i.e.* A *vs*. B *vs*. C). One collar often exhibited more deviance from the other two. For instance, the SE on DOYs 190 and 255, in which fluxes derived from collars A, B and C were 0.295, 0.462 and -0.108 nmol m^{-2} s^{-1}, respectively, on the first date, and 0.106, -0.005 and 0.083 nmol m^{-2} s^{-1}, respectively, on the second date. This is spatial variability not driven by one anomalous collar at a given site, but instead can be generated by any one of the three collars. Table 5 displays the flux data statistics from both T4 and T5. Fluxes from one date at three sites (presented graphically), illustrates this variability (Figure 14). All sites, except T5 RL, exhibited heterogeneity on one or more dates studied, that was greater than the among-site variability on the same transect. Therefore, local differences at one site can mask any spatial trends that may occur along transects. This was further tested by comparing fluxes derived from large collars to those derived from an average of the three small collars. To determine whether or not a larger surface area collar would display an average flux equal to that of three separate, smaller surface area collars, a comparison exercise was undertaken based on five sampling dates and all six sites.

Table 5. Nitrous oxide intra-site variability. Flux measurements were averaged (n=3) and standard deviations (n=3) were taken for each site's three GHG collar measurements. Intra-site variability was established by picking out transect standard deviations (n=9) that were higher or close to the transect means (n=9).

Transect 4						Transect 5					
DOY	Position	Mean (nmol/m2/sec)	StDev (nmol/m2/sec)	Mean of means	StDev of means	DOY	Position	Mean (nmol/m2/sec)	StDev (nmol/m2/sec)	Mean of means	StDev of means
155	FE	0.26	0.07	0.28	0.12	155	**FE**	**0.02**	**0.08**	-0.01	**0.05**
	RL	0.40	0.12				RS	0.02	0.05		
	SE	0.17	0.09				RL	-0.08	0.02		
165	FE	0.31	0.04	0.54	0.38	165	**FE**	**0.12**	**0.18**	0.10	0.02
	RL	0.97	0.33				RS	0.09	0.05		
	SE	**0.34**	**0.29**				RL	0.08	0.04		
170	**FE**	**1.14**	**1.62**	0.91	0.23	170	FE	0.28	0.18	0.39	0.13
	RL	0.68	0.17				RS	0.54	0.27		
	SE	0.91	0.54				RL	0.36	0.16		
171	**FE**	**0.38**	**0.56**	0.52	0.26	171	FE	0.13	0.07	0.21	0.10
	RL	0.82	0.26				RS	0.33	0.18		
	SE	0.36	0.09				RL	0.17	0.11		
190	FE	0.11	0.06	0.08	**0.16**	190	**FE**	**0.01**	**0.14**	0.20	**0.17**
	RL	**-0.09**	**0.07**				RS	0.23	0.03		
	SE	**0.22**	**0.29**				RL	0.35	0.20		
200	**FE**	**0.06**	**0.07**	0.31	0.23	200	**FE**	**0.03**	**0.10**	0.31	**0.28**
	RL	0.35	0.08				RS	0.30	0.11		
	SE	0.51	0.29				RL	0.59	0.37		
206	FE	0.11	0.06	0.18	0.06	206	FE	0.22	0.02	0.28	0.05
	RL	0.21	0.11				**RS**	**0.30**	**0.26**		
	SE	0.21	0.06				RL	0.31	0.15		
220	FE	0.44	0.39	0.33	0.10	220	FE	0.10	0.03	0.53	**0.65**
	RL	0.29	0.12				RS	0.22	0.10		
	SE	0.25	0.19				RL	1.28	0.82		
255	FE	0.14	0.07	0.08	**0.05**	255	**FE**	**0.07**	**0.05**	0.24	**0.20**
	RL	**0.04**	**0.03**				RS	0.19	0.08		
	SE	**0.06**	**0.06**				RL	0.46	0.13		
292	**FE**	**-0.02**	**0.14**	0.03	**0.05**	292	FE	0.06	0.03	0.07	**0.05**
	RL	0.08	0.04				**RS**	**0.13**	**0.12**		
	SE	**0.03**	**0.04**				RL	0.03	0.01		
304	FE	0.21	0.05	0.14	0.06	304	FE	0.16	0.04	0.10	0.06
	RL	0.12	0.03				RS	0.11	0.04		
	SE	0.09	0.05				RL	0.04	0.02		
317	FE	0.16	0.06	0.11	0.05	317	FE	0.12	0.02	0.13	0.04
	RL	0.11	0.15				RS	0.17	0.04		
	SE	**0.07**	**0.10**				RL	0.09	0.02		
333	FE	0.27	0.09	0.05	**0.19**	333	FE	-0.26	0.13	-0.15	0.20
	RL	-0.05	n/a				RS	-0.28	0.04		
	SE	-0.08	0.15				RL	0.08	n/a		

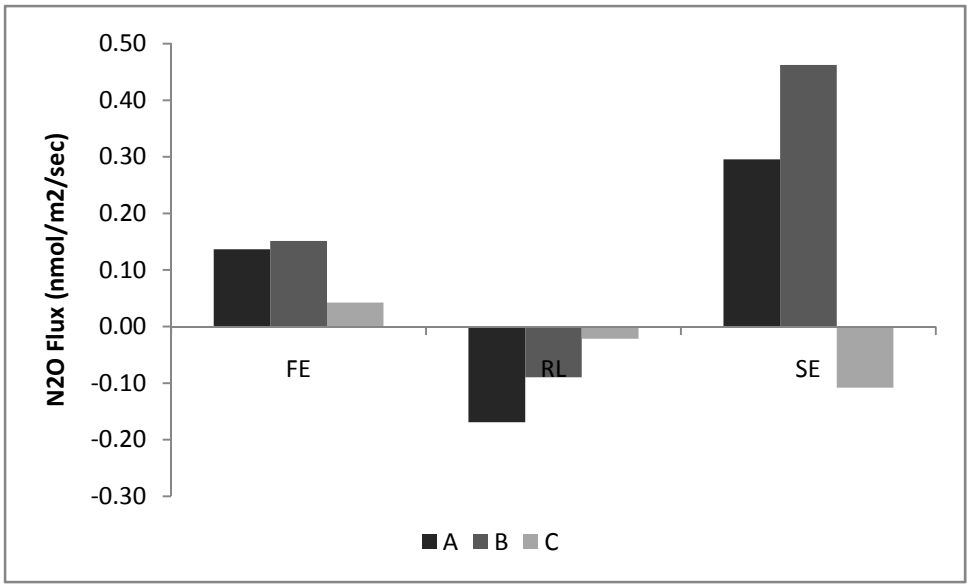

Figure 14. Graphical representation of variability between collars on one sampling date (transect four, on DOY 190).

A wilcoxon signed ranks test was completed to analyze for significant differences between small and large collars (Table 6). This non-parametric test was used as an alternative to a T-test because the data were not normally distributed. At the FE of T4, no significant difference existed between any of the three collars and the large square chamber, however the p value (p=0.075) for collar A suggested a weaker relationship than the other collars. At the RL position on the same transect, two collars (B and C) displayed significant differences between the fluxes derived from them and those from the larger collars. These results may be due to the fact that two large collars were averaged to arrive at one value for this position. Low p values (p=0.075) were calculated for the differences between collars A and B in the RL position of T5, perhaps lending some credibility to the results determined on T4, despite the different setup on the latter transect. One significant difference existed on the RS with collar A; the other two were not significantly different from the large collar.

Table 6. Wilcoxon Signed Ranks Test significance values for small vs. large GHG collars. Each small collar (A, B and C) was compared to the large collar at the same site. Bolded values represent significant differences ($p < 0.05$).

Transect	Site	Asymptotic Significance Values			
		Small A vs. Large	Small B vs. Large	Small C vs. Large	Small vs. Large Avg.
4	FE	**0.075**	**0.116**	**0.249**	**0.306**
	RL	**0.116**	**0.028**	**0.028**	
	SE	**0.249**	**0.600**	**0.116**	
5	FE	**0.463**	**0.345**	**0.463**	
	RS	**0.046**	**0.249**	**0.753**	
	RL	**0.075**	**0.075**	**0.345**	

Scatterplots of N_2O fluxes derived from the one large chamber vs. an average of the three small ones resulted in a poor R^2, signifying a high degree of scattering, however a statistical analysis (Wilcoxon signed rank test) revealed no significant difference ($p > 0.05$) between them, meaning they can be used interchangeably (but perhaps with some caution). Therefore, three collars covering an area of 0.029 m^2 each (0.087 m^2 combined area) capture a similar degree of heterogeneity as a collar that covers an area of 0.21 m^2, over two times greater than the combined area of the small collars.

The purpose of these experiments was to test whether or not the heterogeneity exhibited by the unit of three collars at each site was responsible for the lack of defined trends among sites. Through analysis of the above-stated data, the heterogeneity exhibited within sites was just as high as among sites, suggesting that this was potentially the cause of the unexpected lack of spatial trends from field edge towards the stream. A larger surface area used to capture fluxes at each site revealed no significant difference to that of the means of three smaller surface areas, suggesting that spatial heterogeneity dominates the entire site. Therefore, the placement of GHG collars within a riparian zone may not be important in determining average GHG fluxes from this environment. This also demonstrates the importance of sampling methodology when performing a scientific study, as biases can be easily included without proper considerations. For instance, collar size for gas collection can be tailored directly to the study - if the purpose is to examine patchiness of the site, smaller collars are a better choice. However, if a general flux is desired for larger-scale modeling, larger collars would be more appropriate.

3.2.3 Relationship Between Physical/hydrological Characteristics and Surface Fluxes

3.2.3.1 WFPS and Temperatures vs. N_2O Flux

Hydrological conditions varied among sites, as described in section 3.2.1. As soil moisture is one of the most influential factors for denitrification, relationships between soil moisture (WFPS) integrated over the top 5 cm, and N_2O fluxes were examined. In addition to soil moisture at the surface, both air and soil temperatures can affect N_2O production; these were also examined in relation to observed N_2O fluxes.

Regression analyses were conducted between the three independent variables (WFPS, air temperature and soil temperature) and the dependent variable of N_2O flux (Table 7). Results indicate that temperature was the most well-correlated to the fluxes, with air temperatures displaying slightly better relationships than soil temperatures. Water filled pore space, which is thought to have the most impact upon N_2O emissions, displayed weak relationships. All relationships with WFPS along T5 were negative, even the stronger relationship with collar C at the FE, as well as all SE relationships on T4. This may indicate a clearer pathway through which gases diffuse towards the surface, as high moisture conditions retard diffusive flux. The results were more readily expected at the SE and RL (T4 and T5, respectively) as those are the lowland and positions with the wettest moisture conditions. Further analysis of these trends (i.e. more data collection) would be beneficial. The field edge of T4 displayed very weak correlations with all three variables, indicating that other variables not sampled may have been responsible for N_2O emission controls.

Table 7. R^2 values of independent variables, WFPS, Air Temp and Soil Temp, vs. N_2O flux. Italicized values represent negative relationships, bolded values represent stronger relationships.

		Transect 4			Transect 5		
	Collar	FE	RL	SE	FE	RS	RL
WFPS	A	0.059	0.059	*0.007*	*0.010*	*0.194*	*0.216*
	B	0.065	0.028	*0.315*	*0.047*	*0.333*	*0.420*
	C	*0.022*	0.128	*0.047*	***0.532***	*0.456*	*0.146*
Air Temp	A	***0.081***	**0.291**	**0.561**	**0.043**	**0.555**	**0.176**
	B	***0.012***	**0.417**	**0.587**	**0.236**	**0.455**	**0.061**
	C	**0.274**	**0.179**	**0.293**	**0.518**	**0.588**	**0.067**
Soil Temp	A	*0.066*	0.287	0.351	0.000	0.449	0.356
	B	*0.053*	0.403	0.480	0.132	0.368	0.211
	C	0.140	0.289	0.304	0.405	0.401	0.203

3.2.4 Subsurface Chemistry/Supply (Nutrient Pools and N_2O Concentrations)

To try to explain N_2O fluxes, and their lack of spatial trends within the riparian zone, substrate availability was examined in groundwater, soils and subsurface gases.

3.2.4.1 Nutrient concentrations in groundwater

Because the water table elevation was often deep below the ground surface, piezometers were often dry so no groundwater could be collected. Thus, fewer nutrient determinations could be made at depths > 75 cm, particularly at the FE and RS positions.

3.2.4.1.1 Nitrate and Ammonium

In contrast to the N_2O fluxes, variability among sites occurred in groundwater NO_3 concentrations. As expected, NO_3 concentrations differed between transects as well as along the transects through the riparian zone. Overall groundwater NO_3 concentrations ranged from < dl – 20.6mg-N L^{-1} on T4 and T5 showed a smaller range (< dl – 14.4 mg-N L^{-1}). Nitrate levels were highest at the FE on both transects (Figure 15 a, d) and a general increase with depth is more pronounced at T4. The mid-riparian zone positions differ between the transects (Figure 15 b, e). At T5 the mid-riparian is a RS and at T4 it is RL. It is possible that the NO_3 loss is more complete at the RL positions (ex. T4), or the RS position at T5 is connected to the FE source. Evidence from the former can be seen in Figure 15f where the RL position of T5 shows negligible groundwater NO_3 as does the SE position on T4 (Figure 15 c). On both transects, groundwater NO_3 concentrations declined within 20 m of the FE. As stated above, the shallowest piezometers did not yield water most of the field season, however the three deepest ones did consistently show NO_3 in the order of 150 > 75 > 100 cm.

Ammonium levels were lower than NO_3 at all sites, exhibiting an overall range of < dl – 4.3 mg-N L^{-1} on T4 and a somewhat higher range of < dl – 7.9 mg-N L^{-1} at T5. Ammonium behaved similarly at both transects, with higher concentrations found in lowland zones where the soils are largely organic, and lower concentrations in both upland and mid riparian zones (Figure 15).

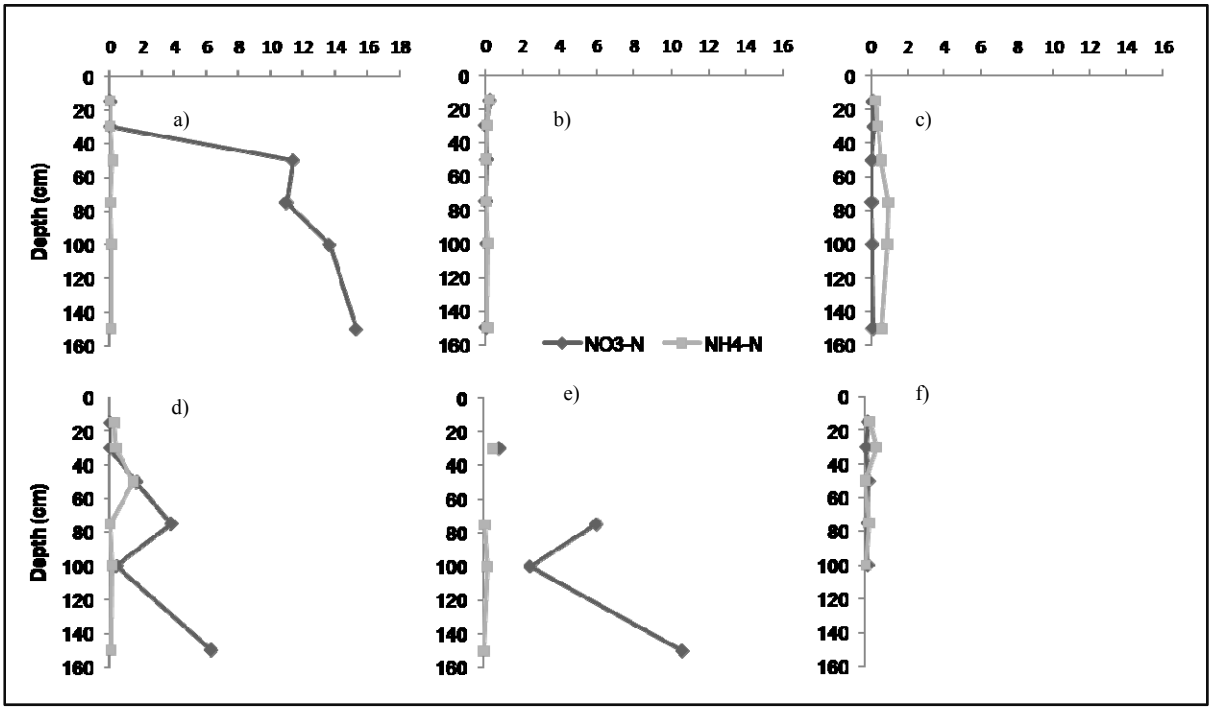

Figure 15. Median nitrate and ammonium concentrations (mg-N L-1). Concentrations are represented with depth for each of the six positions. a) T4 FE; b) T4 RL; c) T4 SE; d) T5 FE; e) T5 RS; f) T5 RL.

Significant outliers in groundwater NH_4 concentrations were uniquely tied to the RL of T5, and mainly at a depth of 75 cm. The most significant period of elevated NH_4 occurred on DOY 220, in the middle of the summer dry period, in addition to hot moments on DOY 170 and 190, both dates following events.

3.2.4.1.2 Dissolved organic carbon (DOC)

Groundwater DOC concentrations on T4 ranged from 12 to 32 mg-C L^{-1}, and on T5 from 7.9 to 38 mg-C L^{-1}. Concentrations were consistent across the riparian zone, with slightly higher levels in the lowland areas on both transects. No consistent depth trends were evident.

3.2.4.1.3 Dissolved oxygen (DO)

Dissolved oxygen readings must be accepted with some caution due to the method of collection (Figure 16). Concentrations ranged from 0.1 to 8.3 mg L^{-1} on T4, with little depth trend. At the SE, DO measurements were below 2 mg L^{-1}, which is considered the boundary for anoxia. At T5, DO ranged between 0.1 and 9.6 mg L^{-1}. DO was highest at the FEs and RS positions, which is consistent

with soil moisture and water table patterns. It was lower at all other positions, where topography was flatter, suggesting zones conducive for denitrification.

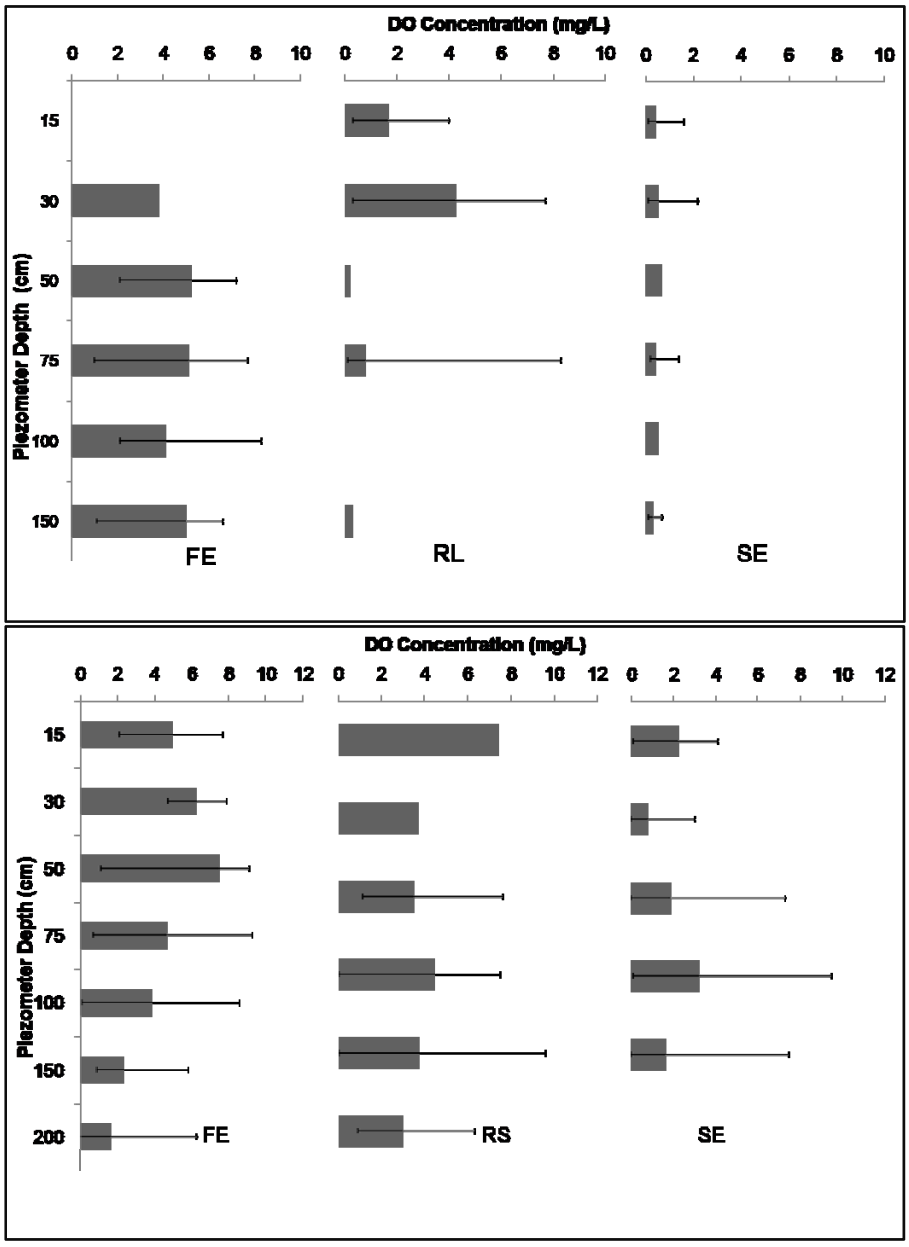

Figure 16. Dissolved oxygen concentrations along T4 (top) and T5 (bottom).

3.2.4.2 Substrate nutrient availability

The C:N ratio of soils is an indication of the overall quality of the soil organic matter (Pierzynski, 2005). Means of C:N ratios for soil profiles sampled to a depth of 1 m for each site demonstrate weak

spatial patterns along both transects. No significant difference existed between the FE and RL along T4, however the SE and RL were significantly different (Figure 17), with the latter displaying a higher ratio. The RL of T5 displayed a significantly greater C:N ratio than either the FE or RS, which were comparable to each other. In general, ratios were varied over a large range from 5.1 to 24.4. Spatial patterns were inconsistent with depth, however at the RLs and the SE, there was a peak at 75 cm below the surface.

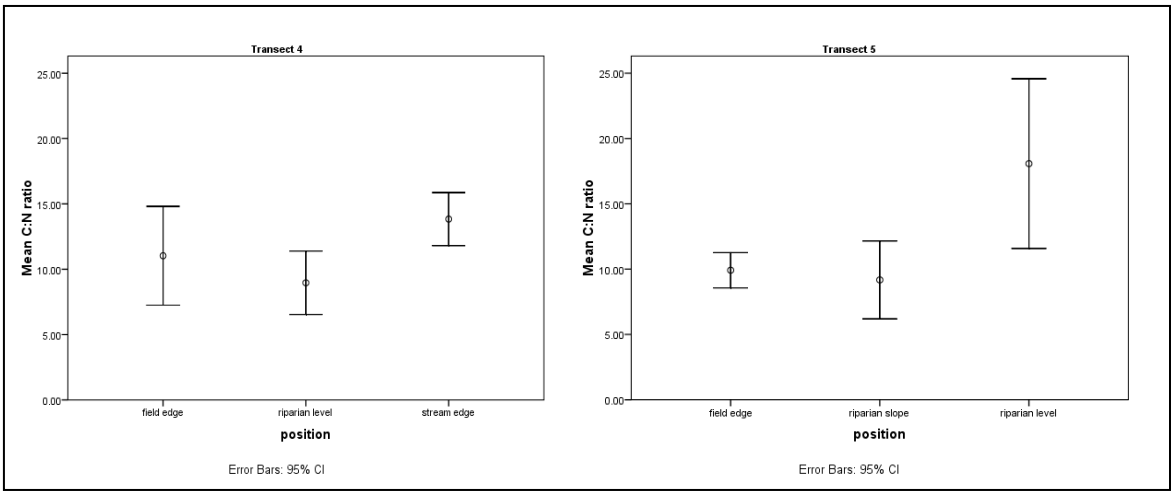

Figure 17. Median soil C:N ratios along both transects (error bars represent 95% confidence intervals).

Extractable NO_3-N and NH_4-N taken from the same soil profiles as the C:N ratios, also displayed a lack of patterning with depth, or with position in the riparian zone. The highest variability for both nutrients was at the FE positions (Figure 18), which displayed the full range of nutrient concentrations extracted (0.17 – 8.93µg g^{-1} for NO_3-N; 0.73 – 30.62µg g^{-1} for NH_4-N). Transect five displayed lower concentrations of both nutrients than T4. Extractable NH_4 concentrations were also higher than extractable NO_3 on both transects and at all positions except the FE of T5, however most of these differences were not significant (Figure 18). In general, extractable NO_3-N and NH_4-N decreased with depth at all sites except the FEs, in which NH_4 peaked at 50 cm (Figure 19).

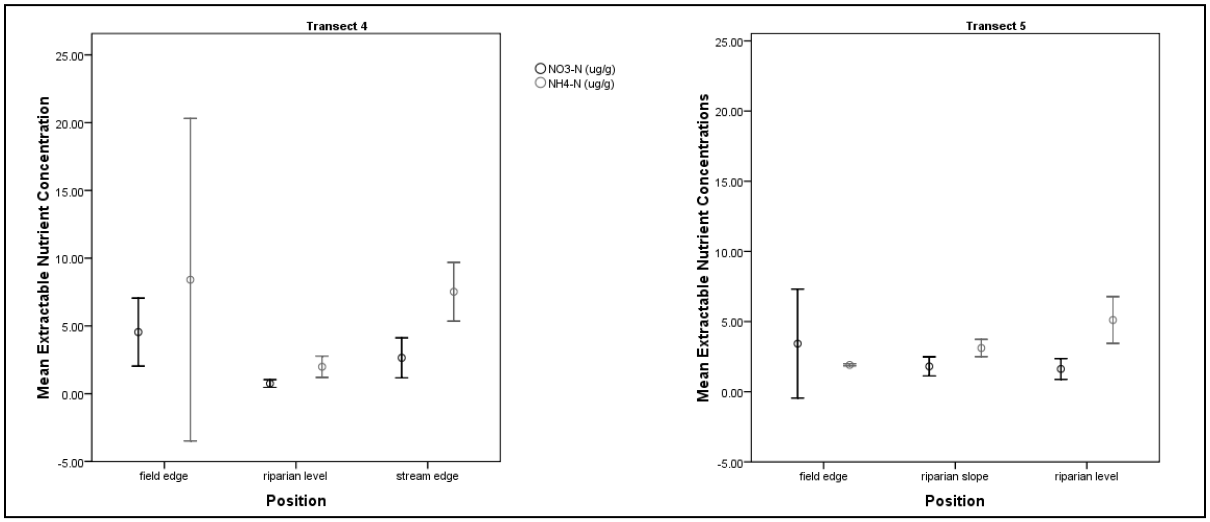

Figure 18. Mean soil extractable NO_3-N and NH_4-N along both transects.

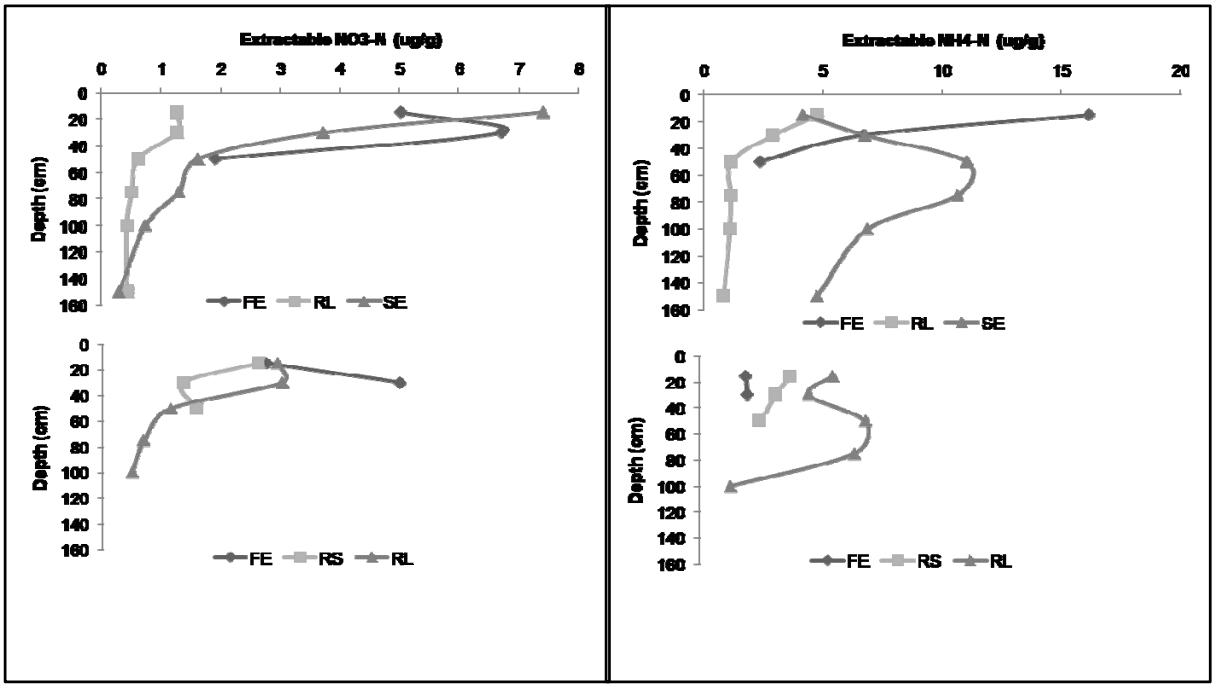

Figure 19. Mean soil extractable NO_3-N and NH_4-N with depth at each position (T4 top, T5 bottom).

3.2.4.3 Subsurface N_2O Concentrations

Similar to substrate and groundwater nutrient concentrations, subsurface N_2O concentrations displayed spatial trends. Nitrous oxide concentrations ranged from 0.16 - 13.7 ppmv on T4, and 0.22 - 45.4 ppmv on T5. Field edge N_2O concentrations were consistently higher than either the RL or SE zones on T4 (Figure 20), following the same pattern as groundwater NO_3 (Figure 15). Nitrous oxide

also increased with depth, and was highest at 75 cm, consistent with the depth of peak C:N ratios. On T5, concentrations increased at 75 cm but were highest below that depth at the RS position (Figure 20Figure), which also follows groundwater NO_3 trends. Differences in concentrations between the two transects were apparent with median concentrations being an order of magnitude greater at the RS as compared to the FE of T4. The similarity of patterns shown by subsurface concentrations of N_2O and NO_3 suggests that one of the expected regulating factors for N_2O production, NO_3 supply, occurs at the FE of both transects and the RS of T5.

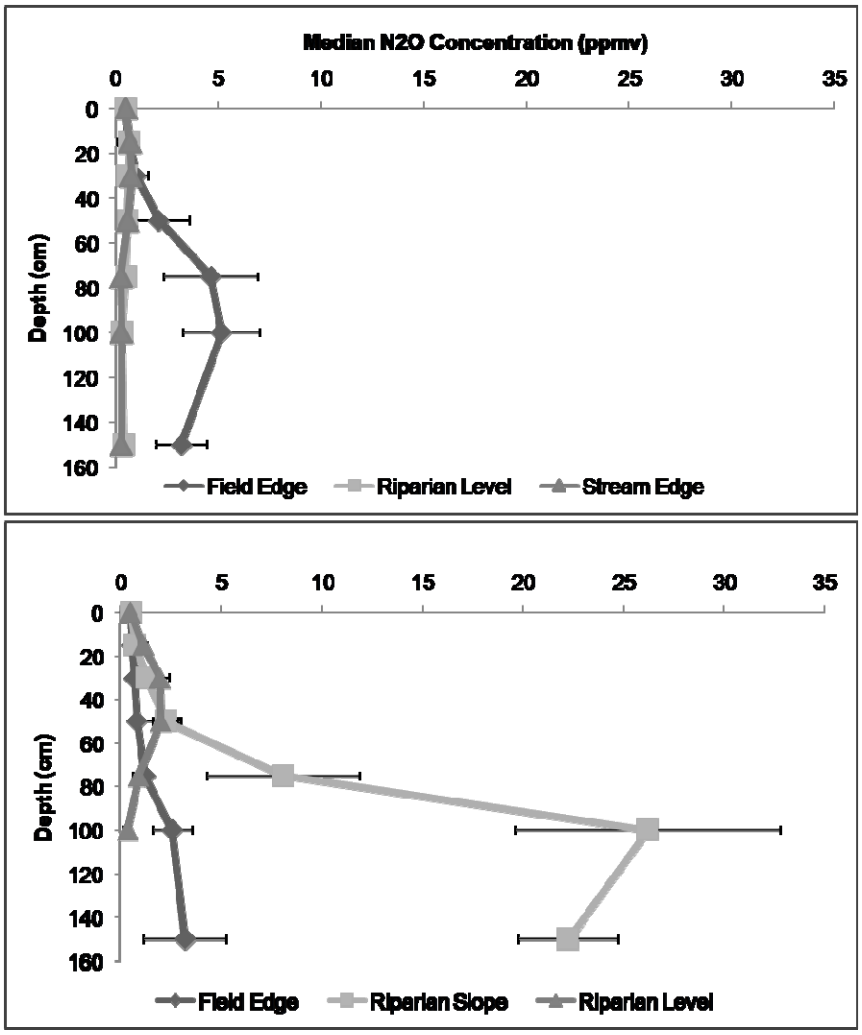

Figure 20. N_2O subsurface concentrations at T4 (top) and T5 (bottom). Notice the dominant N_2O producing positions along each transect (field edge at T4, riparian slope at T5). Error bars represent 95% confidence intervals.

3.2.4.4 Subsurface Chemistry Relationships

Relationships among nutrients and subsurface gases can shed light on processes occurring at depth, without measuring these processes directly. In order to explore the factors that can control N_2O production, relationships between NO_3, NH_4, SO_4 and subsurface N_2O concentrations were examined.

The scatterplot between NO_3 and NH_4 illustrates a mutually exclusive relationship, which means that neither occurs in significant concentrations when the other is present (Figure 21). In all locations except for two, they followed this trend. Both outliers to this trend were found on transect four: the FE at a depth of 150 cm ([NO_3] > 50 ppm, [NH_4] > 3 ppm), and the SE ([NO_3] > 4 ppm, [NH_4] > 1 ppm). Mutual exclusivity represents thermodynamic controls on N_2O production mechanisms (Hedin *et al.*, 1998).

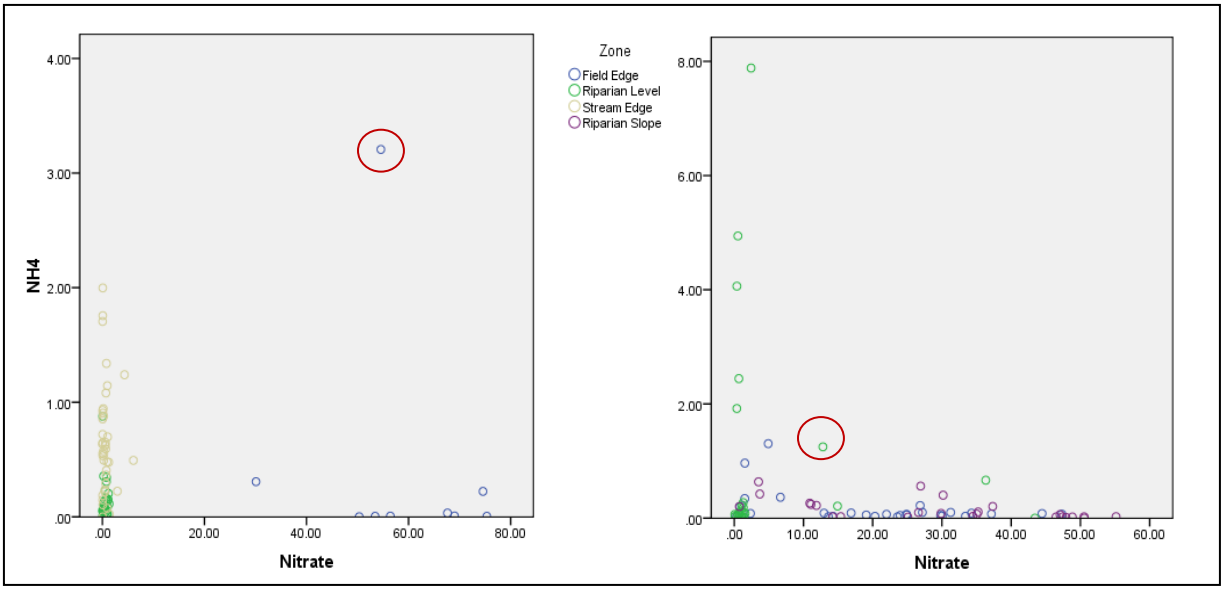

Figure 21. Ground water ammonium vs. nitrate concentrations (T4 left, T5 right). Outliers are circled; aside from the outliers, ammonium and nitrate display a mutually exclusive relationship.

Scatterplots between subsurface N_2O concentrations and groundwater NO_3 reveal a triangular-shaped graph (Figure 22). A clear relationship does not exist with all data points plotted. However, when plotted separately for each position, both positive and negative relationships appeared. At the FE of transect four there were positive relationships at depths of 75 and 100 cm (R^2 0.33 and 0.703, respectively), while the depths of 50 and 150 cm displayed negative relationships (R^2 0.734 and 0.035, respectively). There was only one point available for the shallow piezometers, and therefore they will be disregarded. The RL position displayed relationships at depths of 15, 30, 75, 100 and 150 cm that were all weak and positive, with the exception of the 50 cm depth (R^2 0.703). At the SE, all

relationships are weak (R^2 < 0.2) and positive. On T5, the water table at the FE position was consistently low, and therefore only values 50 cm and below were able to be used for these relationships. All correlations were weak (R^2 < 0.2), with two positive (50 and 100 cm) and two negative (75 and 150 cm). The RS position often experienced low water tables, and therefore minimal data is available for both the 15 and 30 cm depths. Below that, all relationships were weak (R^2 < 0.1), with the 75 and 150 cm depths displaying negative relationships, while the 100 cm depth displayed a positive relationship. At the RL, all relationships were positive and weak (R^2 < 0.1) except for the 50 cm depth which was negative and displayed an R^2 of 0.61.

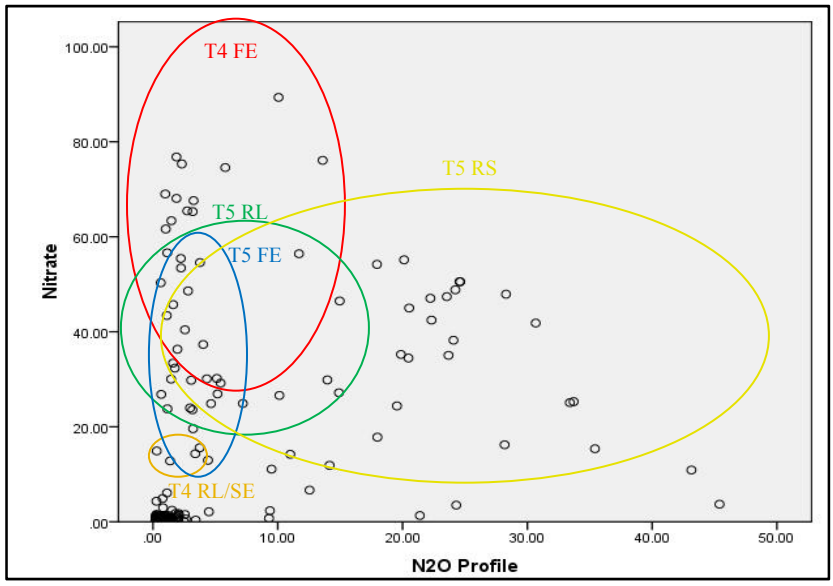

Figure 22. Nitrate vs. N_2O subsurface profile concentrations.

3.2.5 Surface Nitrous Oxide Emissions and Nutrient Supply

Surface fluxes have not shown a relationship to supply and/or subsurface chemistry. For instance, the FE of T4 maintained a high concentration of NO_3 and subsurface N_2O, while the RL displayed little NO_3 and subsurface N_2O, however fluxes of N_2O at the surface-atmosphere interface were not reflective of this. N_2O was equal to or slightly higher at the RL position than the FE (see Figure 12). R^2 values between subsurface concentrations, nitrate/ammonium concentrations and N_2O fluxes revealed no significant relationships (data not shown).

3.2.6 Relationship Between Subsurface Chemical Supply and Soil Physical/Hydrologic Characteristics

Although N_2O movement through the subsurface was not directly studied, an examination of profile concentrations may provide useful information. Soil tortuosity is one of the main soil properties that can influence the movement of gas through the soil profile, and is related to grain size and distribution. Gas diffusion in soils is affected by both bulk density and porosity (related to the tortuosity) – gas movement can become inhibited when pore spaces are minimal, or water-filled, which is encouraged by these soil properties (Ball *et al.*, 2008). Using bulk density and porosity measurements taken at each depth of the profiles, an attempt was made to determine if these properties affected N_2O subsurface profile concentrations.

Upon evaluation of soil properties, one or two depths within each zone were chosen as those that display the highest bulk density and lowest porosity of the profile in that position (Table 8); high BD and low porosity did not consistently correspond to the same depth. Presented graphically, some sites displayed potential decreases in N_2O movement from zones of production (demonstrated by peaks in concentrations) upwards towards the surface (Figure 23). Nitrous oxide profiles from DOY 255 were used instead of means for the whole study period, as this date was closest to the date in which soil cores were collected from the field sites.

Table 8. Soil profile depths characterized by high bulk density and/or low porosity soils.

	Highest Bulk Density		**Lowest Porosity**	
Position	**Transect 4**	**Transect 5**	**Transect 4**	**Transect 5**
Upland	100 cm	75 cm	50 cm	75, 100 cm
Midland	50 cm	75, 100 cm	100 cm	75, 100 cm
Lowland	100 cm	75 cm	100 cm	75 cm

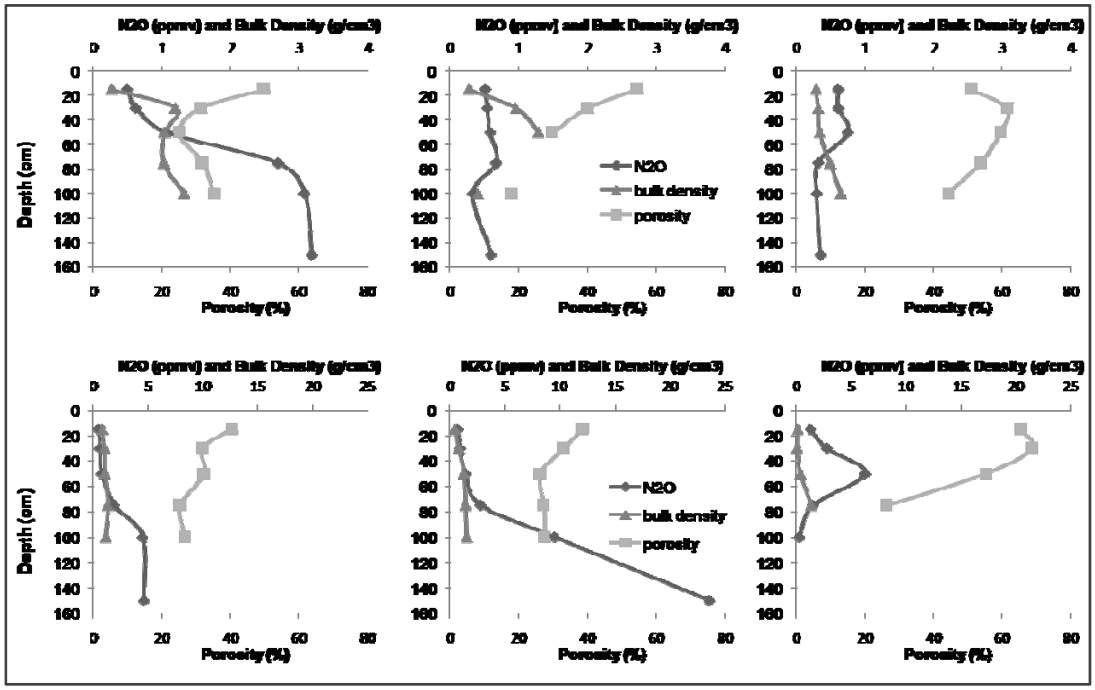

Figure 23. N_2O plotted with porosity and bulk density on DOY 255. a) T4 FE; b) T4 RL; c) T4 SE; d) T5 FE; e) T5 RS; f) T5 RL.

At the FE of T4, there appeared to be a zone of production at 150 cm deep, rising towards the 75 cm depth. At the 50 cm depth, porosity was low (< 30%), and bulk density was increasing. The 100 cm depth high BD zone did not appear to affect the gas concentrations, however N_2O peaks decreased at the 50 cm low porosity zone, which potentially impeded N_2O movement from the area of production below it. At the SE, both low porosity and high density zones occurred at 100 cm, which corresponded to a low point of N_2O concentrations in the profile. However at this site, porosity was > 50%, and therefore not likely a large cause of concentration decreases towards the surface.

Along T5, the FE low porosity zones existed at 75 and 100 cm. Peaks in N_2O were found at 150 cm (and likely deeper) but decreased towards the surface between 100 and 75 cm deep, where low porosity soils were found. At the RS, a general decrease in N_2O concentrations from 150 cm deep towards the 75 cm depth was seen, which may or may not correspond to the low porosity zones between 100 and 50 cm deep (deeper porosity/bulk density cores would aid in this case). At the RL, a peak in N_2O at 50 cm decreased at shallower depths, possibly corresponding to a decrease in porosity. However, in this case, porosity was already high (> 60%) and was likely not the cause of this decrease.

3.2.6.1 Subsurface N_2O Concentrations and Water Table Elevations

Water table elevations were found to be variable between sites and transects, and may impact the location and presence of N_2O gas in the subsurface. Since subsurface N_2O concentrations can act as a proxy for production zones of N_2O, these subsurface gases were examined as a function of water table position.

Subsurface gas profiles displayed marked differences for each position along both transects; peaks of N_2O concentration appeared at different depths among sites, but at approximately the same depth for each date sampled within sites; i.e. different depths spatially, but the same depths temporally (Figures 24 – 26). All positions displayed N_2O concentration peaks at or close to the water table on most of the dates studied.

The FE positions differed from each other more than expected, as they were presumed to receive similar inputs of nutrients and runoff from the adjacent field, and maintained similar soil physical properties (Figure 24). At T4, N_2O concentrations peaked within 60cm of the water table (above and below), with unclear patterning. At T5, on the other hand, there were two groupings of concentrations, in which the driest days in the middle of the summer peaked above the water table, while the sampling dates before and after the dry summer period peaked below the water table, at approximately the same depth as at T4 (with the exception of the flood date on DOY 333). The highest N_2O concentrations at this site were found during the driest periods.

The RL N_2O concentrations all peaked within +/- 25cm of the water table on all sampling occasions (Figure 25). During some periods, namely DOYs 171 and 255, both shortly after a rainstorm, smaller peaks were noticed deeper below the water table. The N_2O concentrations at the RL position on T5 displayed two groupings of peaks: 1) within 20cm above the water table and 5cm below it, and 2) between 30 and 80cm below the water table. The former groupings occurred during the summer and the latter during the spring and fall.

Little variability was visible with N_2O concentrations at the RS position (Figure 26). All profiles peaked between 25 and 75cm below the water table except for one outlier on DOY 190, in which the peaking concentration was the highest and lowest below the water table (45.4 ppmv at a depth of 121cm below the water table). Overall, this site experienced the highest peaks out of all six zones and also displayed the most spatially consistent set of data.

The water table was always close to the surface at the SE, as can be seen with the profile concentrations. All dates analyzed had N_2O peaks within 5 – 10 cm of the water table, with little exception. Two dates during the summer, when the site dried out, experience peaks up to 50 cm below the water table.

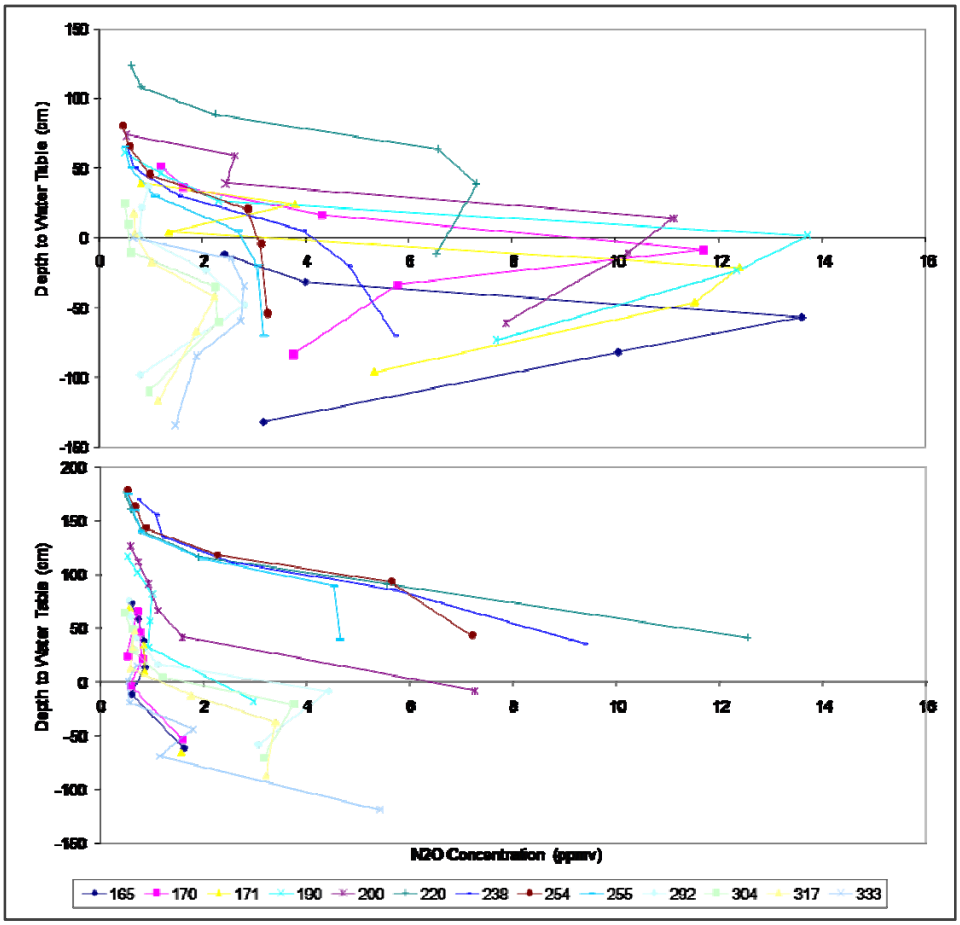

Figure 24. Field edge N_2O concentrations as a function of the water table. The zero line represents the water table elevation. (T4 top, T5 bottom)

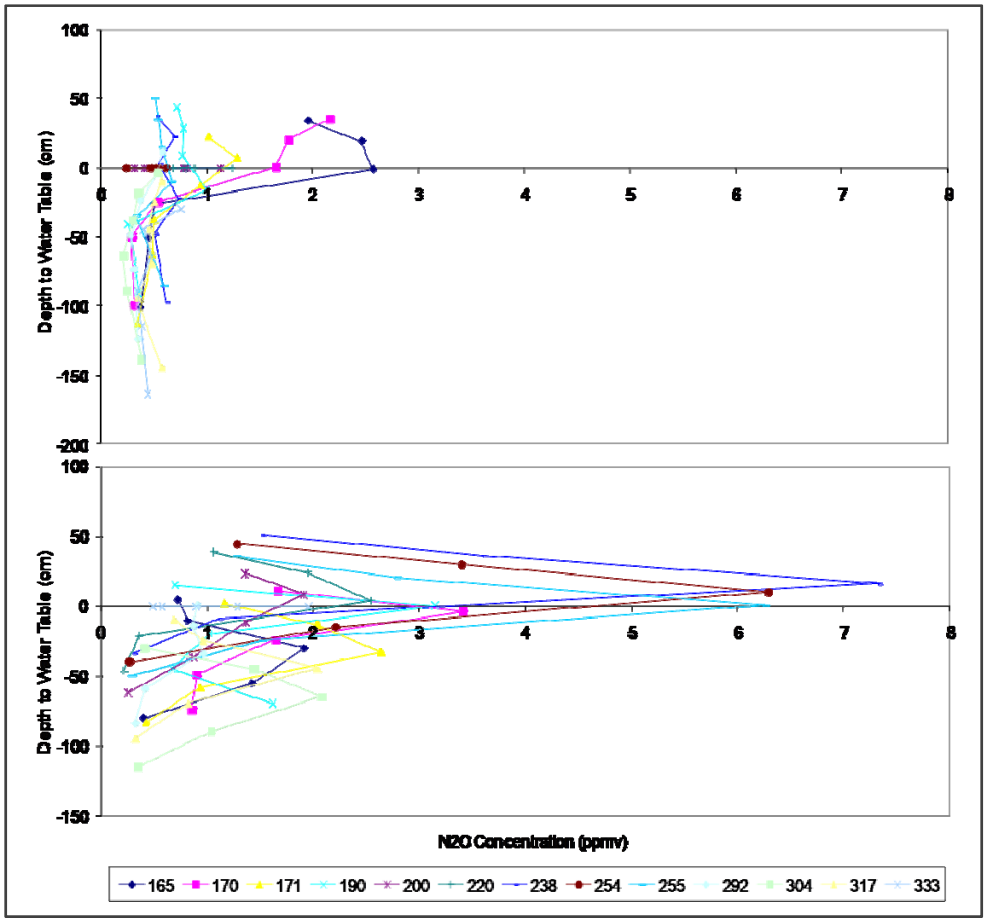

Figure 25. N_2O gas profile concentrations as a function of water table at T4 (top) and T5 (bottom) RL positions.

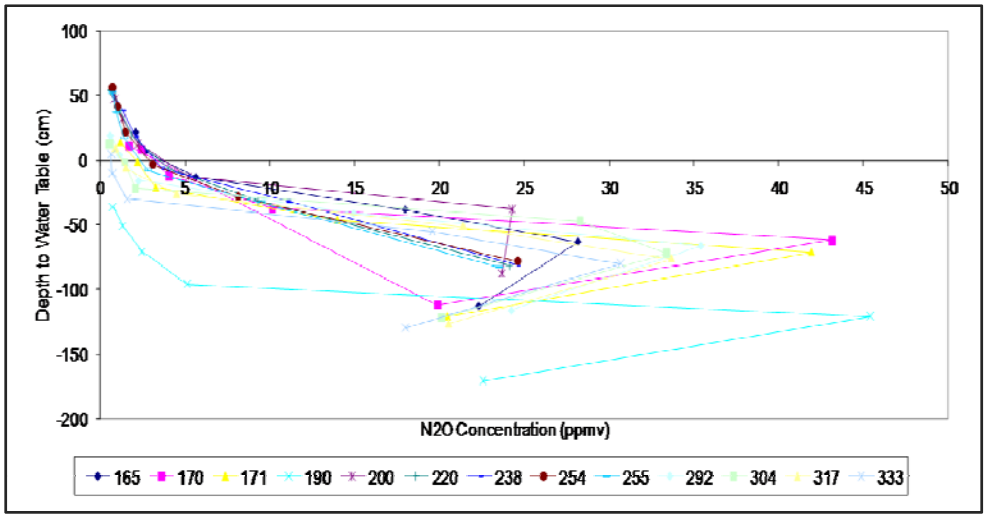

Figure 26. N_2O gas profile concentrations as a function of water table at the RS.

3.2.7 Summary

Nitrous oxide fluxes did not display significant differences between positions along two topographic gradients, as was expected. High spatial heterogeneity may have been partly responsible for the lack of spatial trends. However, positional differences were apparent with both physical and subsurface chemical properties of the six sites studied. Concentrations of NO_3 and NH_4 behaved predictably, with high NO_3 at the field edge, decreasing into the riparian zone towards the stream, and NH_4 highest at the stream edge. Along the non-stream transect (T5), NO_3 was high at the field edge and break in slope, or greatest topographic variation, while NH_4 was low in all locations. Dissolved organic carbon was consistent across the RZ. Subsurface N_2O gas also displayed variation between sites, with high concentrations at the FE, decreasing with distance into the RZ, following the NO_3 trends along T4. Similar to NO_3, N_2O along T5 was highest at the RS. Soil profile trends revealed patterns suggesting strong links between groundwater NO_3 and subsurface N_2O, however this did not result in spatial differences in surface fluxes. High bulk density and low porosity zones within each position may have been responsible for retarded movement of N_2O from zones of production towards the surface.

3.3 Temporal/Seasonal Trends in Nitrous Oxide Emissions and Related Chemistry

Changes in physical and biological factors with time can complicate spatial patterns, in which different sites behave in different ways, as well as maintaining spatial patterns that change with changing conditions. It was important to examine temporal trends to determine if certain periods of time were responsible for driving the visible spatial patterns in subsurface nutrients and N_2O, as well as the lack of spatial patterning with N_2O fluxes across the riparian zone when all data was merged. The results discussed in this section will follow as such: field season hydrology, seasonal/temporal N_2O fluxes, seasonal subsurface supply, and variability throughout a rain event (i.e. the impact of a rainfall event on N_2O fluxes and subsurface gases).

3.3.1 Field Season Hydrology

The seasonal hydrograph can be characterized by a parabolic curve; water table drawdown from the beginning of the season until the end of July, followed by an increase in water table elevation until the

sampling period ended in early November (at which point precipitation became more frequent, and the site was artificially flooded due to a release of the upstream reservoir) (Figure 27).

Precipitation events were somewhat isolated throughout the sampling season until the fall, when precipitation became more frequent. This was reflected in the water table increase around October 11th. Average water table depth below the surface at T4 for the SE was 29.5 cm (standard deviation 13 cm) and for the upland FE was 60 cm (standard deviation 33 cm). At T5, the upland FE average water table depth was 109 cm (standard deviation 54 cm) and the RL lowland was 24 cm (standard deviation 23 cm – highly fluctuating). Transect five was much drier than its counterpart over the whole season, likely due to the water table regulation of the stream at T4.

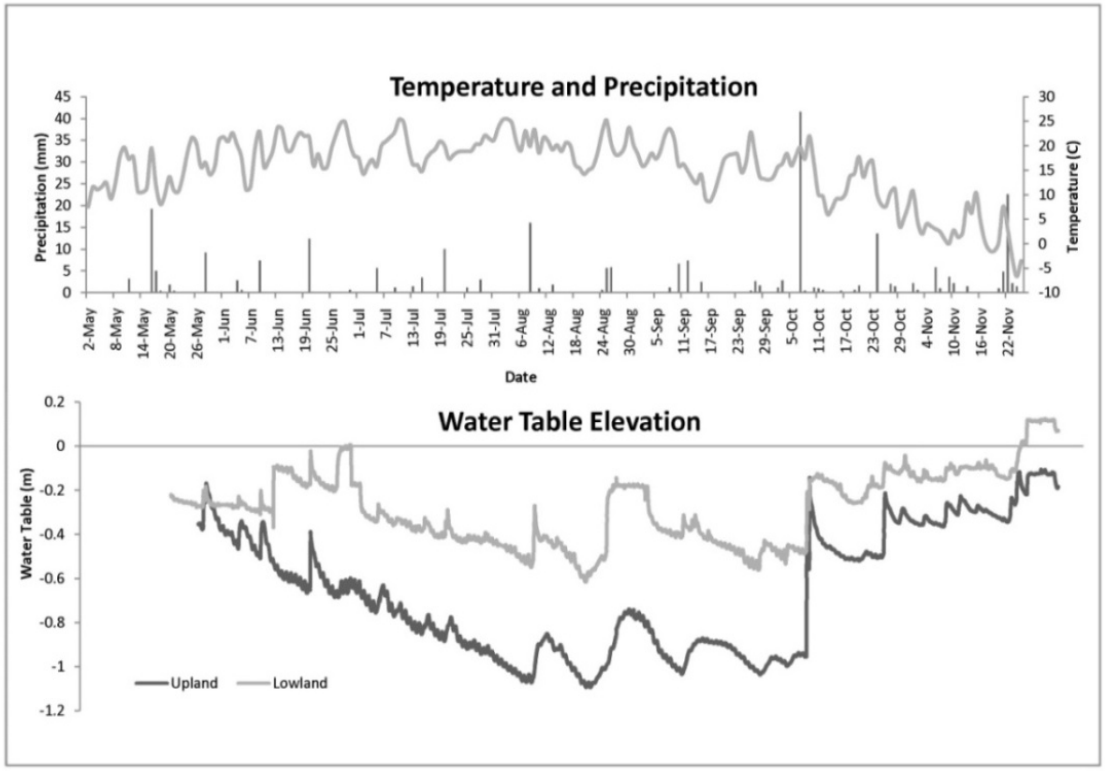

Figure 27. Hydroclimatology for the 2007 field season. The water table elevation graph (derived from T4) depicts many peaks that are not necessarily always tied to rain events – this is due the upstream dam being opened periodically throughout the season.

Maximum and minimum water table elevations plotted with average WT depth displays the seasonal variability on both transects (Figure 9). The FE positions at both T4 and T5 experienced similar ranges of water table depths, with the T5 FE water table consistently deeper than its counterpart. Less variation between max and min existed at the RS on T5, compared to the RL at T4,

however the former water table depths were consistently deeper than at T4. Little variation was visible in the lowland zone, likely due to the influence of the stream. The lowland RL at T5 displayed as much variation in water table depth over the season as the RS position. Water table elevation at both the FE and the SE positions of T4 reveal a drawdown from the beginning of July until the beginning of October, when precipitation events began to increase in magnitude and frequency, rewetting the area. Soil moisture data collected on each sampling event, integrated over a depth of 6 cm (from the surface), displays the same kind of drying out trend as seen with water table (Figure 28). At T5, all sites dried out over the summer more than they did at T4, likely as a result of the stream regulation on water table at T4. This is an important result as it reinforces the hydrologic and likely biochemical variability between T4 and T5 as a result of water table regulation from a stream. Towards the end of the season when the water table was beginning to increase again as a result of more rain events closer together, the RL moisture conditions increased to WFPS close to the SE, demonstrating a wetting up from the stream towards the FE.

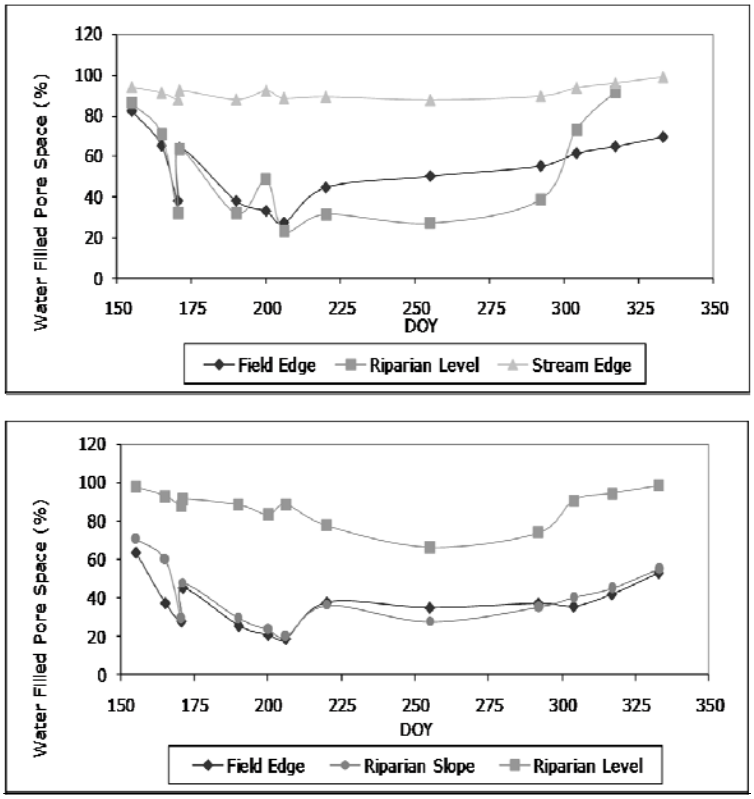

Figure 28. Water-filled pore space at each site over the sampling season.

3.3.2 Temporal Trends in Nitrous Oxide Emissions

The lack of consistent spatial trends is still present when examining the data as a function of season (Figure 29). Seasonality was determined by examining the hydrograph and choosing natural breaks as seasonal divides; spring (n = 4), summer (n= 5), and fall (n = 4). Because sampling was biased towards events, seasonality must be taken with caution. Non-significant trends are apparent, however, during a season, but are not consistent between all seasons. For instance, during the spring and summer at T4, fluxes were highest at the RL. During the fall, however, fluxes decreased from FE to SE. T5 fluxes, on the other hand, displayed an increase into the riparian zone during the summer, a decrease in the fall and highest fluxes at the RS in the spring. The high summer flux in the RL, along with the high RL spring flux on T4, are data points that stand out. Consumption fluxes are more prevalent along T5, especially during the fall. This makes for high variability within datasets.

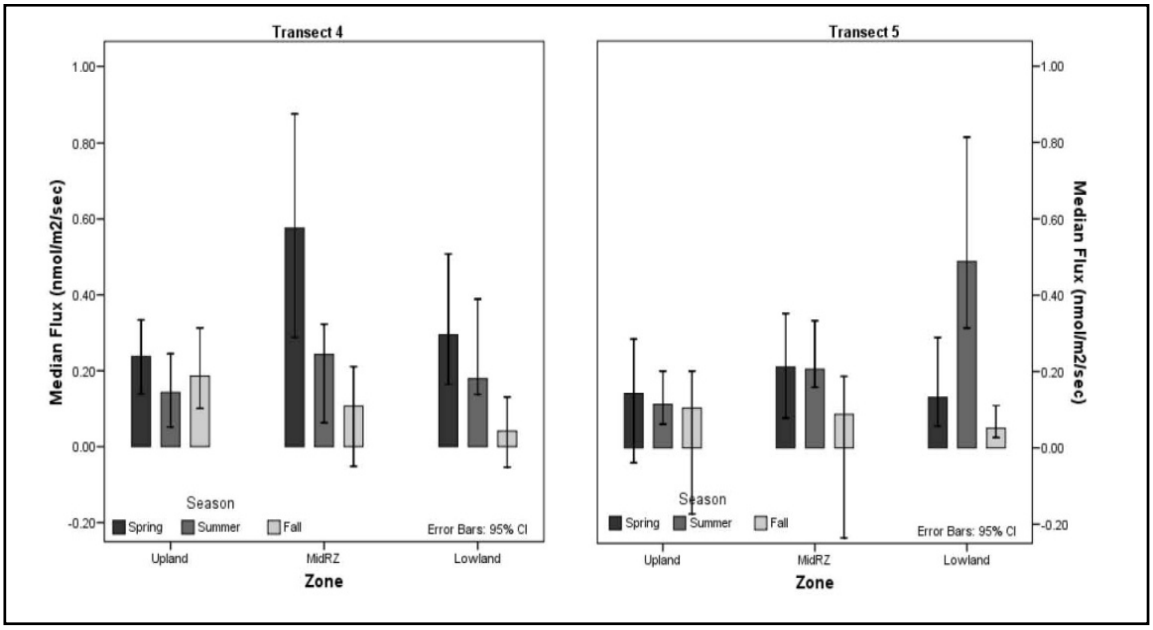

Figure 29. Seasonal nitrous oxide fluxes.

As the variability within datasets for seasonally averaged data was so high, the fluxes were also examined as an average of the three collars for each sampling date of the season (Figure 30). Again, no discernable trends exist. One set of FE fluxes from DOY 170 at T4 (which was taken after a rain event) covers the entire range of N_2O flux data. The three collars produced values on that date of 0.158, 0.238 and 3.01 nmol m^2 sec^{-1}, with WFPS values of 41.3, 35.9 and 36.2%, respectively. All other locations along this transect experienced similarly high within-site variability and high fluxes during the period of time from DOY 165 to 171.

During the drying out period of the summer, DOYs 190 and 200, the SE position experienced higher fluxes than elsewhere along the transect, where values were negative or close to zero. N_2O efflux averages were fairly consistent through the summer except for one FE flux on DOY 220 with higher variability than the rest. During the fall, from DOY 304, the order of greatest to smallest magnitude fluxes was from the FE to the RL to the SE. The last day of sampling, DOY 333 during the flood, the FE position experienced significantly higher fluxes than either of the other two zones, suggesting a possible mobilization of "trapped" N_2O.

Along T5, FE fluxes were generally lower than the RS or level positions, except at the beginning of the sampling season in which fluxes were highly variable and medians were higher than the other sites. Fluxes increased into the summer months to the maximum value reached at the RL on DOY 220, where the WFPS at 6 cm was an average of 77%, with high intra-site variability. The three collars on this date produced values of 0.808, 0.814 and 2.231 nmol m^2 sec^{-1}, with WFPS of 70.5, 84.4 and 78.3%, respectively. Fluxes decreased into the fall, to a minimum flux (consumption) during the flood period, at the FE and RS positions, with average WFPS of 54%. WFPS did not appear to affect the magnitude of a flux on either transect.

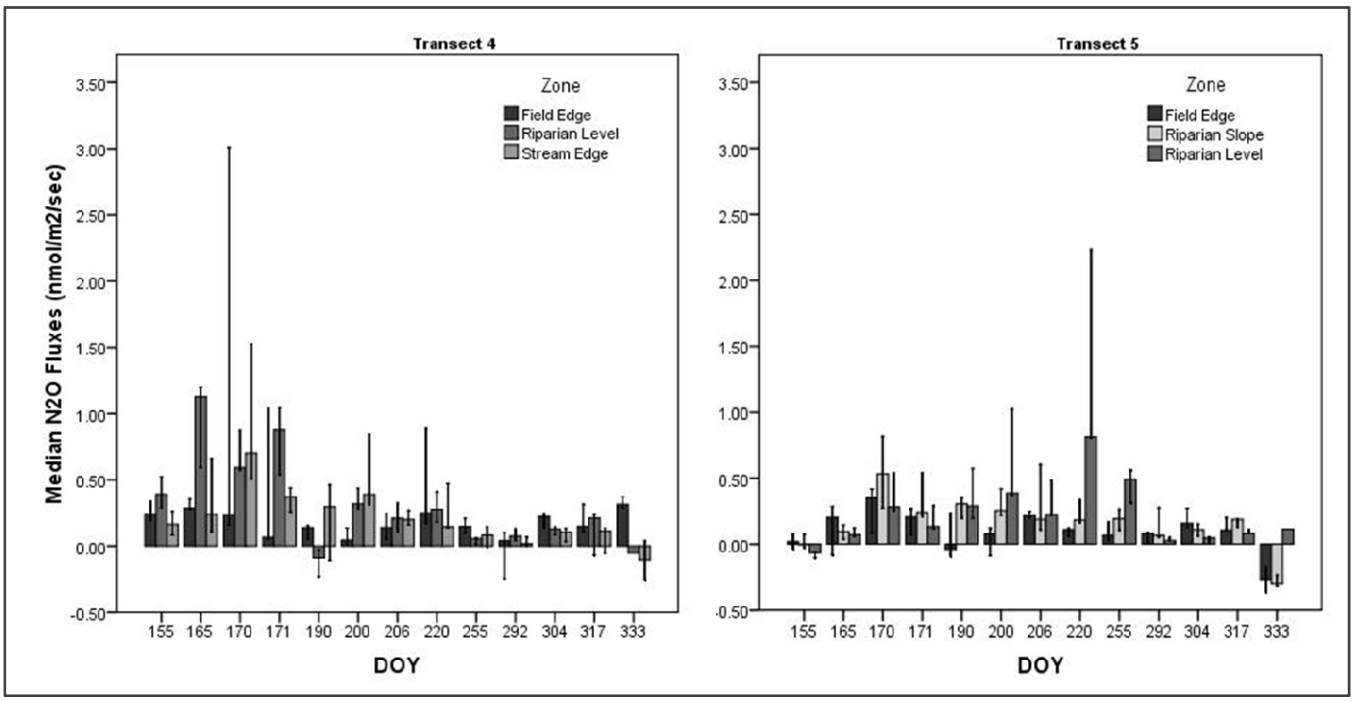

Figure 30. N_2O fluxes on each sampling date.

3.3.3 Seasonal Variability in Soil Nutrient Concentrations

3.3.3.1 Nitrate

Seasonal variability was observed at the FE with slightly higher concentrations in the fall at depth, and the lowest concentrations (of the three seasons) in the summer time (Figure 31). Since the other two sites along this transect displayed such low concentrations of the nutrient, no trends were visible and were considered negligible.

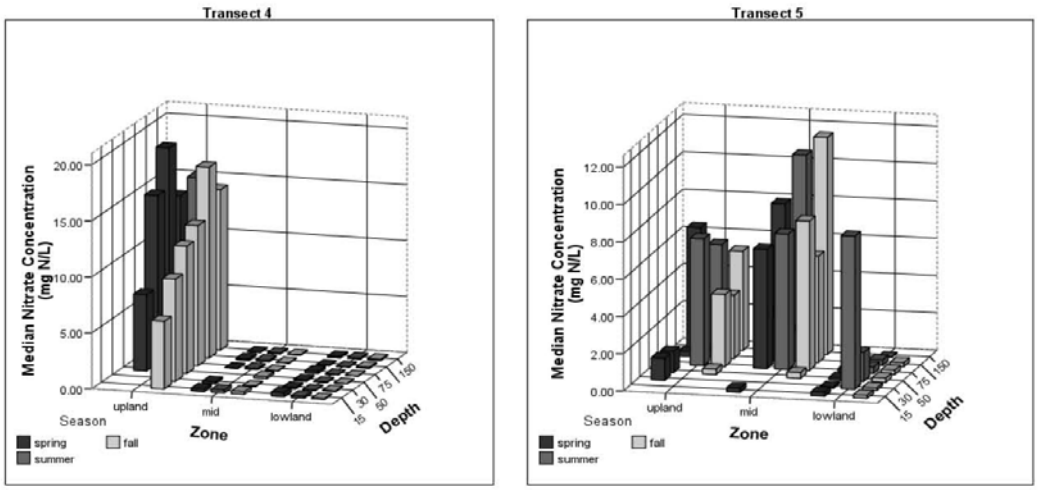

Figure 31. Nitrate concentrations with depth and position along transects 4 and 5. Note the different y-axis scales.

The RL position on T5 displayed low nitrate levels in both spring and fall, contrasting a peak of nitrate in the shallow depths during the summer period, which may have been a result of a perched water table above 75 cm that was observed during periods of dryness in the summer, which could have acted as a "pool" for NO_3 received from upland areas. The RS position maintained the highest concentrations of nitrate, as well as high variability (not shown). The RL displayed very low concentrations of nitrate, similar to the RL of T4 (located approximately the same distance from the adjacent agricultural field).

The FE of T4 was found to maintain significantly higher nitrate concentrations than anywhere else in the riparian zone ($p < 0.05$), specifically at depths of 100 and 150 cm. Temporal periods displaying the highest concentrations (significantly – potentially "hot moments") were found on DOY 165 in the spring (during a non-event, warm sampling date), and 333 in the fall (during the artificially created flood).

Flow reversal periods, on sampling dates 220, 238, 254 and 255, did not seem to affect nitrate concentrations, or distribution of nitrate through the groundwater column. Water levels were low during that sampling period and therefore groundwater was only collected from the deepest depths, and often contained the same or marginally different concentrations of nitrate than at the same depths during regular flow periods.

3.3.3.2 Ammonium

In general, spring concentrations were higher than fall or summer, and increased with depth into the soil profile up until 75 cm and then decreased slightly (Figure 32). Less of a seasonal trend was visible at T5, however fall concentrations at all sites were low, and summer NH_4 levels were on par with springtime concentrations at the FE and RS, but higher ammonium levels deeper in the subsurface were visible at the RL position.

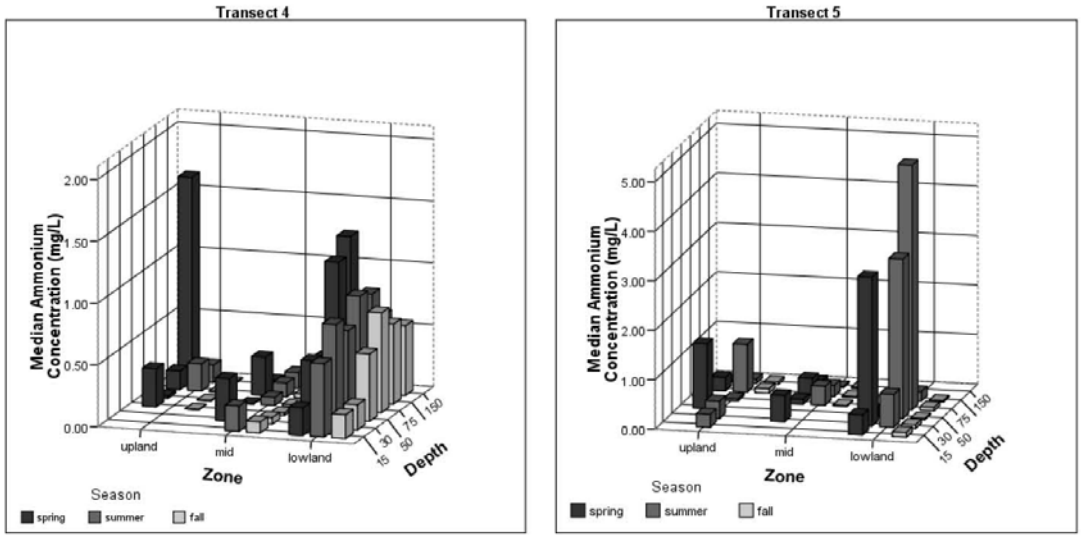

Figure 32. Ammonium concentrations with depth and position along transects 4 and 5.

Concentrations of ammonium displayed a difference between event and non-event samplings, with event-based NH_4 concentrations higher than non-event concentrations. Differences were significant at the FE ($p < 0.05$), but not so at either the RL or SE of T4. There were no significant differences between event/non-event samplings along T5, nor in concentrations between the zones studied.

3.3.3.3 DOC

No discernable trends were apparent in any of the six positions (Figure 33). DOC levels were consistently higher than what has been reported as limiting concentrations for microbial activity (ex.

Hill *et al.*, 2000) and therefore DOC was not considered an important index of N_2O production control at this site (spatially or seasonally).

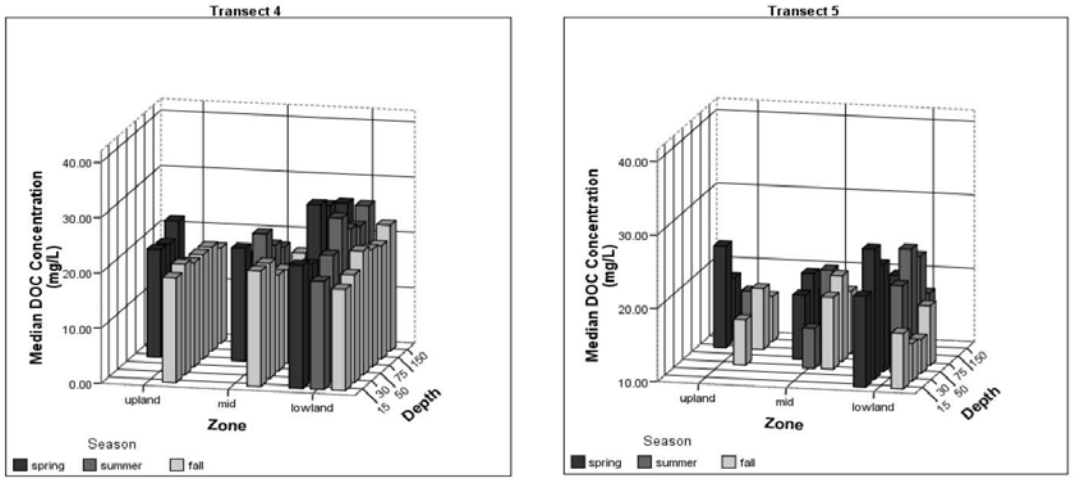

Figure 33. Dissolved Organic Carbon concentrations with depth and position along transects 4 and 5.

3.3.3.4 Dissolved Oxygen (DO)

DO was fairly consistent across the RZ (Figure 34). However, high variability was present in both transects' datasets, and therefore there were no significant differences between sites (not shown), with the exception of a difference between the FE and the SE zones of T4. DO increased slightly in the lower depths on occasions of flow reversals in the riparian zone. This occurred along both transects, but was more prominent along T5; it was expected that T4 would experience more of a change in DO because of input from surface water through the hyporheic zone, however this was not the case.

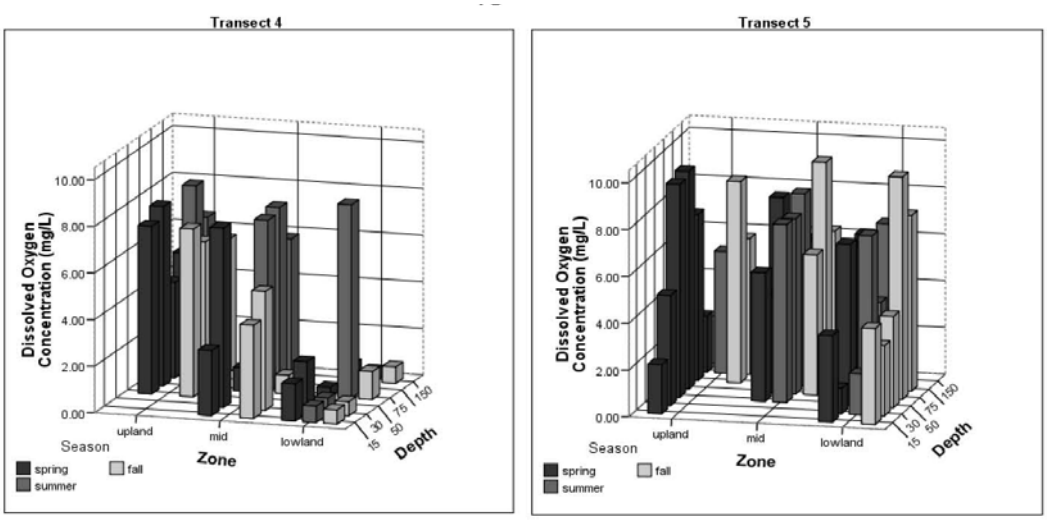

Figure 34. Dissolved Oxygen concentrations with depth and position along T4 and T5.

3.3.3.5 Subsurface N_2O

During both the spring and summer seasons, variability in N_2O concentrations was higher than during the fall, and increased with depth; at 100 cm the most variability was seen during the spring, and the same was seen during the summer at 75 cm (Figure 35). On T5, the upland zone does not appear to be a location in which N_2O is produced in high concentrations, rather the RS took that role in all seasons. N_2O increased with depth at all riparian positions, but to a greater extent at the RL. Little variability was seen in the shallow depths; the highest variability was detected in the RS at 75 cm during the spring.

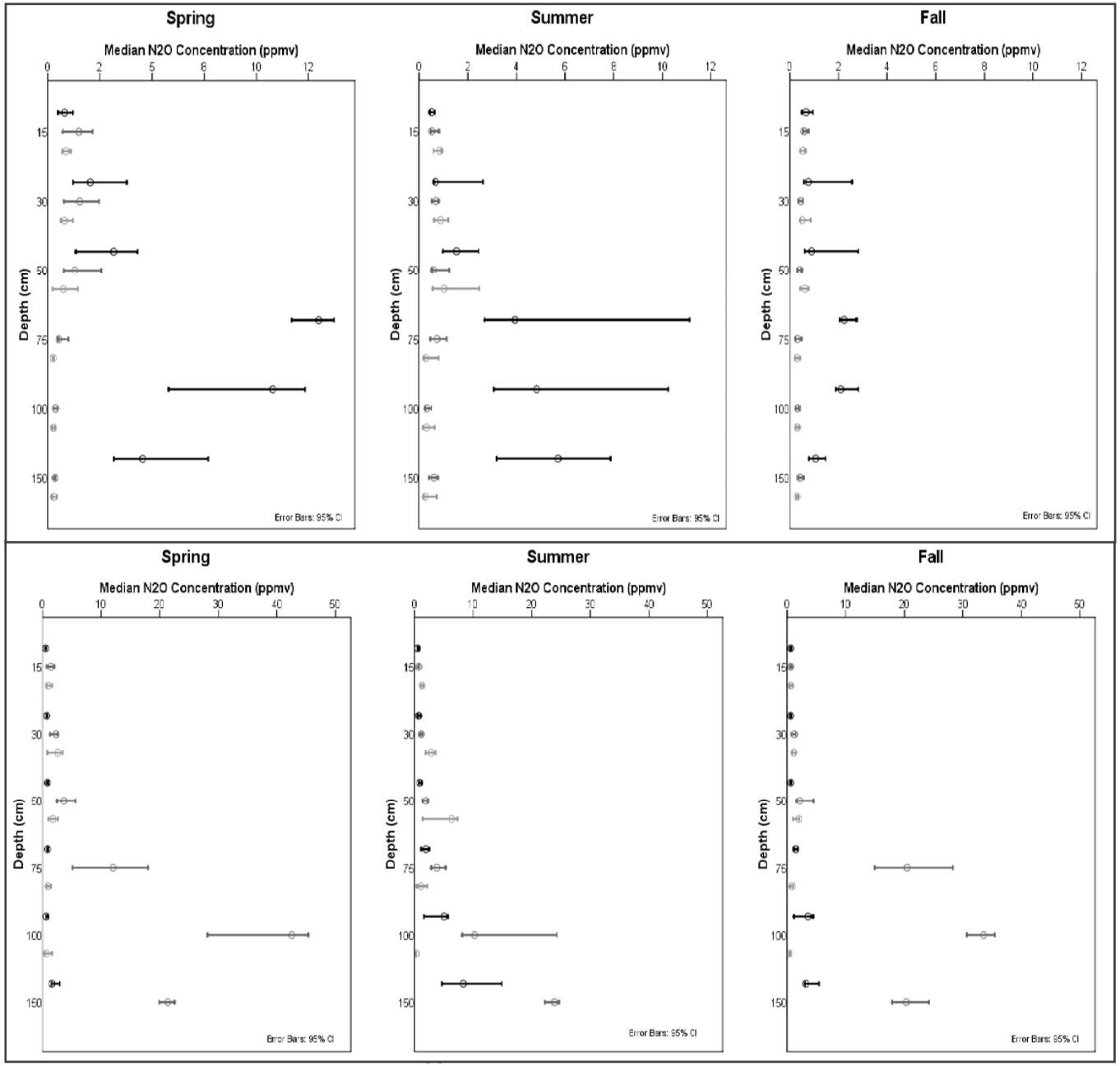

Figure 35. Subsurface N_2O profiles T4 (top), T5 (bottom). Darkest points represent the upland, medium darkness represents zone, and lightest points represent the lowland zones.

3.3.4 Variability in Nitrous Oxide Throughout a Rain Event

Temporal and seasonal factors (such as soil moisture and temperature) were hypothesized to drive the trends (or lack thereof) in N_2O fluxes across the riparian zone. In order to examine these potential driving factors, datasets previously mentioned were examined over time (seasonally), as well as throughout a precipitation event, in which measurements were collected immediately prior to and following a short, intense storm, as well as the following day. These data provide an excellent opportunity to examine the changes in N_2O dynamics over quick changes in moisture, as well as to look at how quickly (or slowly) the system can respond to these changes.

3.3.4.1 N_2O Fluxes

During this event, captured on DOY 170, transect four experienced very little change between antecedent conditions (DOY 165) and immediately following the event (Figure 36). At T5, a greater impact of the precipitation event was noticed. Pre-event, no significant difference was visible in flux between the three positions, however the FE was slightly higher. Immediately following the rain event, all positions experienced an increase in N_2O flux, with the RS and RL positions showing significantly greater fluxes than prior to the event. The RS experienced the greatest increase, and also the greatest variability. A day after the event, fluxes dropped (not significantly), with the RS and RL positions remaining significantly higher than the pre-event conditions, suggesting a lag effect of the rainfall and impact of antecedent moisture conditions on flux dynamics. During this period, ground level moisture conditions displayed a lag in moisture changes as well (Figure 37). Following day 165, which was a wetter period, surface soils dried up until the rain event on DOY 170. The moisture levels taken were directly following the event, and actually displayed smaller values than those from the previous sampling event (DOY 165) because of the dry out between dates. The following day at all sites, however, moisture values had increased as a result of the rain event, but were still lower than WFPS measurements taken on DOY 165. The only exception was at the FE on T5, whose moisture content on DOY 171 was greater than DOY 165.

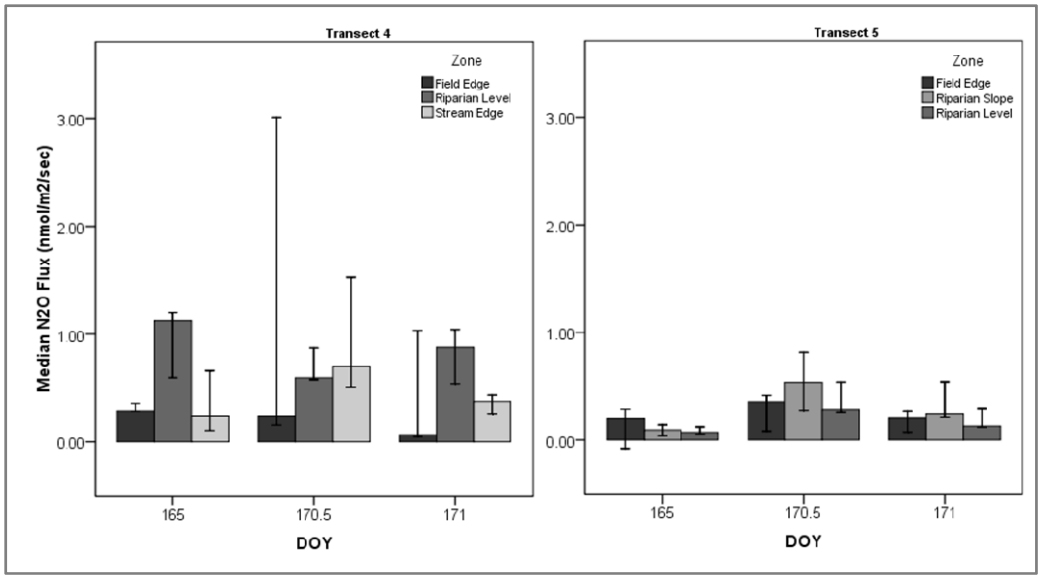

Figure 36. N_2O fluxes through a rain event. Error bars represent 95% confidence intervals, and are highest immediately following the event at the field edge on T4. DOY 170.5 represents the time immediately following the rain event.

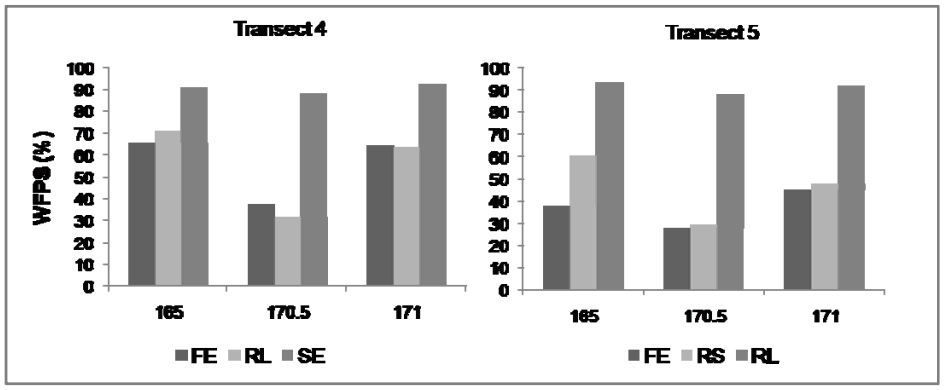

Figure 37. Water-filled pore space through the rain event.

3.3.4.2 Subsurface N_2O Concentrations

The rain event did not make an impact at all locations, specifically the field edges that were the driest. At the FE position of T4, peak concentration depth was at the 75 cm depth level all four measurement events (5 days prior to the event, immediately before and after, and then the following day) (Figure 38 a). Peak concentrations were slightly higher before the rain event, decreasing immediately following the event, maintaining the same profile shape, with the production zone still prevalent. After the rain event, on the following day, a new peak was detected (above the water table). This suggests a microsite was created, possibly due to infiltration of precipitation, allowing for a zone of low-oxygen and ideal conditions for denitrification. The FE of transect five behaved differently than its

counterpart on T4 – there was little to no change in the peak depth of N_2O, nor in the concentration (Figure 38 b).

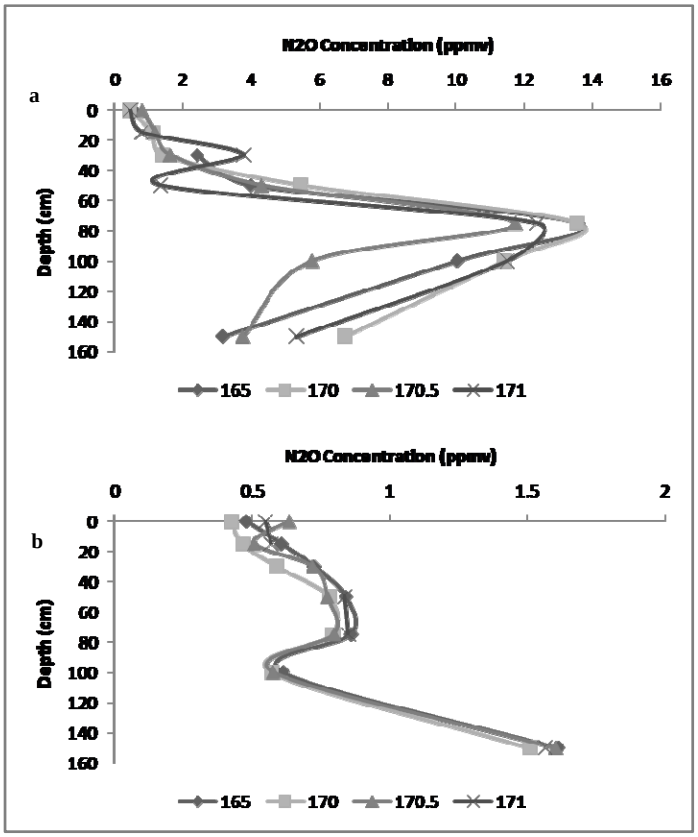

Figure 38 N_2O subsurface gas concentrations during a rain event. a) T4 FE; b) T5 FE.

The RL position of T4 experienced the greatest peak of N_2O concentration (at the water table) on DOY 165, five days prior to the event (Figure 39 a). The water table was also a location in which the soil temperatures peaked (data not shown). The N_2O peak remained at the same depth, with a lower concentration, just before the rainfall. Following the rain event, the peak increased in elevation with the rising water table, but did not reach the same concentrations as had previously been detected prior to the event. Concentrations were lowest the following day. The RL on T5 displayed the most noticeable change with precipitation. Peaks of N_2O were greatest immediately before and immediately after the rainfall event, with the post-event peak at a lower depth than the pre-event peak (Figure 39 b), which means that the denitrification zone may have shifted deeper below the water table post-rainfall.

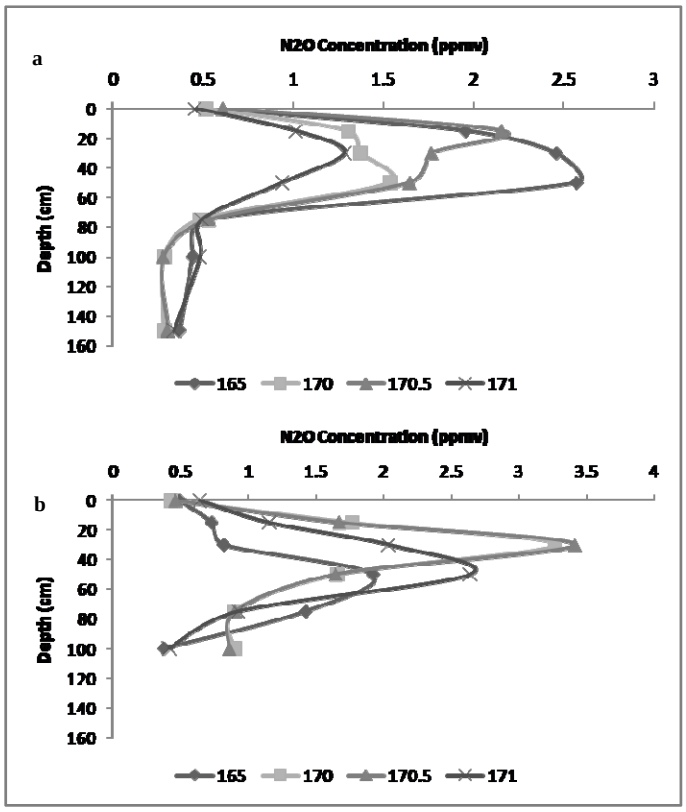

Figure 39. N_2O subsurface profile concentrations at the RL positions during a rain event. a) T4, b) T5.

The SE maintained low N_2O concentrations throughout this rain event, with an increase in peak concentrations and peak depth, the day following the rainfall (Figure 40). Before the event, peak N_2O concentrations were shallow and low. Following the event, peaks occurred between 20 and 30 cm below the water table, with smaller peaks at the shallowest profile array (15 cm).

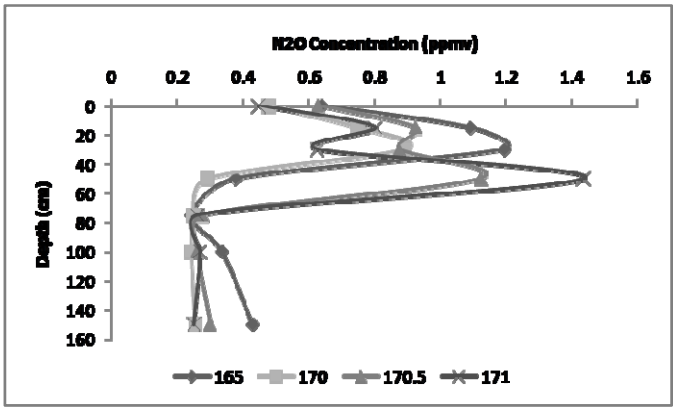

Figure 40. N_2O subsurface concentrations during a rain event at the SE.

The RS along T5 experienced the highest N_2O peaks of all six zones (Figure 41). The peaks appeared at approximately 60 cm below the water table before and after the rain event. The highest concentration was apparent just before the rain event, and decreased slightly following the precipitation, and again the day after. However these decreases in peak concentration were minimal and insignificant.

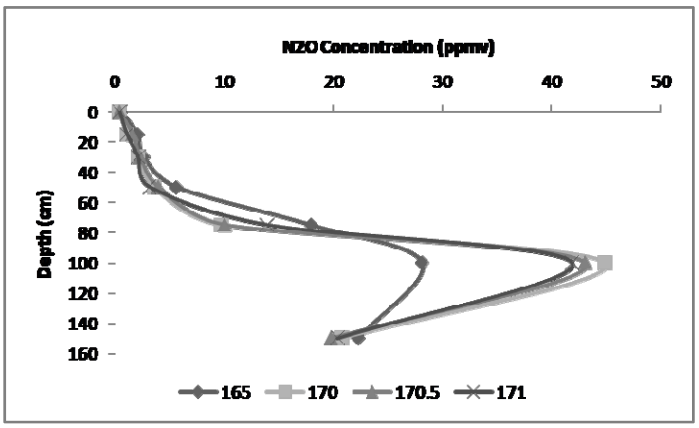

Figure 41. N_2O subsurface gas and temperature profiles in the RS zone.

It is important to note that all differences seen between samples taken before, during or after the event, may not be significant due to natural variability beneath the surface. Two more gas profiler arrays located at each site (sampling in triplicate) would have aided in determining whether or not these differences were significant. With this caveat, it appears that the rain event captured did not greatly affect subsurface concentrations of N_2O, as was expected.

Chapter 4
Discussion

4.1 Spatial Distribution of Nitrous Oxide and Associated Controls on Nitrous Oxide Production

Topography affects the spatial distribution of soil moisture, temperature and organic matter content (Florinsky, *et al.*, 2002), which have all been linked to N_2O. Because of the topographical nature of riparian zones, and in particular the one studied here, and with varying inputs of both surface and groundwater, N_2O production was expected to be highly variable, and dependent upon many factors *in situ*. A summary of N_2O fluxes from similar studies can be found in Table 9. Hefting *et al.* (2003) found low FE fluxes (0.5 nmol m^{-2} sec^{-1}) with little seasonal variation, high mid riparian zone fluxes in each of spring, summer and fall, and similar fluxes at the SE, not significantly different from the mid riparian zone. Venterea *et al.*'s (2003) results differed from Hefting's with a consumption flux summer average (negative values) and a fall average of 0 nmol m^{-2} sec^{-1}. Machefert *et al.* (2002) reviewed N_2O studies performed in various European ecosystems (n = 33); three were riparian zones or forested wetlands. Fluxes determined during this study fell within the range of those previously completed in similar riparian environments. Within these studies, Hefting's (2003) were similarly spread out across the riparian zone, and demonstrated differences between the three sites, specifically between the FE and the mid- and lowland riparian zones. Despite results of other studies, such as Hefting *et al.* (2003), and an expectation of spatial patterning resulting from topography, no significant differences were found in this study among topographic positions. The climate during the 2007 field season was abnormally dry, which may have led to the lack of difference in N_2O emissions among sites. When soil is aerated and dry, nitrification dominates and NO is often a more common byproduct than N_2O (Davidson *et al.*, 2000) because production of N_2O is inhibited (Davidson *et al.*, 2004). This is important for future attempts at determining riparian zone N_2O budgets, as these results imply a lack of importance for placement of GHG collection chambers during dry years, but other results suggest that average moisture or wet years might display more dominant spatial trends.

Table 9. Ranges and means of N_2O fluxes in similar environments and studies.

Location	Ecosystem	**N_2O Flux (nmol m^{-2} sec^{-1})**	**Source**
Netherlands	Forested Riparian Zone	0.5 – 4.0	Hefting *et al.*, 2003
Massachusetts, USA	Forest (Pine, Hardwood)	-5.0 – 0	Venterea *et al.*, 2003
Europe (n = 3)	Riparian Zones and Forested Wetlands	0.05 – 2.76	Machefert *et al.*, 2002
Louisiana, USA	Coastal Riparian Zone	0.05 (mean)	Yu *et al.*, 2008
Brittany, France	Forested Riparian Zone	3.73 (mean)	Clement *et al.*, 2002
Southern Ontario	Forested Riparian Zone	-0.28 – 1.3	DeSimone *et al.*, 2009 (present work)

4.1.1 Subsurface Production Controls

The purpose of collecting subsurface N_2O and nutrients concentrations was to try to elucidate process, and especially location of processes occurring, in order to better understand what drives production and movement of gases subsequently released at the soil-atmosphere interface.

Groundwater concentrations of nutrients, specifically nitrate, behaved predictably, with high levels at the FE, and very low levels within the riparian zone along T4. However higher concentrations in the mid riparian zone, or riparian slope position were seen along T5. It is well known that most natural and anthropogenically introduced nitrate that enters riparian zones is attenuated within a short distance (Hill *et al.*, 2000; Hanson *et al.*, 1994; Peterjohn and Correll, 1984). The denitrification of nitrate is recognized as being the main production mechanism for N_2O in the subsurface, therefore nitrate concentrations are an important indicator and pair for comparison with subsurface gases to infer process and zones of production. High nitrate concentrations suggest a sustainable source or supply for denitrification microbes. However, since the sampling occurred as a "snapshot" of subsurface activities, a depleted supply of nitrate could also imply quick turnover of N. For instance, Hedin *et al.* (2000) found low NO_3 concentrations just inland of the soil-stream interface zone. Through isotopic analysis of ^{15}N in NO_3 and NH_4, they determined that the depletion was a result of rapid denitrification and loss of NO_3 via N_2O release. There were only a few positions in which strong relationships were found between nitrate and subsurface N_2O, suggesting that other nutrients or substrate may have been responsible for the microbial denitrification activity, or that the rate of NO_3 into the system was more important than the concentration at any given time (ex. Willems *et al.*, 1997; Groffman and Tiedje, 1989). Phosphorus is often a limiting nutrient for microbial activity, however it was not examined in this study due to sample and budgeting restrictions. DOC was found

in high concentrations across the riparian zone and thus should not be deemed as limiting microbial activity (Hill *et al.* (2000) found a threshold for DOC at approximately 8 mg L^{-1}). Soil C:N ratios, determined on one occasion at various depths along both transects, can help to elucidate the health of the environment for microbial activity. On average, microbes require eight parts of carbon for every part of nitrogen, however because only a fraction of the carbon incorporated into microbes is used for cell development, they need to find approximately 24 parts of carbon for every one of nitrogen (Brady and Weil, 1999). High organic carbon to inorganic nitrogen ratios can stimulate microbial growth and consumption of nitrogen species, while low ratios can result in excess NH_4 and NO_3 (relative to microbial requirements) (Pierzynski *et al.*, 2005). In this study, the average C:N ratio was 12.3, which is fairly low, but has been seen in similar environments (ex. Maljanen *et al.*, 2003; Hedin *et al.*, 1997). These low ratios may be an indication of mineralization as a main source of ammonium production (Hedin *et al.*, 1998), as higher ratios, in the order of 25:1, would indicate a balance between mineralization and immobilization (Pierzynski *et al.*, 2005), therefore resulting in minimal NH_4 in the subsurface. Despite the low ratios found in this study, however, concentrations of both NH_4 and NO_3 in the subsurface (in groundwater and extractable nutrients from the soil profile) were comparable to other studies (Table 10), suggesting their presence was common for this type of environment.

Subsurface N_2O concentrations exhibited high spatial heterogeneity among sites, with below ambient concentrations to high peaks up to 35ppmv. This range is slightly higher than other researchers' findings, but does not appear to be significantly different (Table 11). Spatial patterning was apparent along each transect, lending credibility to the hypothesis that production mechanisms among sites would differ, however the release of those gases at the surface did not follow subsurface trends. Soil depths with high nitrate concentrations in the upland displayed high concentrations of N_2O, below the measured water table level. Highest N_2O concentrations in the subsurface at the T5 RL were found in conjunction with high nitrate concentrations at depth in this zone, possibly suggesting denitrification activity at this level, or at least the potential for denitrification. However, analysis of N_2O profile concentrations, suggested that gases produced at a depth of 100 cm were not reaching the upper portion of the soil profile (the shallowest gas profile array collected gases from a depth of 7.5 to 22.5 cm below the surface).

Table 10. Ranges of extractable NO_3-N and groundwater NO_3-N from similar study sites.

Location	Ext. NO_3 (ug/g as N)	GW NO_3 (mg/l as N)	Source
Maryland, USA		0.7 – 11	Peterjohn and Correll, 1984
Michigan, USA	0 – 12		Groffman and Tiedje, 1989
Rhode Island, USA		0.1 – 7.0	Hanson *et al.*, 1994
Michigan, USA		0 – 3.8	Hedin *et al.*, 1997
Pennsylvania, USA	0.8 – 2.1		Bowden *et al.*, 2000
Brittany, FR	1.1 – 8.9 (g N /kg)	0.98 – 9.3	Clement *et al.*, 2002
Maryland, USA	0 – 0.75		Groffman *et al.*, 2002
Southern Ontario, CA	0.2 – 8.9	0.0 – 13	DeSimone *et al.*, 2008 (present work)

Table 11. Subsurface N_2O concentrations.

Location	Mean Subsurface N_2O (ppmv)	Source
Southern England	10 – 99	Clough *et al.*, 1999
Eastern Finland	0.3 – 8.5	Maljanen *et al.*, 2003
Germany	0.3	Muller *et al.*, 2004
Germany	2.9 (ppm)	Reth *et al.*, 2008
Southern Ontario	35	DeSimone *et al.*, 2009 (present work)

4.1.1.1 Denitrification Potential and Activity

Denitrification rates were not analyzed for this specific project, however another study at this site examined four depths along a transect adjacent to T4, and found that denitrification potential was highest in the surface horizon, and decreased with depth, regardless of distance into the riparian zone or season (Leoni, 2008). As the gas sampler arrays displayed higher N_2O concentrations with depth (to a point, peaking at the apparent optimum production environment), a limiting factor must have existed that did not allow the microbial potentials to be reached.

Denitrification is understood to be limited by organic carbon, nutrient availability and low oxygen conditions (Clement *et al.*, 2002). In this study, DOC was consistent across the riparian zone and with depth. Extractable nitrate and ammonium were analyzed from the same samples as C:N concentrations, and were sampled just once during the study period due to budgeting reasons (extractable nutrients have been found to be relatively stable on a seasonal timescale (ex. Groffman and Tiedje, 1989)). Extractable nitrate was highest at shallow depths, especially at the field edges and mid riparian zones on both transects. Extractable nutrients have been demonstrated to maintain significant spatial patterns, specifically with depth (Clement *et al.*, 2002). Some studies have

determined that no significant relationships exists between extractable NO_3-N and measured denitrification potential (Schnabel *et al.*, 1997; Zak and Grigal, 1991), while others determined that they are strongly correlated (Groffman *et al.*, 2002). At this site, correlations were only found during the spring season ($r^2 = 0.933$, $p < 0.01$ (Leoni, 2008)). At other sites, areas with extractable NH_4 as the dominant inorganic nitrogen species displayed lower N_2O emissions than those with NO_3 as a dominant species (Davidson *et al.*, 2000). In this study extractable NH_4 was consistently, but not significantly, higher than NO_3, which might explain why N_2O lacked spatial trends. Substrate concentrations of nitrate and ammonium collected regularly during sampling events, displayed trends with depth and across the riparian zone, with peaks often coinciding with subsurface concentration peaks of N_2O. This might suggest that these locations maintain optimal conditions for denitrification, i.e. have a high denitrification potential. Despite this, higher fluxes of N_2O at these locations were not present.

4.1.1.2 Discrepancy Between Subsurface N_2O Concentrations and N_2O Fluxes

Nitrous oxide in the subsurface air and porewater is an indication of denitrification activity at a snapshot in time. In this study, there were differences in subsurface N_2O with depth and across the riparian zone (among positions and between transects). This may suggest that denitrification is controlled by something other than DOC and nitrate availability (oxygen may be depleted in pockets within the soil profile, even above the water table). In all the N_2O profiles, highest concentrations were at depth, most often below the water table. These concentrations always decreased towards the surface and approached ambient air concentrations. In order for a gas to diffuse towards the surface and then into the atmosphere, a concentration gradient is required (see section 1.3.1). However, regardless of the fact that subsurface N_2O concentrations just below the surface were at and sometimes below ambient concentrations, N_2O fluxes were still recorded. And, despite there being significant differences in subsurface production and concentrations of N_2O at depth, no significant differences in fluxes were detected at the surface. The contribution of subsurface-produced N_2O to the surface fluxes is still poorly understood (Well *et al.*, 2001), however these data may suggest several mechanisms. One, most of the microbially-produced N_2O that reaches the surface is produced in the very shallow upper layer of the soil profile, in microsites of low oxygen (as the water table may not reach the surface on all occasions). In this case, the surface fluxes must not be driven by production at depth (i.e. concentration gradients driving gas diffusion at the surface are based upon the production occurring within the shallow subsurface) because of the lack of spatial trending across the riparian

zone specific to this study. However researchers have found both that N_2O fluxes were a result of gases produced > 20 cm below the surface (Muller *et al.*, 2004; Well *et al.*, 2001), and at depths < 20 cm of the soil profile (Cannavo *et al.*, 2004; Clement *et al.*, 2002). Ball *et al.* (1997) found that production of N_2O was likely controlled by soil processes below 20 cm, while emission processes were controlled in the top 0-10 cm of the soil profile, thereby presenting a complex set of processes that control two aspects of N_2O dynamics in these types of landscapes. Another possibility is one that may be related to the drought conditions experienced during this study's sampling period. Florinsky *et al.* (2004) found similar results when they examined the topographic controls on denitrification and N_2O, in which dry soil moisture conditions resulted in a lack of dependence of spatial distribution of soil moisture (soil morphology). The low soil moisture conditions may have created a sort of "oxic blanket" across the ecosystem, affecting the N_2O:N_2 ratio. As N_2O produced at denitrification sites diffuses towards the surface, the N_2O:N_2 ratio decreases (Clough *et al.*, 1999). Several studies reporting N_2O fluxes have noticed negative or consumption fluxes, which have also been found at this field site, but few of these studies have discussed why these results might occur, unless to say that there was a lack of understanding of N_2O uptake in soils (ex. Yates *et al.*, 2006; Verchot *et al.*, 1999; Jordan *et al.*, 1998), and net N_2O uptake has not been specifically studied (Chapuis-Lardy *et al.*, 2007). However, the soil mechanisms that can uptake atmospheric N_2O may also be responsible for the lack of difference among topographic positions in this study, in which the climate was anomalously dry. Nitrifier denitrification occurs in low-oxygen environments in which ammonium is oxidized to nitrite, and then reduced to nitric oxide, N_2O and finally N_2, by the *same* group of organisms; it is thought to play a role in the production and release of N_2O in natural systems (Wrage *et al.*, 2001). It may also play a role in the consumption of N_2O, as some nitrifiers have been found to possess the capability of denitrification, thereby reducing N_2O to N_2 (Chapuis-Lardy *et al.*, 2007). Aerobic denitrification occurs in specific microbial species that have developed the capability of reduction in the presence of oxygen (Robertson *et al.*,, 1995; Lloyd *et al.*, 1987). This may also contribute to the decline in N_2O as the gas diffuses into upper, dryer layers of the soil profile, where aerobic denitrifiers can reduce N_2O to N_2. This latter process is still not very well understood (Chapuis-Lardy *et al.*, 2007). A third contributive mechanism for the lack of spatial trending in N_2O emissions is the soil physical properties, and zones of low porosity/high bulk density. These layers may act as confining layers (high tortuosity), causing a retardation of gas diffusion towards the surface, resulting in low emissions across the riparian zone, despite differences in production concentrations among topographic positions (see 4.1.5 for more information).

4.1.1.3 Natural Heterogeneity Overshadowing Spatial Trends

Natural sites are often heterogeneous with respect to microbial activity and resulting nutrient transformations, likely resulting from microsites of optimal moisture levels and organic carbon concentrations. High spatial variability in N_2O fluxes have been demonstrated in other research studies, ranging from 15 to 350%, for replicates of three to eight samples (Freibauer and Kaltschmitt, 2003). One objective of this study was to determine whether or not intra-site heterogeneity, or variability, overshadowed the differences between sites along each transect. The hypothesis was that there would be differences between sites as a result of varying hydrology and topography. When the results of this study showed the contrary, the data were examined to determine whether or not heterogeneity was the root of the unexpected results. This was accomplished by taking triplicate gas flux measurements at each site, and then comparing the standard deviation to the triplicate mean in order to point out sampling periods and sites with high variability. Standard deviations were also calculated for between-site comparisons using the means from the three sites along each transect. Results indicated several areas and dates of study in which the intra-site variability did seem to overshadow the potential differences between sites.

Experimentation with another set of greenhouse gas collars, whose surface area was greater than the total surface area from this study's three small collars combined, also examined the question of spatial patterning in the riparian zone and intra-site variability. Integrating the flux measurements over a larger surface area, may reduce the effects of spatial heterogeneity, and comparing that with contemporaneous fluxes from three smaller chambers, helped to corroborate the previously stated results. In this experiment, it was found that there were no significant differences between the two sets of collars. If this is the case, then it would imply that intra-site variability did not necessarily account for the lack of spatial variability, suggesting it simply did not exist in this riparian zone. This corroborates other findings in this study that suggest placement for GHG collection chambers within a heterogeneous riparian zone was unimportant. These results could also be resultant from the unusually dry field season in which the data were collected, essentially creating an "oxic blanket" effect across the riparian zone through which a fairly consistent flux of N_2O could reach the surface, regardless of volume of production below the surface (as discussed above).

4.1.2 Nutrient relationships as a proxy for process delineation

Relationships between nutrient concentrations can elucidate production mechanisms related to the redox potential in the soil profile. The distribution of electron donors (oxidizable carbon such as

DOC) is often organized in a thermodynamically derived order with depth into the soil profile (Hedin *et al.*, 1998). Because of this, nutrient cycling by microbes follows the redox sequence: denitrification, sulphate reduction, methanogenesis. It stands to reason then, that the concentrations of various nutrients and electron donors, specifically NO_3, NH_4, SO_4 and DOC, would relate to one another in a way that demonstrates the thermodynamics of the redox sequence. For instance, nitrate and ammonium cannot exist together in equilibrium unless they are present in zones of active nitrification (Hedin *et al.*, 1998), which occurs in aerobic environments. Most studies performed in similar environments indicate that the dominant nitrate removal process is denitrification, and that this process is also responsible for the majority of N_2O gas produced (Cannavo *et al.*, 2004; Clement *et al.*, 2002; Cey *et al.*, 1999; Willems *et al.*, 1997; Peterjohn and Correll, 1984). The scatterplots between NH_4 and NO_3 determined in this study revealed a mutually exclusive relationship, suggesting denitrification as a dominant process. This was found in all sampling events except for two, indicating thermodynamic disequilibrium and likely zones of active nitrification: T4 FE and SE (at depth). Nitrification is performed by microbes that require oxygen, and therefore aerobic environments. Dissolved oxygen levels at a depth of 150 cm on T4 FE were largely above 2 mg L^{-1} (median of 5 mg L^{-1}), which has shown to be a cutoff for aerobic/low-oxygen environments (Oh and Silverstein, 1999). The presence of oxygen at this depth, even at the FE where the water table was always low, suggests a flow path for oxygenated groundwater, originating from outside of the riparian zone. At the SE, however, DO levels were consistently low at all depths, with values ranging from 0.3 to 0.7 mg L^{-1}. It seems unlikely that nitrification would be occurring at such low oxygen levels. Therefore we might assume that the concentrations of both nitrate and ammonium that made this site an apparent outlier to the general regression trend were not significantly different enough to suggest a zone of active nitrification, or this outlier may also be an indication of aerobic denitrification. These are only speculations as conclusive evidence via collected data are not available in this study.

The relationship between NO_3 and subsurface N_2O is scattered and lacks patterning. If NO_3 concentrations decrease upon N_2O production, the relationship should be inverse and potentially linear. However this was not the case. Similar results were found in Weller *et al*. (1994) study in a similar forested riparian zone. Conversely, Hedin *et al*. (1998) found a strong positive relationship between these compounds. Weller suggested their results were due to other denitrification controls (i.e. other nutrients), while Hedin related it more to NO_3 supply and similar spatial trends in both datasets. Both results indicate that NO_3 concentrations as a snapshot in time and space may not be as important a detail as NO_3 flux into the environment.

4.1.3 Soil Moisture and Water Table Influences on Nitrous Oxide

Soil moisture values differed between transects; T4 moisture was mediated by the stream, and did not dry out as much as did T5. Differing moisture levels is hypothesized to have an effect on N_2O production and emission, specifically on a seasonal or event basis. However, N_2O fluxes did not exhibit a seasonal trend, nor a positional one with seasonality. During wetter conditions, denitrification activity and N_2O emissions were more highly correlated to soil moisture than during dry conditions (Florinsky *et al.*, 2004), a result that may have led to the lack of spatial trends along the topographic transects. Reasons behind this might be answered by examining the controls on N_2O production in the subsurface, namely soil moisture and water table level, on a seasonal basis.

Scatterplots of N_2O flux versus surface soil moisture content (0-6 cm) did not reveal any significant relationships in this study, despite being a well-known relationship between the two. Spatial trends along RZs (among upland and lowland site) have been found by other researchers, with little to no relationship between fluxes and soil moisture (Dhont *et al.*, 2004; Paludan and Blicher-Mathiesen, 1996). Production in the subsurface is likely influenced by several different variables, including soil moisture and water table position, as is gas diffusion from sites of production to the soil-atmosphere interface. High subsurface concentrations of N_2O, which for these purposes, may be assumed to act as a proxy for production zones, displayed significant peaks when normalized for water table depth. In these graphs, most of the N_2O peaks were at or slightly above or below the water table, suggesting a strong influence of moisture on denitrifying bacterial activity. In all cases, N_2O concentrations were highest at the water table and decreased upward towards the surface where the soil was drier and therefore more oxic. The relative concentrations at each site are significantly different from one another, some being orders of magnitude different; specifically, the FE at T4 and the RS at T5, display peak concentrations an order of magnitude greater than the other four sites. These concentrations are consistent with peaks found in other studies (Clough *et al.*, 1999; Rolston *et al.*, 1976). Despite discrepancies in subsurface peak concentrations among sites, none of the concentrations appeared to affect the flux at the surface; a result similar to that found in other studies (Reth *et al.*, 2008; Hosen *et al.*, 2000). There could be a time lag related to gas diffusion through the subsurface. One study used ^{15}N-labeled N_2O, injected at 155cm below the surface to determine this lag time; the labeled molecule was recovered at the surface after seven days (Reth *et al.*, 2008). Another study recovered only 0.4% of the applied ^{15}N after 38 days of sampling (Clough *et al.*, 1999). Therefore, it is possible that N_2O produced at depth does reach the surface, or takes an extended period of time, explaining the lack of correlation between subsurface profiles and surface fluxes.

Soil moisture is a strong factor influencing diffusion coefficients in the subsurface. Highly moist subsurface environments can act as sinks for moving gases, as diffusion is dramatically decreased. Aerobic, dry environments can increase diffusion coefficients compared to wet soils, potentially leading to faster movement of gases from their zones of production to the surface as a flux. In this study, especially during the summer months, soil moisture was low at the FEs, RS, and RL (at T4). On one sampling occasion, profile and flux samples were taken consecutively over 2 days (with another sampling date five days prior; DOY 165, 170, 171). An examination of time staggered profiles and fluxes was not able to demonstrate this time lag, however a study specifically addressing this issue would likely be able to add insight to the time lag concern.

4.1.4 Soil and Ambient Temperature Influences on Nitrous Oxide

Temperature positively influences microbial activity, and therefore should influence N_2O production through enhanced denitrification activity. On a microscale in the subsurface, temperature measurements were taken during every sampling period, at the same depths as the gas profilers, in order to determine if temperature was a determinant factor in N_2O production at this field site. An examination of temperature versus N_2O concentrations revealed weak positive relationships (data not shown) with R^2 values less than 0.2. Nitrous oxide dissolves more easily at lower temperatures (Dhont *et al.*, 2004), which could mean the relationship should have been negative, however microbial activity is heightened at higher temperatures. Therefore, these negative relationships may more readily indicate production of N_2O as opposed to "storage" of the gas at a particular depth. Examining profiles of N_2O and temperature revealed that sampling dates occurring on days with lower soil temperatures has higher N_2O concentrations (not significant). Relationships between surface fluxes and soil/air temperatures revealed stronger R^2 values, contrary to Dhont *et al.*'s (2004) findings, however possibly lending credibility to the hypothesis that production was occurring at the surface of this riparian zone, and there was little connection between the subsurface biogeochemical conditions and N_2O at the surface-atmosphere interface.

4.1.5 Soil Physical Properties Influence on Nitrous Oxide Flux and Subsurface Concentrations

The soil physical properties at this site have implications for the transport and movement of gases through the soil profile (see 1.2.2). To calculate diffusion rates of a particular gas, a diffusion coefficient must be employed; however this value must take into account soil tortuosity, which is a

function of the connectivity of pores within the soil profile. Tortuosity of unity occurs when there is full connectivity between pores, and increases as air content decreases. At the same value of soil air content, the tortuosity in wet soils is larger than in dry soils, and also larger in undisturbed profiles as compared to sieved and repacked soils (Moldrup *et al.*, 2001). Also, natural soils often maintain smaller gas diffusivity levels due to microsites of higher than average bulk density and/or water content that retards gaseous flow (Moldrup *et al.*, 2001). Therefore, soils with lower porosities (i.e. less volume for air-filled porosity), will experience slower gas diffusion rates. This has implications for N_2O produced at depth in soils with high bulk density/low porosity and high water content: the residence time of N_2O in the soil column could increase due to a reduction of the gas diffusion coefficient (Clough *et al*., 2005), resulting in dissolution of N_2O or reduction to dinitrogen gas. It was expected that the soil properties examined in this project would display a visible impact upon the subsurface N_2O profile concentrations. Both porosity and bulk density appeared to affect gas movement, which was displayed by rapid decreases in peak N_2O subsurface concentrations above areas with low porosity and high bulk density. Porosity appeared to affect the movement of N_2O slightly more than bulk density in some cases. Ball *et al.* (1997) suggest that particular soil factors may not always be of equal importance, or have the same effect on N_2O production/movement/emission, when conditions vary, due to complexities of the natural system. These results suggest the importance of experiments in which environmental and soil properties are controlled in a laboratory setting in order to attempt to sift out the dominating variables.

Hydraulic soil properties such as the proportion of water filled pore space have been highly correlated to denitrification rates (see Table 1). Under dry conditions N_2O production rates are normally lower than they are when soil moisture is higher. Loamy soils showed a smaller decrease in N_2O production rate upon drying than did clay soils, whereas during wet conditions highest production rate was in loamy sands, then peat, and then clay (Pihlatie *et al.*, 2004). Sandy soils had lower N_2O emissions in a study in Saskatchewan than finer-textured soils (Corre *et al.*, 1996). This is contrary to that found by other researchers in which fine textured soils maintained higher denitrification rates than course grained soils (Groffman and Tiedje, 1989). In this study, soil types did not differ enough within the profile, or among sites, to make a significant difference. In a recent study conducted at this site, Leoni (2008) found that soil texture had no bearing on denitrification potential (denitrification enzyme activity [DEA]).

4.2 Temporally-Controlled Spatial Distribution of N_2O and Related Production Controls

Nitrous oxide fluxes did not display spatial trends, partly due to the high degree of natural heterogeneity in the system, and possibly also a result of the unusually dry collection period. Examining the data as one entire field season of points was also considered to be a potential reason for a lack visible trends due to overshadowing by certain sampling dates and/or seasons. Therefore, they were also analyzed as a seasonally-averaged collection of points, attempting to parse out any overshadowing effects of seasonality. However, despite examining the data in this way, consistent spatial trends were sparse. This was an unexpected result as significant differences have been found in other studies (ex. Hedin *et al.*, 2001), and the current understanding of N_2O production might suggest that hydrological and physical differences between sites would produce significantly different fluxes of this gas (Groffman and Tiedje, 1989).

Event fluxes were higher than non-event fluxes (not significant), and spatial heterogeneity at each site was more pronounced during events samplings. These results are likely due to hotspots being created as microsites within the soil profile (or near the surface), following soil moisture increases to potentially optimum N_2O production levels (McClain *et al.*, 2003).

Subsurface N_2O was used as a proxy for denitrification activity. There were no trends in time with subsurface gas concentrations. Other studies have found that denitrification rates are lowest in the summer and higher during shoulder seasons, possibly due to a lack of competition for NO_3 by trees and other vegetation, and a high availability of organic carbon (Groffman and Tiedje, 1989). The field edge of T4 always experienced the highest concentrations of N_2O, highest in the spring time, a shoulder season. Springtime was also the season in which the highest concentrations were analyzed at the riparian slope position of T5; concentrations were slightly lower during the fall, and lowest in the summer.

The reason suggested for the lack of spatial trending in N_2O fluxes over the study period (averaged over the entire period, as well as during the spring and summer) may be a result of the "oxic blanket" that "covered" the site. Fall samples should not have followed this theory due to the high moisture conditions experienced as a result of increased precipitation and artificial flooding, thereby displaying spatial trends. However, this was not the case. Subsurface N_2O concentrations were lower during the fall than other seasons on both transects, and soil temperatures were also lower than other seasons,

therefore production of N_2O was likely slowed (as compared to spring and summer), muting trends that might have been present.

4.2.1 Hydrology and Soil Physical Properties

A hypothesis of this study was that temporal or seasonal variability would be driven more by physical processes including hydrology and moisture, temperature and soil physical properties, than by biotic factors such as substrate. In order to examine this hypothesis, site hydrology and moisture conditions were studied.

The seasonal hydrograph at T4 displayed small peaks related directly to rainfall events, as well as large wide peaks, such as the one seen between August 24th and September 5th (Figure), which are a result of the upstream reservoir water being incrementally released due to accumulation of precipitation, increasing the water level in this riparian zone. Soil moisture levels at a depth of 6 cm display a difference between the stream-regulated T4 and non-regulated T5. These were apparent with the degree to which both transects dried out over the summer, with the latter drying out more than T4.

The hydrology of a riparian wetland zone is often highly complex (Cey *et al.*, 1999), and is sensitive to changes in both surface and groundwater regimes (Baird *et al.*, 2005). Although hydrological analysis was not the main goal of this study, some important information was derived. Flow across the riparian zone at T4 was mainly oblique to the stream, from the FE to the SE, but changed during the year as influence of the stream was modified by regulation of the upstream reservoir (Leach, 2008). Furthermore, Leach (2008) showed that the RL and SE positions were along different flow paths, dependent upon water table elevation. During periods of very low water table, the site experienced flow reversals, with water moving from the stream area towards the FE. Such flow reversals have the potential to influence groundwater nutrient concentrations if the stream and hyporheic sources are different than the upslope sources. Nitrate, ammonium and DOC showed no differences in concentrations as a result of the changes in riparian zone flow. The deepest piezometers measured were 150 cm below the surface, whereas other researchers have examined groundwater at depths greater than 2 m (Duke *et al.*, 2007; Hill *et al.*, 2000; Cey *et al.*, 1999; Peterjohn and Correll, 1984). Alternatively, several other studies examined only shallow ground water depths, similar to those in this study (Banaszuk *et al.*, 2005; McGlynn *et al.*, 1999; Willems *et al.*, 1997). Results from both sets of studies indicate the importance of flow paths to the efficacy of riparian zone functionality and nutrient concentrations. These findings suggest that flow reversals might affect nutrient

concentrations, specifically ammonium, which is generally only found at the SE on T4 and the RL of T5, as it is often associated with high organic soils due to bonding with negatively charged organic matter (Brady and Weil, 1996). Therefore, it was expected that reversals would cause a movement of ammonium towards the mid-riparian zones of both transects. This was not the case, however. There were no apparent differences in the ammonium concentrations, nor in any other nutrient datasets, that would indicate a change or movement as a result of flow path reversals. One reason for this might be the low hydraulic conductivities at this site, restricting movement of water and increasing residence times in the riparian zone (silt/loams generally have a hydraulic conductivity of approximately 10^{-3} – 10^{-8} m s^{-1} (Bear, 1972), which could indicate slow-moving water).

4.2.2 Nitrous Oxide Variation Through a Rain Event

It has been documented that there is high transfer of nutrients during storm events (Macrae *et al.*, 2007) due to increased connectivity between landscape units. One event was studied over the field season, in which data were collected before, immediately after, and one day following a relatively large rain event. This storm event was expected to demonstrate this transfer of nutrients, especially NO_3 from the upland FE to the slopes and lowland areas of the transects studied, in the form of large changes between concentrations in the subsurface and/or in the fluxes at the surface. This, however, did not appear in the results.

At the two locations in which N_2O production is greatest, T4 and T5 RLs, error bars increased the most after the rain event, indicating high heterogeneity, likely resultant from microsites of hotspot activity after changes in soil moisture post-infiltration of precipitation. All sites experienced increases in N_2O fluxes, with a short time lag, but not necessarily related to increases in surface soil moisture. WFPS did increase following the rain event, however not to the levels it was at 5 days prior to the event. The fact that fluxes and surface soil moisture did not follow each other linearly, as expected (especially if production and emission were occurring at or near the soil surface), might suggest that antecedent conditions play a larger role in the release of N_2O as a flux at the soil-atmosphere interface. This was found by Groffman and Tiedje (1988), in which denitrification was stimulated differently depending on whether the soil was wetting or drying, due to hysteresis in the soil matrix. Subsurface N_2O concentrations responded to the rain event as well, however not consistently. Evidence of microsites or hotspots of production were visible at the FE of T4, where a small peak of N_2O was present a day following the rain event. Despite this small change, neither of the two FEs demonstrated change hypothesized to occur. The RL and RS sites demonstrated the most change as a

result of precipitation. These areas fluctuated the most in terms of water table and soil moisture over the season.

Chapter 5
Conclusions

Riparian zones are efficient in non-point source pollution mitigation from agricultural runoff, which is often rich in nutrients like nitrate, which can be toxic to surface water environments. When runoff and groundwater with high concentrations of nitrogen species enter riparian zones, they are often mitigated within the first five to 10 m. These nitrogen species, like nitrate and ammonium (along with phosphorus in fertilizers), act as energy sources for microbial activity. Through the redox sequence in low oxygen soils and microsites of the soil profile in riparian wetlands, nitrate is reduced to N_2O, which is released into the atmosphere. The processes that reduce non-point source pollution to surface water bodies are the same processes that lead to nitrous oxide production and release at the surface-atmosphere interface.

Despite the importance of nitrous oxide as a greenhouse gas, the ideal conditions for production in riparian wetlands, and the prevalence of agriculturally-dominated catchments in Ontario (and beyond), it has received little attention in the literature compared to the other popular trace greenhouse gases, CO_2 and CH_4. The literature that has been published focuses on N_2O efflux from agricultural fields, with little emphasis on riparian zones adjacent to these fields, which are responsible for mitigating agriculturally-related pollution. A better understanding of nitrogen cycling and the consequent release of N_2O is necessary in order to create more accurate models for climate change predictions.

The purpose of this study was to examine the dynamics of N_2O across an agriculturally-impacted riparian wetland. Specific research questions were related to spatial variability in fluxes from the field edge to the lowland zone, and to driving factors. It was hypothesized that spatial differences in N_2O fluxes across the riparian zone would be most strongly related to N supply from different sources (agricultural field and stream), whereas temporal variability at each site would be driven by changes in soil moisture.

The flux data and related geochemical data were examined as averages of all data, for spatial patterns across the riparian zone; none were found in flux data, despite spatial trends in moisture, temperature, nutrient supply and subsurface N_2O concentrations. It was hypothesized that seasonal trends in flux data may have overshadowed expected spatial trends, therefore, the datasets were also "binned" into seasons and again analyzed spatially across the riparian zone. Once again, despite

trends in variables that are responsible for N_2O production control, no spatial trends were apparent in N_2O fluxes.

Heterogeneity exhibited within all sites was just as high as heterogeneity among sites, suggesting that this was one of the causes of the unexpected lack of spatial trends across the riparian zone. A larger surface area GHG flux measurement collar (2 times greater than the total surface area of the small collars) used to capture fluxes at each site revealed no significant difference to that of the means of three smaller surface areas, suggesting that spatial heterogeneity dominates the entire site. Although the literature supports the finding of high variability in N_2O fluxes, the strong trends spatial and seasonal trends in the driving forces of N_2O production were found, and the lack of connection between the surface and the subsurface chemistry is contrary to what was expected. Another hypothesis, that requires further study, is related to the drought season in which this study took place, potentially applying an "oxic blanket" over the riparian zone. Both nitrification and nitrifier denitrification are processes that occur under oxic conditions; although both produce N_2O as a byproduct, both can also reduce N_2O to N_2 if given enough of a residence time, leading to a lack of difference in N_2O fluxes along the transects studied. Precipitation events did not significantly affect N_2O emissions, nor subsurface gas concentrations. This may also relate to the general dryness of the season, and the importance of antecedent conditions on soil moisture characteristics. Physical soil properties like low porosity and high bulk density can also act to the inhibit movement of N_2O towards the surface. If these layers of lower conductivity exist across the riparian zone, a general paucity of N_2O would reach the surface.

Chapter 6
Recommendations

Future studies in this area would benefit from taking a more "mechanistic" approach to analyzing N cycling *in situ*. A higher density of sampling locations, including at least two subsurface gas profiler arrays at each site, measurements of redox potential at all sampling locations and depths, and a longer study time period (i.e. over at least 2 full field seasons), would provide a better understanding of processes occurring beneath the surface. Special attention to antecedent moisture and temperature conditions would be beneficial, as well as adding a concurrent laboratory component related to antecedent conditions, monitoring results both *in situ* and in the controlled setting of the lab.

A factorial laboratory design, controlling independent variables such as moisture, temperature, nitrogen (NO_3 and NH_4) concentrations and rates of addition, would also provide the "mechanistic" approach necessary. In this design, monoliths of soil could be stored in controlled growth chambers (available at the University of Waterloo). Moisture, temperature, redox and soil gas probes, inserted at various depths, would provide a great deal of information as conditions were altered. In addition to this, the processes responsible for gas movement from the subsurface zones of production to the surface could be examined using the closed chamber approach with both vented and non-vented chambers. Both advective and diffusive fluxes are responsible for the movement of gas through the subsurface, however they become dominant over one another under different conditions. A vented chamber allows for the influence of wind speed (which controls advective flux), while a non-vented chamber removes this process from the equation. Examining both types of chambers, and controlling for the extra variable of wind speed might help to determine the dominant gas movement process under different conditions.

An important missing piece of knowledge coming out of this study was that of time lags between gas production and the gas' release at the surface. Taking time intensive measurements of N_2O flux as well as subsurface gas concentrations following an induced/natural rain event would help to understand the mechanics of gas transport. Isotope analysis has become a popular way of being able to "fingerprint" nutrients and the transformation processes leading creating them. Labeling of nitrate and/or ammonium additions (in an induced rain event) with N^{15} would help to determine whether denitrification or nitrification was responsible for N_2O production, as well as helping to track the movement of this gas through the subsurface.

Appendix 1

Sample Calculations

Water-filled Pore Space Calibration (from Theta probe)

	Water-filled pore space (WFPS)						Theta probe reading					
Saturation increment	A1	A2	A3	B1	B2	B3	A1	A2	A3	B1	B2	B3
0	100.3	104	96.9	98.5	100	111.5	1105	1103	1097	1096	1100	1101
1	100	103.8	96.7	98.3	99.7	111.2	1089	1090	1087	1079	1082	1070
2	99.7	103.5	96.5	98	99.4	110.8	1077	1078	1072	1070	1077	1064
3	98.6	102.5	95.4	97.3	98.6	109.8	1064	1064	1055	1050	1054	1047
4	95.5	99	92.1	93.3	95.4	105.8	1039	1037	1034	1039	1045	1019
5	94.3	97.8	90.8	92.1	94.2	104.3	1049	1036	1035	1044	1042	1025
6	90	93.7	87.3	87.8	90.2	98.5	1041	1025	1034	1035	1035	1017
7	89.6	93.3	86.7	87.4	89.9	98	1094	1076	1091	1088	1088	1078
8	88.7	92.5	85.8	86.8	89.1	97	1050	1021	1037	1038	1037	1019
9	85.8	89.5	82.4	84.4	86.2	93.9	1039	993	1029	1023	1026	1001
10	78.6	83.5	77.7	79.5	80.2	87.7	1029	939	1020	1020	1007	976
11	71	75.1	69.2	71.6	72.1	78.6	997	858	992	982	984	958
12	70.2	74.2	68.3	70.8	71.2	77.6	1000	829	990	988	978	897
13	63.4	66.1	59.5	63.1	63	68.9	961	742	958	963	917	817
14	58.9	61.2	55.5	58.6	58.8	63.4	953	701	957	944	878	752
15	55.2	57.1	52.4	55.2	55.4	58.9	913	704	914	852	838	727
16	52	53.6	49.3	52.3	52.5	55.1	818	647	836	880	787	633
17	37.1	35.3	35.6	37.3	36.5	35.3	393	527	810	428	633	582
18	32.1	29.1	30.1	31.1	29.2	27.4	546	400	647	352	422	425
19	30.3	27	27.9	29.1	26.9	25.1	372	326	507	328	370	377
20	26.8	24.2	25.1	26	23.5	22.3	270	273	449	318	334	304
21	21.3	16.6	17.1	19.1	15	14.9	222	242	306	218	270	228
22	19.2	14.4	15.1	17.4	12.9	13.4	139	222	287	201	229	215
23	17.7	12.9	13	16.2	10.7	12	189	187	201	222	174	195
24	16	10.9	11.6	14.6	9	10.8	137	164	206	217	119	183
25	7.2	3.8	3.3	7.6	2.7	5.1	103	53	73	126	35	107
26	5.9	2.1	2.4	6.3	1.3	3.4	79	45	48	95	33	107
27	6.3	4.3	3.3	7.1	3.4	5.1	78	44	41	87	20	81
28	4.1	2.4	1.6	4.7	1.9	2.8	62	40	41	76	20	79
29	1.5	1.6	1	1.7	1.3	1.4	24	17	22	29	14	45

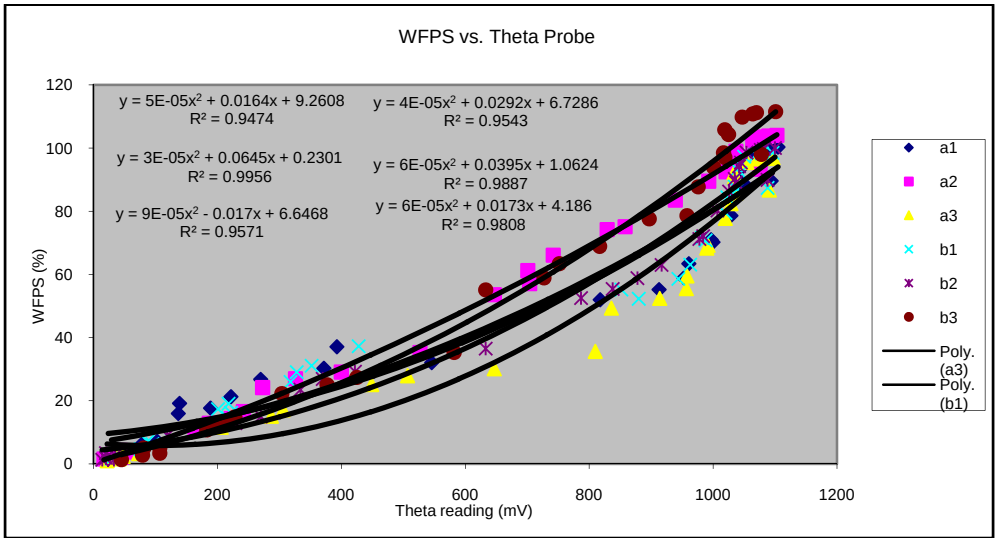

If the equation defining the above relationships is equal to: $y = ax^2 + bx + c$, then the average of *a*, *b* and *c* from all 6 test sites will provide an average relationship between WFPS and Theta readings.

	a	b	C
a1	5.00E-05	0.0164	9.2608
a2	3.00E-05	0.0645	0.2301
a3	9.00E-05	-0.017	6.6468
b1	4.00E-05	0.0292	6.7286
b2	6.00E-05	0.0395	1.0624
b3	6.00E-05	0.0173	4.186
AVG	0.000055	0.024983	4.685783
STDEV	2.07E-05	0.027149	3.526507

Therefore, the equation is:
$Y = 0.000055x^2 + 0.024983x + 4.685783$
Where y = WFPS and x = theta

N_2O Flux Calculations

1) Collar Volume

Measurements were taken at each sampling event to determine the collar "topography" (either one reference level taken at the same point on the collar each time, or 5 measurements, averaged). These were used to calculate the volume of the air inside the collar.

Mean depth (or reference depth) x inside cross-section area of the collar

Ex. Mean depth = 8.2cm, x-section area = 291cm^2

8.2 x 291 = 2386.2 cm^3, the volume of air in the collar (2.4 L)

This value is added to the volume of the chamber put on top to determine the total volume (1.46L). Only the collar volume changes at each sampling event.

2) Flux calculation

Gas concentrations (from GC) are plotted to determine the slope of the concentration change (uL L^{-1} min^{-1}). This value is converted to moles (using temperature from chamber and chamber volume). The new units are now nmoles per minute. The collar/chamber area is taken into account and flux is now in units of: nmol m^{-2} min^{-1}.

Ex. N_2O concentrations (times 0, 10, 20 and 30 minutes): 0.4917, 9.4916, 0.6506, 0.7444 (uL L^{-1})

In Excel: "=Slope(known y's, known x's), where y = concentration, x = time (0-30 min)

= 0.00917

Divided by 60 seconds per minute,

= 0.00015 uL L^{-1} s^{-1}

3) Flux conversion

Molar volume is needed to convert uL L^{-1} to nmoles using the following equation:

22.414 x (273 + air Temp / 273) x (101.3 / ambient barometric pressure)

Current values in units of uL L^{-1} s^{-1} are divided by the total collar + chamber volume

Ex. 0.00015 uL L^{-1} s^{-1} x (2.4 + 1.6 L) = 0.0006 ul s^{-1}

Divided by the molar volume:

0.0006 ul s^{-1} / (22.414 x ((273+20)/273) x (101.3/100) = 2.46e-5 moles s^{-1}

Divided by the collar's cross sectional area:

2.46e-5 moles s^{-1} / 0.0291 m^2 = 7.16e-7 moles m^{-2} s^{-1} (or 0.072 nmoles m^{-2} s^{-1})

References

Achtnich, C., F. Bak and R. Conrad. 1995. *Competition for electron donors among nitrate reducers, ferric iron reducers, sulfate reducers, and methanogens in anoxic paddy soil*. Biol Fertil Soils. 19: 65-72.

Akimoto, F., A. Matsunami, Y. Kamata, I. Kodama, K. Kitagawa, N. Arai, T. Higuchi, A. Itoh, H. Haraguchi. 2005. *Cross-correlation analysis of atmospheric trace concentrations of N_2O, CH_4 and CO_2 determined by continuous gas-chromatographic monitoring*. Energy. 30: 299-311.

Ashby, J.A.; Bowden, W.B.; Murdoch, P.S. 1998. *Controls on denitfication in riparian soils in headwater catchments of a hardwood forest in the Catskill mountains, USA*. Soil Biology and Biochemistry. 30(7): 853-864.

Balestrini, R., C. Arese, and C. Delaconte. 2007. *Lacustrine wetland in an agricultural catchment: nitrogen removal and related biogeochemical processes*. Hydrology and Earth System Sciences Discussions. 4: 3501-3534.

Ball, B.C., G.W. Horgan, H. Clayton, and J.P. Parker. 1997. *Spatial variability of nitrous oxide fluxes and controlling soil and topographic properties*. Journal of Environmental Quality. 26: 1399-1409.

Banazuk, P., A. Wysocka-Czubaszek, P. Kondratiuk. 2005. *Spatial and temporal patterns of groundwater chemistry in the river riparian zone*. Agriculture, Ecosystems and Environment. 107: 167-179.

Bateman, E.J., and E.M. Baggs. 2005. *Contributions of nitrification and denitrification to N2O emissions from soils at different water-filled pore space*. Biology and Fertility of Soils. 41(6): 379-388.

Bear, J. 1972. Dynamics of Fluids in Porous Media. Dover Publications. 782pgs.

Bowden, R.D., G. Rullo, G.R. Stevens, and P.A. Steudler. 2000. *Soil fluxes of carbon dioxide, nitrous oxide and methane at a productive temperate deciduous forest*. Journal of Environmental Quality. 29: 268-280.

Brady, N.C. and R.R. Weil. 1999. The Nature and Property of Soils (12th edition). Prentice-Hall Inc.: New Jersey. 881pgs.

Burt, T.P. 2005. *A third paradox in catchment hydrology and biogeochemistry: decoupling in the riparian zone*. Hydrological Processes. 19: 2087-2089.

Butterbach-Bahl, K., M. Kesik, P. Miehle, H. Papen, and C. Li. 2004. *Quantifying the regional source strength of N-trace gases across agricultural and forest ecosystems with process based models*. Plant and Soil. 260: 311-329.

Cannavo, P; Richaume, A; LaFolie, F. 2004. *Fate of nitrogen and carbon in the vadose zone: in situ and laboratory measurements of seasonal variations in aerobic respiratory and denitrifying activities*. Soil Biology and Biochemistry. 36: 463-478.

Carpenter, S.R., N.F. Caraco, D.L. Correll, R.W. Howarth, A.N. Sharpley, and V.H. Smith. 1998. *Nonpoint pollution of surface waters with phosphorus and nitrogen*. Ecological Applications. 8(3): 559-568.

Cey, E.E., D.L. Rudolph, R. Aravena and G. Parkin. 1999. *Role of the riparian zone in controlling the distribution and fate o fagricultural nitrogen near a small stream in southern Ontario*. Journal of Contaminant Hydrology. 37: 45-67.

Chantigny, M.H.; Angers, D.A.; Rochette, Philippe. 2002. *Fate of Carbon and Nitrogen from animal manure and crop residues in wet and cold soils*. Soil Biology and Biochemistry. 34: 509-517.

Chapuis-Lardy, L., N. Wrage, A. Metay, J.-L. Chotte, and M. Bernoux. 2007. *Soils, a sink for N2O? A review.* Global Change Biology. 13: 1-7.

Clement J-C., G. Pinay and P. Marmonier. 2002. Seasonal dynamics of denitrification along topohydrosequences in three different riparian wetlands. J. Environ. Qual. 31: 1025-1037.

Clough, T.J.; Sherlock, R.R.; Rolston, D.E. 2005. *A review of the movement and fate of N2O in the subsoil*. Nutrient Cycling in Agroecosystems. 72: 3-11.

Clough, T.J., S.C. Jarvis, E.R. Dixon, R.J. Stevens, R.J. Laughlin, and D.J. Hatch. 1999. *Carbon induced subsoil denitrification of ^{15}N-labeled nitrate in 1m deep soil columns.* Soil Biology Biochemistry. 31: 31-44.

Conrad, R. 1996. *Soil microorganisms as controllers of atmospheric trace gases (H2, CO, CH4, OCS, N2O and NO)*. Microbiological Reviews. Dec.: 609-640.

Conrad, R. 2002. Trace Gas Exchange in Forest Ecosystems. R Gasche *et al*. (eds.). Pg: 3-33.

Corre, M.D., C. van Kessel, and D.J. Pennock. 1996. *Landscape and seasonal patterns of nitrous oxide emissions in a semi-arid region.* Soil Sci. Soc. Am. Journal. 60: 1806-1815.

Dahm, C.N., N.B. Grimm, P. Marmonier, H.M. Valett and P. Vervier. 1998. *Nutrient dynamics at the interface between surface waters and groundwaters*. Freshwater Biology. 40: 427-451.

Davidson, E.A., F.Y. Ishida, and D.C. Nepstad. 2004. *Effects of an experimental drought on soil emissions of carbon dioxide, methane, nitrous oxide, and nitric oxide in a moist tropical forest.* Global Change Biology. 10: 718-730.

Davidson, E.A., M. Keller, H.E. Erickson, L.V. Verchot, and E. Veldkamp. 2000. *Testing a conceptual model of soil emissions of nitrous and nitric oxides*. BioScience. 50(8): 667-680.

Deacon, J. 2007. *The Microbial World: The nitrogen cycle and nitrogen fixation*. Institute of Cell and Molecular Biology, The University of Edinburgh. http://helios.bto.ed.ac.uk/bto/microbes/nitrogen.htm

den Elzen, M.G.J., A.H.W. Beusen and J. Rotmans. 1997. *An integrated modeling approach to global carbon and nitrogen cycles: Balancing their budgets*. Global Biogeochemical Cycles. 11(2): 191-215.

Dohnt, K., P. Boeckx, G. Hofman, and O. Van Kleemput. 2004. *Temporal and spatial patterns of denitrification enzyme activity and nitrous oxide fluxes in three adjacent vegetated riparian buffer zones*. Biol. Fertil. Soils. 40: 243-251.

Duke, J.R., J.D. White, P.M. Allen, and R.S. Muttiah. 2007. *Riparian influence on hyporheic-zone formation downstream of a small dam in the Blackland Prairie region of Texas*. Hydrological Processes. 21: 141-150.

Environment Canada. 2008. *Climate Normals or Averages 1961-1990.* http://climate.weatheroffice.ec.gc.ca/climate_normals/index_1961_1990_e.html

Fetter, C.W. 1999. Contaminant Hydrogeology (2nd Edition). New Jersey: Prentice-Hall Inc.

Fiedler, S. and M. Sommer. 2004. *Water and redox conditions in wetland soils – Their influence on pedogenic oxides and morphology*. Soil Science Society of America Journal. 68: 326-335.

Florinsky, I.V., R.G. Eilers, G.R. Manning, L.G. Fuller. 2002. *Prediction of soil properties by digital terrain modeling*. Environmental Modelling and Software. 17: 295-311.

Foloronuso, O.A. and D.E. Rolston. 1984. *Spatial variability of field-measured denitrification gas fluxes*. Soil Sci. Soc. Am. Journal. 48(6): 1214-1219.

Freibauer, A and M. Kaltschmitt. 2003. *Controls and models for estimating direct nitrous oxide emissions from temperate and sub-boreal agricultural mineral soils in Europe*. Biogeochemistry. 63: 93-115.

Galloway, J.N., F.J. Dentener, D.G. Capone, E.W. Boyer, R.W. Howarth, S.P. Seitzinger, G.P. Asner, C.C. Cleveland, P.A. Green, E.A. Holland, D.M. Karl, A.F. Michaels, J.H. Porter, A.E. Townsend, and C.J. Vorosmarty. 2004. *Nitrogen cycles: Past, present, and future*. Biogeochemistry. 70: 153-226.

Galloway, M.E. and B.A. Branfireun. 2004. *Mercury dynamics of a temperate forested wetland.* Science of the Total Environment. 325: 239-254.

Groffman, P.M., A.J. Gold, and K. Addy. 2000. *Nitrous Oxide production in riparian zones and its importance to national emissions inventories*. Chemosphere – Global Change Science. 2(3-4): 291-299.

Groffman, P.M. and J.M. Tiedje. 1989. *Denitrification in north temperate forest soils: spatial and temporal patterns at the landscape and seasonal scales*. Soil Biol. Biochem. 21(5): 613-620.

Groffman, P.M., N.J. Boulware, W.C. Zipperer, R.V. Pouyat, L.E. Band, and M.F. Colosimo. 2002. *Soil nitrogen cycle processes in urban riparian zones*. Environ. Sci. Technol. 36: 4547-4552.

Grunfeld, S., and H. Brix. 1999. *Methanogenesis and methane emissions: effects of water table, substrate type and presence of Phragmites australis*. Aquatic Botany. 64: 63-75.

Hanson, G.C., P.M. Groffman, and A.J. Gold. 1994a. *Denitrification in riparian wetlands receiving high and low groundwater nitrate inputs*. Journal of Environmental Quality. 23: 917-922.

Hanson, G.C., P.M. Groffman, and A.J. Gold. 1994b. *Symptoms of nitrogen saturation in a riparian wetland*. Ecological Applications. 4(4): 750-756.

Hanson, P.J., N.T. Edwards, C.T. Garten and J.A. Andrews. 2000. *Separating root and soil microbial contributions to soil respiration: A review of methods and observations*. Biogeochemistry. 48: 115-146.

Heagy, A.E. 1993. *Natural Areas Report: Beverly Swamp.* Ontario Ministry of the Enviornment Natural Heritage Information Centre. http://nhic.mnr.gov.on.ca/areas/areas_report.cfm?areaid=5328

Heagy, A.E. 1995. *Hamilton-Wentworth Natural Areas Inventory.* The Earth Science Features of Hamilton-Wentworth Region, Ontario. Hamilton Naturalists' Club: Hamilton ON. Vol 1: 1-1 - 1-28.

Hedin, L.O., J.C. von Fischer, N.O. Ostrom, B.P. Kennedy, M.G. Brown, G.P. Robertson. 1998. *Thermodynamic constraints on nitrogen transformations and other biogeochemical processes and soil-stream interfaces*. Ecology. 79(2): 684-703.

Hill, A.R., K.J. Devito, S. Campagnolo, and K. Sanmugadas. 2000. *Subsurface denitrification in a riparian zone: Interactions between hydrology supplies of nitrate and organic carbon*. Biogeochemistry. 51: 193-223.

Hinton, P.R., C. Brownlow, I. McMurray and B. Cozens. 2004. SPSS Explained. Routledge: USA. 377pgs.

Hosen, Y., H. Tsuruta and K. Minami. 2000. *Effects of the depth of NO an dN_2O productions in soil on their emission rates to the atmosphere: analysis by simulation model.* Nutrient Cycling in Agroecosystems. 57: 83-98.

Hutchinson, G.L. and A.R. Mosier. 1981. *Improved soil cover method for field measurements of nitrous oxide fluxes.* Soil Science Society of America Journal. 45: 311-316.

Intergovernmental Panel on Climate Change. 2001. *Climate Change 2001: The Scientific Basis. Contribution of Working Group I to the Third Assessment Report of the Intergovernmental Panel on Climate Change* [Houghton, J.T.,Y. Ding, D.J. Griggs, M. Noguer, P.J. van der Linden, X. Dai, K. Maskell, and C.A. Johnson (eds.)]. Cambridge University Press, Cambridge, United Kingdom and New York, NY, USA, 881pp.

Jordan, T.E., D.E. Weller, D.L. Correll. 1998. *Denitrification in surface soils of a riparian forest: effects of water, nitrate and sucrose additions.* Soil Biology and Biochemistry. 30: 833–843.

Karrow, P.F. 1963. *Pleistocene geology of the Hamilton-Galt region area*. Ontario Department of Mines and Geological Report. 16: 66.

Kaufman, S.C., J.M. Waddington, and B.A. Branfireun. 2005. *Hydrogeomorphic controls on runoff in a temperate swamp*. Hydrology and Earth System Sciences Discussions. 2: 483-508.

Knowles, Roger. 1982. *Denitrification*. Microbiological Reviews. Mar.: 43-70.

Lashof, D.A. and D.R. Ahuja. 1990. *Relative contributions of greenhouse gas emissions to global warming*. Nature. 344:529-531.

Lemke, R.L., R.C. Izaurralde, and M. Nyborg. 1998. *Seasonal distribution of nitrous oxide emissions from soils in the Parkland region*. Soil Science Society of America Journal. 62: 1320-1326.

Leoni, L. 2008. *An analysis of riparian zone denitrification potential in relation to soil texture and chemistry*. [UG Thesis]. McMaster University, Hamilton ON.

Lloyd, D., L. Boddy, and K.J.P. Davies. 1987. *Persistence of bacterial denitrification capacity under aerobic conditions: The rule rather than the exception*. FEMS Microbiology Letters. 45(3): 185-190.

Machefert, S.E. and N.B. Dise. 2004. *Hydrological controls on denitrification in riparian ecosystems*. Hydrology and Earth System Sciences. 8(4): 686-694.

Machefert, S.E., N.B. Dise, K.W.T. Goulding, and P.G. Whitehead. 2002. *Nitrous oxide emissions from a range of land uses across Europe*. Hydrology and Earth System Sciences. 6(3): 325-337.

Livingston, G.P. and G.L. Hutchinson. 1995. Methods in Ecology: Biogenic Trace Gases: Measuring Emissions from Soil and Water (Matson, P.A. and R.C. Harriss [eds.]). Blackwell Science Ltd, Oxford, UK. Pgs 14-50.

Maljanen, M., A. Liikanen, J. Silvola, and P.J. Martikainen. 2003. *Measuring N2O emissions from organic soils by closed chamber or soil/snow N2O gradient methods*. European Journal of Soil Science. 54: 625-631.

McClain, M.E., E.W. Boyer, C.L. Dent, S.E. Gergel, N.B. Grimm, P.M. Groffman, S.C. Hart, J.W. Harvey, C.A. Johnston, E. Mayorga, W.H. McDowell, G. Pinay. 2003. *Biogeochemical hot spots and hot moments at the interface of terrestrial and aquatic ecosystems*. Ecosystems. 6(4): 301-312.

McGlynn, B.L., J.J. McDonnell, J.B. Shanley and C. Kendall. 1999. *Riparian zone flowpath dynamics during snowmelt in a small headwater catchment.* Journal of Hydrology. 222: 75-92.

Mitsch, W.J. and J.G. Gosselink. 2007. Wetlands (Edition 4). John Wiley and Sons.

Moldrup, P., T. Olesen, T. Komatsu, P. Schjonning, and D.E. Rolston. 2001. *Tortuosity, diffusivity, and permeability in the soil liquid and gaseous phases.* Soil Science Society of America Journal. 65: 613-623.

Mosier, A.R., J.M. Duxbury, J.R. Freney, O. Heinemeyer, and K. Minami. 1996. *Nitrous oxide emissions from agricultural fields: Assessment, measurement and mitigation*. Plant and Soil. 181: 95-181.

Muller, C., R.J. Stevens, R.J. Laughlin, H.-J. Jager. 2004. *Microbial processes and the site of N_2O production in a temperate grassland soil*. Soil Biology and Biochemistry. 36: 453-461.

Naiman, R.J. and H. Décamps. 1997. *The ecology of interfaces: Riparian zones*. Annual Review of Ecological Systems. 28: 621-658.

Nommik, H. 1956. *Investigations on denitrification in soil*. Acta agricultura Scandinavica, Section B. Soil and plant science. 6: 195-227.

Oh, J. and J. Silverstein. 1999. *Oxygen inhibition of activated sludge denitrification.* Water Research. 33(8): 1925-1937.

Peaman, I., Etheridge, D., De Silva, F., Fraser, P.J. 1986. *Evidence of changing concentrations of atmospheric CO_2, N_2O and CH_4 from air bubbles in Antarctic ice*. Nature. 320: 248-250.

Peterjohn, W.T. and D.L. Correll. 1984. *Nutrient dynamics in an agricultural watershed: observations on the role of a riparian forest.* Ecology. 65(5): 1466-1475.

Pierzynski, G.M., J.T. Sims, G.F. Vance. 2005. Soils and Environmental Quality, Third Edition. CRC Press. 569pgs.

Reth, S., W. Graf, O. Gefke, R. Schilling, H.K. Seidlitz, J.C. Munch. 2008. *Whole-year-round observation of N2O profiles in soil: A lysimeter study.* Water Air Soil Pollution: Focus. 8:129-137.

Robertson, L.A., T. Dalsgaard, N.-P. Revsbech, and J.G. Kuenen. 1995. *Confirmation of 'aerobic denitrification' in batch cultures, using gas chromatography and ^{15}N mass spectrometry*. FEMS Microbiol. Ecol. 18: 113-120.

Robertson, G.P. and J.M. Tiedje. 1987. *Nitrous oxide sources in aerobic soils: nitrification, denitrification and other biological processes.* Soil Biol. Biochem. 19(2): 187-193.

Sallam, A., W.A. Jury, and J. Letey. 1984. *Measurement of gas diffusion coefficient under relatively low air-filled porosity.* Soil Science Society of America Journal. 48: 3-6.

Schnabel, R.R., J.A. Shaffer , W.L. Stout, L.F. Cornish. 1997. *Denitrification distributions in four valley and ridge riparian ecosystems.* Environmental Management. 21(2): 283-290.

Simek, Miroslav; Jisova, Linda; Hopkins, David W. 2002. *What is the so-called optimum pH for denitrification in soil?*. Soil Biology and Biochemistry. 34: 1227-1234.

Sutka, R.Ll, N.E. Ostrom, P.H. Ostrom, J.A. Breznak, H. Gandhi, A.J. Pitt, and F. Li. 2006. *Distinguishing nitrous oxide production from nitrification and denitrification on the basis of isotopomer abundances*. Applied and Environmental Microbiology. 72(1): 638-644.

Triska, F.A., J.H. Duff, and R.J. Avanzino. 1993. *The role of water exchange between a stream channel and its hyporheic zone in nitrogen cycling at the terrestrial-aquatic interface*. Hydrobiologia. 251: 167-184.

US Environmental Protection Act. 1996. www.epa.gov

van Kessel, C., D.J. Pennock and R.E. Farrell. 1993. *Seasonal variations in denitrification and nitrous oxide evolution at the landscape scale*. Soil Science Society of America Journal. 57: 988-995.

Verchot, L.V., E.A. Davidson, J.H. Cattanio *et al*. 1999. *Land use change and biogeochemical controls of nitrogen oxide from soils in eastern Amazonia*. Global Biogeochemical Cycles. 13: 31-46.

Vitousek, P.M., J.D. Aber, R.W. Howarth, G.E. Likens, P.A. Matson, D.W. Schindler, W.H. Schlesinger, and D.G. Tilman. 1997. *Human alteration of the global nitrogen cycle: Sources and consequences*. Ecological Applications. 7(3): 737-750.

Wang, Y.-P., B.Z. Houlton, and C.B. Field. 2007. *A model of biogeochemical cycles of carbon, nitrogen and phosphorus including symbiotic nitrogen fixation and phosphatase production*. Global Biogeochemical Cycles. 21, GB1018, doi: 10.1029/2006GB002797.

Walker, R.F., S.E. Hixson, and C.M. Skau. 1992. *Soil denitrification rates in a subalpine watershed of the eastern Sierra Nevada.* Forest Ecology Management.50: 217-231.

Warren, F.J., J.M. Waddington, R.A. Bourbonniere, and S.M. Day. 2001. *Effect of drought on hydrology and sulphate dynamics in a temperate swamp*. Hydrological Processes. 15: 3133-3150.

Well, R., J. Augustin, J. Davis, S.M. Griffith, K. Meyer, D.D. Myrold. 2001. *Production and transport of denitrification gases in shallow ground water*. Nutrient Cycling in Agroecosystems. 60: 65-75.

Whalen, S.C. 2000. *Nitrous oxide emission from an agricultural soil fertilized with liquid swine waste or constituents*. Soil Science Society of America Journal. 64: 781-789.

Willems, H., M. Rotelli, D. Berry, E. Smith, R. Reneau, S. Mostaghimi. 1997. *Nitrate removal in riparian wetland soils: effects of flow rate, temperature, nitrate concentration and soil depth*. Water Resources. 4: 841-849.

Woo, M-k. 1979. *Impact of power line construction upon the hydrology of part of a mid-latitude swamp*. Catena. 6: 23-42.

Woo, M-k. and J. Valverde. 1981. *Summer streamflow and water level at a mid-latitude forested swamp.* Forest Science. 27(1): 177-189.

Wrage, N., G.L. Velthof, M.L. van Beusichem, and O. Oenema. 2001. *Role of nitrifier denitrification in the production of nitrous oxide*. Soil Biology and Biochemistry. 33(12): 1723-1732.

Yates, T.T., B.C. Si, R.E. Farrell, and D.J. Pennock. 2006. *Probability distribution and spatial dependence of nitrous oxide emission: temporal change in hummocky terrain*. Soil Sci. Soc. Am. Journal. 70: 753-762.

Young, M.E. 2001. *Hydrological and Biogeochemical Controls on Mercury Fate and Transport in a Southern Ontario Forested Wetland*. Master of Science Thesis, Department of Geography, University of Toronto.

Yu, K., S.P. Faulkner, and W.H. Patrick Jr. 2006. *Redox potential characterization and soil greenhouse gas concentration across a hydrological gradient in a Gulf coast forest*. Chemosphere. 62: 905-914.

Zak, D.R. and D.F. Grigal. 1991. *Nitrogen mineralization, nitrification and denitrification in upland and wetland ecosystems*. Oecologia. 88:189-196.

Zhang, Z. 2007. *Effect of hydrological regimes on groundwater phosphorus transfer in a riparian wetland*. [Thesis] University of Waterloo, Waterloo, ON.

Zumft, W.G. 1997. *Cell and molecular basis of denitrification*. Microbiology and Molecular Biology Reviews. Dec.: 533-616.